A STRATIGRAPHIC AND PETROPHYSICAL STUDY OF IN-SITU GEOTHERMAL RESERVOIR QUALITY OF THE CAMBRO-ORDOVICIAN STRATA IN THE SUBSURFACE AT CORNELL UNIVERSITY, ITHACA, NEW YORK

A Thesis

Presented to the Faculty of the Graduate School

of Cornell University

In Partial Fulfillment of the Requirement for the Degree of

Master of Science

by

Jood Ahmad A. Al Aswad

August 2019

ABSTRACT

Geothermal energy is an attractive energy source which may significantly offset fossil fuels because of its potential to produce sustainable, widespread, and affordable heat. Cornell University is exploring the subsurface at its Ithaca, New York campus to access the naturally hot deep rocks and produce geothermal fluids for direct use as a thermal source with which to heat campus buildings. A reconnaissance fairway analysis of the geothermal potential of the Appalachian Basin revealed that rocks with suitable natural permeability and heat for geothermal reservoirs are likely to be at 2.3 - 3 km depth. This study investigates the in-situ geological properties and geothermal reservoir potential of the Cambro-Ordovician limestones, dolostones and sandstones underlying the Knox Unconformity at ~2.3 km to 2.8 km depth in Ithaca, New York. This new evaluation is based on repurposing geophysical well logs, drill cuttings and core reports, supplemented by new cuttings analyses, from 78 pre-existing hydrocarbon industry boreholes in central and western New York.

Gamma ray, neutron porosity hydrogen index, density and photoelectric factor logs are utilized to derive estimates of the lithologies and porosity of the Cambro-Ordovician strata. Coupled with the logs are cuttings reports and analyses for the interpolation of depths and thickness through the construction of cross-sections and isopach maps. Three intervals of strata are identified as potential reservoirs: the zone at which the basal Ordovician Little Falls Formation limestone or dolostone is interbedded with the upper Galway Formation sandstone known as the Rose Run member in New York; the interbedded sand and dolomite beds of the Galway Formation informally labeled in this study as the Yellowjacket member in New York; and the feldspathic sandstones of the basal Ausable member of the Potsdam Formation. These occur at depths below Ithaca of roughly 2.55 km, 2.7 km and 2.8 km +/ 0.2 km, respectively.

BIOGRAPHICAL SKETCH

Jood Al Aswad was born in Riyadh, Saudi Arabia and raised in the United States, Canada and Saudi Arabia by two PhD professors and diplomats who valued and encouraged the pursuit of knowledge and education. She majored in Earth Sciences at George Mason University, and solidified her love for the geosciences during her field camp experience while studying and mapping the geology of the Black Hills with South Dakota School of Mines and Technology. She was awarded a grant by the Office of Scholarship, Creativity and Research at George Mason to conduct independent geodetic research under the guidance of Dr. Linda Hinnov, which whetted her appetite to conduct research even more. While at George Mason University, she was awarded a full-ride scholarship from the King Abdullah Scholarship Program and graduated as the top student in her program and one of the first female geologists from her country.

In 2017, she began to study stratigraphy and petrophysics for the Earth Source Heat group under the tutelage of the wonderful Dr. Teresa Jordan. During her time at Cornell, she was awarded a fellowship by the King Abdullah Scholarship Program and served as president of the Cornell chapter of the American Association of Petroleum Geologists club. She greatly enjoyed the unique opportunity presented with studying potential geothermal reservoirs within Cornell's subsurface. Upon graduation, Jood plans to continue on in her academic career and pursue a PhD at Stanford University.

To my parents and role models,

Fatimah Al Sulaim and Ahmad Al Aswad.

ACKNOWLEDGEMENTS

There are so many people I would like to thank for their support:

- A deep, sincere gratitude to my major advisor, Dr. Teresa Jordan, who has been a perfect mentor and helped me develop into the scientist I am today. Word cannot express the gratitude I feel for such a wonderful advisor.
- My minor advisor, Dr. Warren Allmon, and Dr. Jefferson Tester, the P.I. of Earth Source Heat, thank you for all the time and support you have given me .
- The King Abdullah Scholarship Program for their financial support during my time here.
- My parents, my sister Jada Al Aswad, and my brother Majid Al Aswad for their faith in me and encouragement whenever things got hard. You are my rocks.
- Dr.'s Muawia and Nimat Barazangi, who have become like an extended Arab family to me during my time here. I greatly enjoyed our conversations, and making sure to get to you within +/- 5 minutes of the times we agreed to meet.
- DDU Team and friends— Ole Gustafson, Steve Beyers and Tasnuva "Ming" Khan. Special thanks to Dr. Jared Smith, who was a great help and wonderful source of knowledge. Thank you all for the fresh perspectives you've given me on my data.
- Tom and Sharon Pasquini, whom I personally would love to thank for their generosity and mentorship as hosts during my time taking a short course at Houston, TX.
- A great thank you to Savannah Williams, Judy Starr, Judy Wiiki, Polly Marion and Crystal Doner for making Snee a welcoming place.
- Dennis Earl from Petra/iHS and his boundless patience with my questions regarding the software.

- My friends in the department who include but are not limited to Caren Shin, Corey Hanson, Irene Del Real, Katie Grant, Patricia MacQueen, Joey Durkin, Paul Morgan, Paula Bürgi, and Khalid Abdulrahman and his wife Alaa..

TABLE OF CONTENTS

Biographical Sketch……..……ii
Dedication……..……...iii
Acknowledgements...……iv
List of Figures…….....……....viii
List of Abbreviations……..x
List of Symbols.....xi

Chapter 1: Introduction.....1
1.1: Background and Motivation.....1
1.2: Tectonic and Paleogeographic Setting 4
1.3: Stratigraphic Setting.....7
1.4: Objectives.....13

Chapter 2: Data and Methods.....21
2.1: Log Data Acquisition.....21
2.2: Well Logs.....22
2.3: Gamma Ray Log Normalization.....24
2.4: Picking Formation Tops and True Vertical Depth.....25
2.5: Corrections for Shale and Gas Effects in Neutron Logs.....26
2.6: Well Cuttings.....30

Chapter 3: Overall Petrophysical and Stratigraphic Analysis of the Subsurface Cambro-Ordovician Units of Central New York.....35
3.1: Abstract.....35
3.2: Introduction.....36
3.3: Top Picking Criteria from Well Logs.....36
3.4: Depth and Thickness of the Sedimentary Strata Beneath the Knox Unconformity.....37
3.5: Wells Used for NPHI Log Corrections.....43
3.6: Tribes Hill: Porosity and Permeability.....45

3.7: Little Falls: Porosity and Permeability.....49
3.8: Galway: Porosity and Permeability.....51
3.9: Potsdam: Porosity and Permeability.....66
3.10: Synthesis of Overall Regional Analysis of Porosity and Permeability.....79
3.11: Interpolation of Subsurface Stratigraphic Tops at Cornell University.....81

Chapter 4: The Effect of the Knox Unconformity on the Porosity of Underlying Strata: A Comparison of Western and Central New York.....85
4.1: Abstract.....85
4.2: Introduction.....86
4.3: Well Selections.....90
4.4: Results and Discussion.....92
4.5: Conclusion.....99

Chapter 5: Conclusions and Recommendations.....102

LIST OF FIGURES

Figure 1.1: The most favorable Play Fairways in the Appalachian Basin……...3
Figure 1.2: Tectonic setting of Laurentia and Gondwana 490 Ma……..6
Figure 1.3: Stratigraphy of the Cambro-Ordovician at central New York……..9
Figure 1.4: Map of formations that directly subcrop the Knox Unconformity at New York……12
Figure 2.1: Well logs of the Avoca 4 well with top picks and lithologies…….....27
Figure 2.2: Comparison of raw NPHI porosity with NPHI corrected for gas and shale.....31
Figure 2.3: Map of several counties in central and western New York with county lines.....32
Figure 3.1: Map of all wells evaluated for stratigraphic top picks in central and western New York.....39
Figure 3.2.: Structural map of the depth to the top of the shallowest formations above the Galway that directly subcrop the Knox Unconformity.....40
Figure 3.3: Isopach thickness map for Beekmantown Group in central and western New York from wells measured in meters TVD and meters MD.....42
Figure 3.4: Map of wells used for petrophysical analyses in Chapter 3.....44
Figure 3.5: Comparison and regression of Stevenson 1 well GR and corrected NPHI.....48
Figure 3.6: Porosity, permeability and density of Cambrian and Ordovician units encountered in the subsurface at the Miller # 2 well in Jamestown, western NY 50
Figure 3.7: Type log of a well with the Galway Formation informal member names, and log patterns corresponding to those informal members.....53
Figure 3.8: Well logs and informal stratigraphic partitions for the Galway Formation from the Avoca 4 well in Steuben County, central NY.....55
Figure 3.9: Comparison of the Galway Formation member divisions and their associated type logs of this study and Smith et al.'s 2010 report.....56
Figure 3.10: Well logs associated with the Galway Formation at the Auburn Geothermal well.....59
Figure 3.11: Comparison of porosity results for a portion of the Yellowjacket member of the Galway formation from the analyses conducted by Kolkas and Smith et al.....61
Figure 3.12: Air Permeability results of a core section from the Olin [N-650-S] well conducted by Kolkas in 1998.....63

Figure 3.13: Comparison of cuttings porosity analysis conducted by Kolkas (1998) and corrected porosity log at the Mitchell # 1 well.....65
Figure 3.14: N-S cross-section of wells at Avoca, Steuben Country, central NY, flattened at the top of the Potsdam Formation.....67
Figure 3.15: Core plug air permeability of the Potsdam Formation at the Robert Olin 1 (N-650-S) well (API: 31-101-03924-0000), conducted by Kolkas in 1998.....69
Figure 3.16: Logs of the Mitchell 1 and Avoca 4 wells in Steuben County, central NY.....72
Figure 3.17: Corrected log porosity of the Potsdam sandstone from feet at the Mitchell 1 and Avoca 4 wells in Steuben County, central NY.....73
Figure 3.18: Well logs of the Mitchell 3 (M3) well in Steuben County, central NY from the Potsdam to the basement.....75
Figure 3.19: Geologic and isopach map of the Potsdam in the Ottawa Embayment and Quebec Basin.....77
Figure 3.20: Box and whiskers plots of formations of the Beekmantown Groups and their corrected porosities.....79
Figure 3.21: North-South cross-section of wells used for the interpolation of Cambro-Ordovician strata at Cornell's subsurface.....81
Figure 4.1: Comparison of stratigraphy of the Sauk megasequance at central NY with the stratigraphy of the Sauk megasequence in Ohio 87
Figure 4.2: Map of formations that directly subcrop the Knox Unconformity in western and central New York.....89
Figure 4.3: Map of the three wells located in Wyoming County, western New York, and 5 wells used in Steuben County, central New York, for the analyses conducted in this chapter..... 91
Figure 4.4: Histograms of porosity distributions, coupled with porosity versus depth figures, of the wells evaluated in central New York.....93
Figure 4.5: Histograms of porosity distributions, coupled with porosity versus depth figures, of the wells evaluated in western New York.....95
Figure 4.6: Effective porosity of the Yellowjacket member of the Galway for a well in western New York versus a well in central New York.....98
Figure 5.1: Stratigraphic column of expected depths to the Trenton-Black River and Beekmantown Groups in central New York, at Cornell's location.....106

LIST OF ABBREVIATIONS

API	American Petroleum Institute
ESH	Earth Source Heat
ESOGIS	Empire State Organized Geologic Information System
FLOW	Flowmeter
GR	Gamma Ray
LLS	Shallow laterolog
LLD	Deep laterolog
M1	Mitchell 1
M3	Mitchell 3
md	millidarcy
MD	Measured Depth
NPHI	Neutron Porosity Hydrogen Index
NY	New York
PEF(Z)	Photoelectric Factor
POTA	Potassium
RHOB	Density
SSTVD	Sub-Sea True Vertical Depth
TVD	True Vertical Depth

LIST OF SYMBOLS

Φ_d	Density Porosity
Φ_{cn}	Corrected Neutron Porosity
Φ_n	Neutron Porosity
Φ_{sh}	Neutron Porosity of Shale
ρ_b	Bulk Density
ρ_d	Matrix density of dolomite
ρ_f	Fluid Density
ρ_l	Matrix density of limestone
ρ_{ma}	Matrix Density
ρ_s	Matrix density of sandstone
γ_{log}	GR response in zone of interest
γ_0	GR response in the cleanest formations
γ_{100}	GR response in shales or zones of high radioactive decay
I_{sh}	Shale Index
P_e	Photoelectric Absorption Factor
V_{sh}	Shale Volume

CHAPTER 1:

INTRODUCTION

1.1 Background and Motivation:

Earth has a vast amount of geothermal resources with the potential to sustainably provide clean and affordable heat and/or electricity in a variety of regimes worldwide (Axelson, 2010; Beckers et al., 2014). Sedimentary basins, which are commonly explored for hydrocarbon production, also have potential for deep (> 1 km) geothermal exploration because they are widespread and have reasonable geothermal gradients (e.g., Aguirre, 2014; Stutz et al, 2015; Smith, 2016; Camp, 2017). Studies examining the possibility for geothermal production in the Appalachian basin have repurposed tools and data from existing oil and gas exploration wells for geothermal field evaluations. These studies reveal that although temperatures in the Appalachian Basin are much less than is ideal for electric power production, low temperature (<100°C) geothermal heat production at economic depths of less than 4 km is feasible (e.g., Black, 1979; Hendry et al., 1982; Hodge and Fromm,1984; Hodge, 1996; Blackwell et al., 2011; Shope, 2012; Jordan et al., 2016; Stutz et al., 2015; Smith, 2016).

Cornell University is located in Northeast United States in the Appalachian Basin, which is a cold-climate area with high heat demand. In September 2013, Cornell University faculty, staff and students developed a detailed plan to reach its goal of becoming carbon-neutral by 2035, titled the Climate Action Plan (Cornell University, 2013). Subsequent analyses of options by which to help the university reach this goal identified geothermal energy as a potential important energy source, leading to an endeavor titled Earth Source Heat (ESH). The aim is to explore and develop direct-use geothermal production to circulate heat for a campus of 30,000 people in 14 million square feet of buildings that annually consume ~240,000 MW_{th}-hrs of heat

(Gustafson et al., 2018). Currently, research needed to assess ESH advances through a project funded by the Department of Energy. Since no wells have been drilled yet at the Ithaca campus of the university, the project is in the data gathering and analysis phase in which existing well data from oil, gas, and other companies, provided by the New York State Museum's Empire State Organized Geologic Information System (ESOGIS), is repurposed for geothermal assessment (Camp and Jordan, 2017).

In 2017, a low-temperature geothermal play fairway analysis was reported for the Appalachian Basin. The quantitative analysis assessed utilization and potential geological risks to create Play maps with the use of data from existing wells in the entire basin. Results of the play fairway indicate Cornell's area in Ithaca, NY, is located in one of the most favorable play fairways in the Appalachian (Figure 1.1) (Cornell University, 2017).

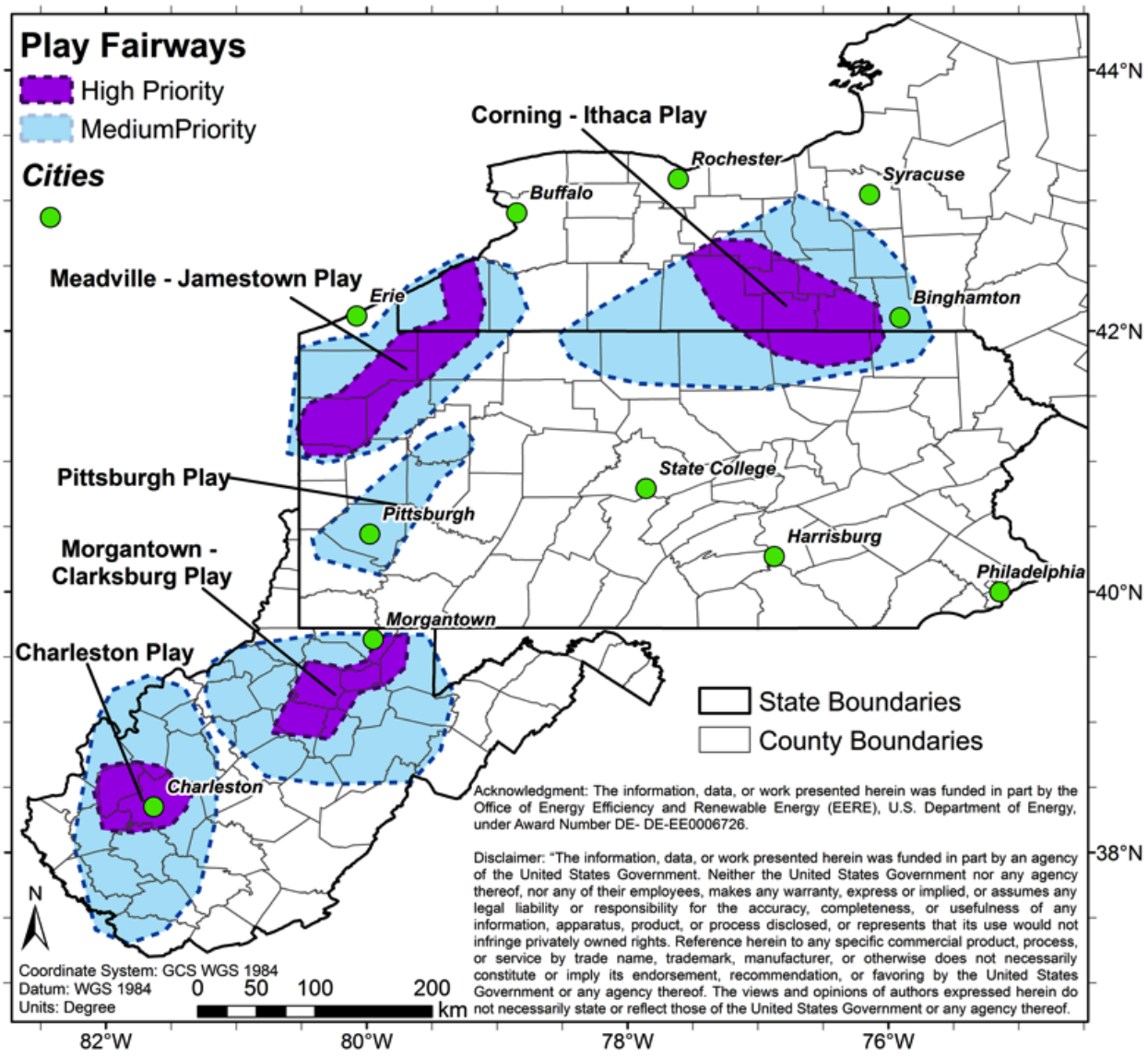

Figure 1.1: The most favorable Play Fairways in the Appalachian Basin. Cornell's location in Ithaca is indicated as 'High Priority' (for further investigation) at the Corning-Ithaca Play (Cornell University, 2017).

The goal of this thesis is to apply stratigraphic principles to the analysis and interpretation of petrophysical parameters, to enable assessment of the suitability of the sedimentary layers beneath Cornell for geothermal production. The analysis utilizes the subsurface data available near the Cornell University Ithaca campus in central New York (NY). The subsurface strata of interest range from 2.3 to 3.0 km in depth, which have been determined in previous studies to be depths with suitable temperatures (>70 °C) for low-temperature geothermal heating (Jordan et al., 2016). Limestones, dolostones, and sandstones are commonly found at these depths and overlie the Precambrian Grenville basement rock at near 3.0 km depth.

1.2 Tectonic and Paleogeographic Setting

Approximately 1.0 billion years ago, at the final stage of the assembly of the Rodinia supercontinent, the metamorphic and igneous basement of New York was formed by the continent-continent collisional events of the Grenville Orogeny**.** Rodinia began to rift during the late Precambrian (~620 Ma) and formed the Laurentia paleocontinent, which contained the continental crust of what is presently New York. Due to the rifting, New York's location in Laurentia was situated on a promontory that received little to no sediment during the Neoproterozoic to the Late Cambrian, or from ~1.0 Ga to ~510 Ma. As a result, an extensive unconformity of roughly 200 million years duration occurred between the time of the Grenville Orogeny and the deposition of the first sediments in New York approximately 510 Ma.

At around 615 Ma, a shallow tropical ocean known as the Iapetus Ocean emerged on the eastern margin of Rodinia as it began to rift from Gondwana. Much later, New York began to develop a carbonate bank as deposition started in a passive margin basin (O'Brien and van der

Pluijm, 2012). New York's location at the time was south of the equator on a passive margin facing the Iapetus Ocean (Hatcher, 2010).

Approximately 490 million years ago, near the Cambrian-Ordovician boundary, the tectonic setting shifted from a passive margin to that of an active margin as the continents began to drift back toward each other and the nearby Taconic Island Arc began to subduct beneath Laurentia (Figure 1.2). The collision of the island arc with Laurentia ~450 Ma was at a time of active tectonism and mountain building known as the Taconic Orogeny (Sloss, 1963; Fisher, 1977). The collision of the Taconic Island Arc with Laurentia triggered block faulting and tilting across the region. This resulted in the uplift of the western region of New York and subsidence of the eastern end further beneath the Iapetus Ocean. The Cambrian-lower Ordovician strata are mostly attributed to post-rift subsidence (Wise and Ganis, 2009). The transtensional tectonics of the Taconic Orogeny led to the formation of grabens and fractures that later became dolomitized by several stages of hydrothermal fluids posited to originate from the basement (Rasmussen et al., 2003; Slater and Smith, 2012). The Appalachian Basin, an elongate flexural foreland basin with a shallow inland sea, was formed by tectonic loading that began with the Taconic Orogeny and spanned the interval from the Ordovician through the Carboniferous in New York (Hatcher, 2010). In sequential order, the shift to an active margin gave rise to the following orogenic events: the Taconic Orogeny during the Middle Ordovician, the Acadian Orogeny in the Middle Devonian, and the Alleghenian (Appalachian) Orogeny spanning the Late Carboniferous to Permian.

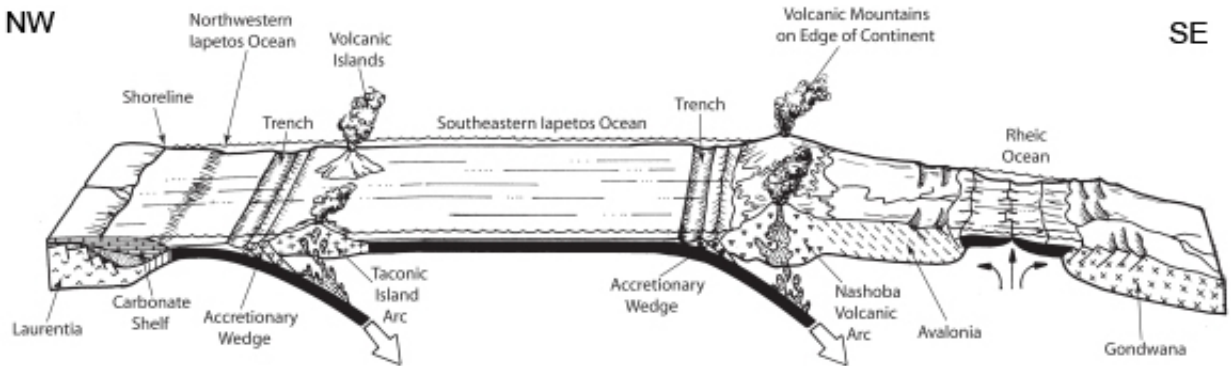

Figure 1.2: A depiction of the rifted margin of Laurentia (present day New York) to the left and Gondwana to the right, with the Iapetus Ocean between, during the early Ordovician. The Taconic Island Arc formed in the middle of the ocean and began to subduct and later collide with Laurentia, which initiated the Taconic Orogeny (image from Coleman, 2005).

Sea level rise during the time of the Acadian Orogeny, combined with sediment erosion from remnants of the Taconic Orogeny, contributed to sediment loading and compaction of the underlying Cambrian, Ordovician, and Silurian strata. Deposition continued into the Carboniferous and Permian periods, when the formation of the Appalachian Mountains (~300-250 Ma) caused further southward inclination of sediments as well as the formation of joints and faults (Rickard, 1973). The Alleghenian Orogeny is the cause for the regression of the sea from the Appalachian Basin and, in part, the formation of the supercontinent Pangaea (Hatcher, 2010). Roughly coeval to the end of the Alleghenian Orogeny in the Late Permian (250 Ma) was a global ice age originating from the South Pole that caused sea levels to drastically fall (Knoll et al., 1997). Both of these events initiated extensive erosion of Carboniferous and Permian sediments, which persisted regionally until the glaciations of the Late Cenozoic. The net result over the approximately 260 million years of erosion since the Alleghenian Orogeny was the loss of 3-4 kilometers thickness of strata in central NY (Miller and Duddy, 1989). Currently, the only preserved strata underlying the Quaternary ice age deposits in central New York's subsurface originated during the Paleozoic.

The tectonic events described in this thesis are not an exhaustive list. However, the list highlights the most important regional structural controls on the porosity, permeability, compaction, depths, thicknesses, and geographic spread of the Cambro-Ordovician sediments examined in this thesis, all of which contribute to reservoir quality.

1.3 Stratigraphic Setting

A previous study by Camp in 2017 was conducted on the feasibility of the Upper Ordovician Trenton-Black River Group limestones and dolostones as reservoirs for geothermal

production. This thesis focuses on the underlying Upper Cambrian and Lower Ordovician strata found in target depths of ~2.3-3 km in central New York: the Potsdam, Galway, Little Falls and Tribes Hill Formations (Figure 1.3). Together, these formations are a part of the succession of the Sauk megasequence in New York State. The Sauk megasequence includes all strata below the Knox Unconformity, which is at the base of the Black River Group in central New York, and above the nonconformity cut on the Precambrian basement (eg. Sloss, 1977; Haq et al, 1988; Fisher, 1977). The nomenclature 'Beekmantown Group' is used variably to either include all sedimentary formations below the Knox Unconformity in central NY, or to include all but the Potsdam Sandstone. This thesis will adopt the former usage. Henceforth in this study, the Potsdam Formation is included in the Beekmantown Group.

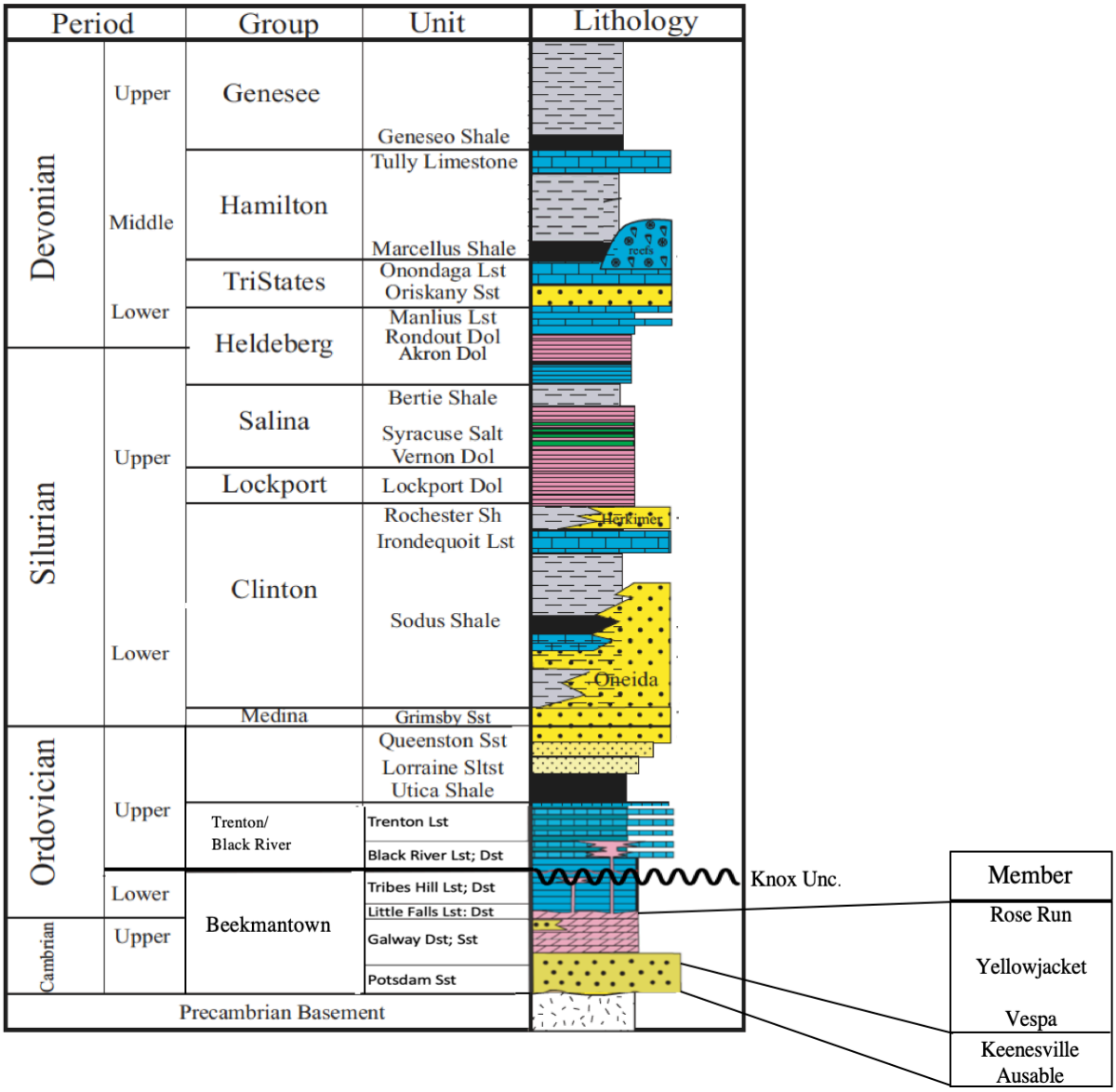

Figure 1.3: Stratigraphic succession in the subsurface of Central New York, from Precambrian to Devonian (modified from Smith et al., 2010). Cambrian and Ordovician units and the members depicted here are modified, while the Silurian and Devonian units have not been changed from Smith et al., 2010. Lst represents limestone, Dst represents dolostone/dolomite, Sst represents sandstone, Sh represents shale, and Unc. represents an unconformity. To the right are informal members of the Galway in Chapters 3 and 4, and formal members of the Potsdam Formations discussed in this thesis.

A Cambro-Ordovician terrestrial-to-shelf sequence onlapped the Precambrian basement, starting at ~510 Ma. Because the Upper Cambrian to Lower Ordovician Potsdam Sandstone represents the earliest onlap of autochthonous rocks, the distribution and physical characteristics of the Potsdam Sandstone are largely influenced by the geometry of the erosional surface of the underlying basement rock (Selleck, 1997). The Potsdam has two subdivisions: the basal non-marine Ausable Member arkosic sandstone and conglomerate, and the upper marine Keenesville Member quartz arenite. A thin layer of subaerial terrigenous detritus that unconformably overlies the basement is discontinuously present in the subsurface today. This material is originally called 'granitic wash' or 'feldspar wash' (Fisher, 1997). The basal Ausable member may be what is referred to as the 'feldspar wash,' and is assumed to be so in this study. It was postulated to have originated from the accumulation of eroded granite in rift basins during the late Proterozoic.

The Potsdam is overlain by the Upper Cambrian Galway Formation, which is made up of interbedded dolomite and sandstone facies deposited in a shallow marine environment. The lowermost portion of the Galway is mainly sandstones, while the middle consists of interbedded dolomite and sandstone, and the top consists of clean arenitic sandstone, known as the Rose Run member. The Rose Run member is equivalent to the Rose Run Formation in Ohio, where it is a prolific gas reservoir, which implies that it possesses significant permeability (Smith et al., 2010). This member is depicted as the yellow piece at the top of the Galway formation in Figure 1.3.

The uppermost portion of the Galway Formation grades in to the limestones of the Upper Cambrian Little Falls Formation. Some occurrences of interbedded dolomite and shale exist in the Little Falls, as well as small amounts of sandstone and siltstone (Kreidler, 1975). Overlying

the Little Falls is the Lower Ordovician Tribes Hill Formation, which contains shaly limestone or dolostone (Smith et al., 2010).

After the deposition of the Tribes Hill Formation in central New York, sea level fell sharply and exposed New York to subaerial erosion, producing the Knox Unconformity. In the subsurface, the unconformity cuts progressively deeper into the strata to the west and north, so that in the southeast it overlies the Lower Ordovician Rochdale Formation and in the northwest it directly overlies the Proterozoic basement (Figure 1.4). At Cornell University's location in Ithaca, Tompkins County, central New York, the Knox Unconformity overlies the Tribes Hill Formation (Smith, 2012).

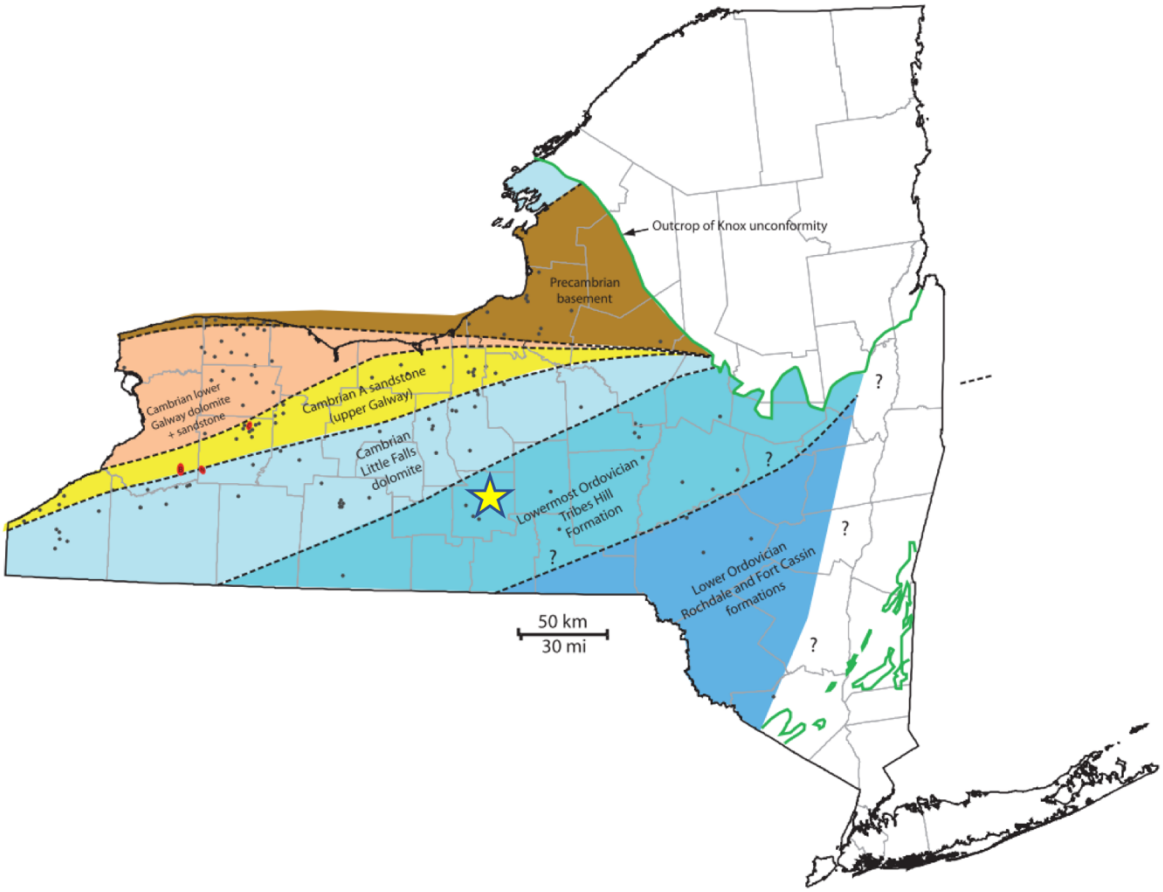

Figure 1.4: Map of formations that directly subcrop the Knox Unconformity (from Smith et al., 2010). The location of Cornell University is marked by the yellow star. Black dots denote wells used by Smith et al. (2010) to create the map, and dashed lines delineate interpreted boundaries between lowermost formations.

1.4: Objectives

There is reservoir potential in all pre-Knox Unconformity sedimentary layers. Historically, the Potsdam Formation was a producer of gas in New York until 2008. There is also reservoir potential in the Galway and Little Falls formations, which have been gas producers since 1991 and 2000, respectively (data acquired from New York State Department of Environmental Conservation at www.dec.ny.gov, 2019). As a zone of interest for brine and liquid disposal as well as gas storage, the Beekmantown Group has been researched on the basis of reservoir quality (e.g. Smith et al., 2005; Lugert et al., 2006; Kolkas, 1998; Bass et al., 1996, Guo et al., 1996; McCann et al., 1968); Based on these studies and reports that the Potsdam, Galway and Little Falls formations are expected to yield zones of favorable reservoir quality in the Beekmantown Group of central New York, in order of highest to lowest potential.

To assess their suitability as reservoirs for low-temperature geothermal production, well logs, cuttings and permeability reports from 78 existing exploration and production wells in western and central New York, archived by ESOGIS, are used for petrophysical and stratigraphic evaluation. Parameters of the assessment include determining for potential reservoirs their depths, thicknesses, lithologies and porosity, as well as reviewing published permeability data. These evaluations are coupled with analyses of paleogeomorphic and structural features that, if present, may affect the quality and distribution of the potential reservoirs. In particular, the following will be tested to analyze reservoir quality:

1) The interval from the Knox Unconformity to the bottom of the Little Falls Formation: Does the erosional effect of the Knox Unconformity increase porosity?
2) Which interval in the Beekmantown Group seems to have the best reservoir quality?

REFERENCES

Aguirre, G.A., 2014, Geothermal resource assessment: A case study of spatial variability and uncertainty analysis for the states of New York and Pennsylvania. MS Thesis. Cornell University, Ithaca, NY.

Allaz, J., Selleck, B., Williams, M.L., and Jercinovic, M.J., 2013, Microprobe analysis and dating of monazite from the Potsdam Formation, New York: A progressive record of chemical reaction and fluid interaction: American Mineralogist, v. 98, p. 1106–1119.

Axelsson, G., 2010, Sustainable geothermal utilization–Case histories; definitions; research issues and modelling. Geothermics, *39*(4), pp.283-291.

Bass, J.P., Sarwar, G., Guo, B. and Friedman, G.M., A preliminary assessment of suitable site for new high-deliverability salt-cavern storage facilities in south central New York. Northeastern Geology and Environmental Sciences, v. 18., pp. 36-48.

Blackwell, D., Richards, M., Frone, Z., Ruzo, A., Dingwall, R., and Williams, M., 2011, Temperature-at-depth maps for the conterminous US and geothermal resource estimates: Geothermal Resource Council Transactions, v. 35, p. 1545-1550.

Beckers, K.F., Lukawski, M.Z., Anderson, B.J., Moore, M.C., and Tester, J.W., 2014, Levelized costs of electricity and direct-use heat from Enhanced Geothermal Systems: Journal of Renewable and Sustainable Energy, v. 6, no. 1, 013141 p.

Camp, E.,R. 2017, Repurposing petroleum reservoirs for geothermal energy: a case study of the Appalachian basin. PhD Dissertation. Cornell University, Ithaca, NY.

Camp, E.R., and Jordan, T.E., 2017, Feasibility study of repurposing Trenton–Black River gas fields for geothermal heat extraction, southern New York. Geosphere; 13 (1): 22–35. doi: https://doi.org/10.1130/GES01230.1

Cornell University, 2013, 2013 Climate Action Plan update & roadmap 2014-2015.

Coleman, M.E., 2005, State geological and natural history survey of Connecticut. Special Publication no. 2. Hartford, CT U.S.A.: Connecticut Department of Environmental Protection

Cornell University, 2017, Final Report: Low Temperature Geothermal Play Fairway Analysis for the Appalachian Basin. Retrieved from https://gdr.openei.org/submissions/899

Fisher, D.W., 1977, Correlation of the Hadrynian, Cambrian and Ordovician rocks in New York State: New York State Museum Map and Chart Series No. 25, 75 p.

Gustafson, J.O., Smith, J.D., Beyers, S.M., Al Aswad, J.A., Jordan, T.E., and Tester, J.W., 2018, Earth Source Heat: Feasibility of deep direct use of geothermal energy on the Cornell campus, GRC Transactions, vol. 42.

Guo, B., Friedman, G.M., Bass, J.P., and Sarwar, G., 1996, Underground gas storage in the Cambro-Ordovician succession of Southeastern New York: A preliminary study. Northeastern Geology and Environmental Sciences, v. 18, pp. 49-58.

Harris, D.C. and Baranoski, M.T., 1996, Play Cpk: Cambrian pre-Knox group play, in Roen, J.B. and Walker B.J. eds. The atlas of Appalachian gas plays, West Virginia Geological and Economic Surver Publication V-25, Morgantown, pp. 188-192.

Hatcher, R. D., Jr., 2010, The Appalachian orogen: A brief summary, *in* Tollo, R. P. Bartholomew, M. J., Hibbard, J. P., and Karabinos, P. M., eds., From Rodinia to Pangea: The lithotectonic record of the Appalachian region: Boulder, Colorado, Geological Society of America Memoir 206, p. 1–19.

Haq, B. U., J. Hardenbol, and P. R. Vail, 1988, Mesozoic and Cenozoic chronostratigraphy and cycles of sealevel change, in C. K. Wilgus, B. S. Hastings, C. G. St. C. Kendall, H. W.

Posamentier, C. A. Ross, and J. C. Van Wagoner, eds., Sealevel changes: An integrated approach: SEPM Special Publication 42, p. 71 – 108

Hatcher, R. D., Jr. , 2010, The Appalachian orogen: A brief summary, in From Rodinia to Pangea: The Lithotectonic Record of the Appalachian Region, Geological Society of America Memoir 206, edited by R. P. Tollo et al., pp. 1–19, GSA, Boulder, CO

Hodge, D.S., 1996, Assessing geothermal energy potential in upstate New York. Final report: New York State Energy Research and Development Authority, 197 p.

Hodge, D.S., and Fromm, K., 1984, Heat flow and subsurface temperature distributions in central and western New York. Final report, New York State Energy Research and Development Authority, 217 p.

Hornbach, M., Frone, Z., Ferguson, C., Bolat, R., and Magnani, M.B., 2016, Low-Temperature geothermal play fairway analysis for the Appalachian basin, Geothermal Data Repository, https://gdr.openei.org/submissions/638.

Husinec, A., and Donaldson, J.A., 2014, Lower Paleozoic Sedimentary Succession of the St. Lawrence River Valley, New York and Ontario: Field Trip A-1, *in* Chiarenzelli, J., and Valentino, D., eds., Geology of the Northwestern Adirondacks and St. Lawrence River Valley, p. A1 – A28

Isachsen Y.W., Landing, E., Lauber, J.M., Rickard, L.V., and Rogers, W.B., 2000, Geology of New York: a simplified account, 2nd edn. New York State Museum, Albany

Jacobi, R. D. and Fountain, J.C, 2002, The character and reactivation history of the of the southern extension of the seismically active Clarendon-Linden Fault System, western New York State, in Neotectonics and Seismicity in the Eastern Great Lakes Basin, R. H. Fakundiny, R. D. Jacobi, and C. F. M. Lewis (eds.): Tectonophysics, v. 353, p. 215-262.

Jordan, T., Camp, E., Smith, J., Whealton, C., Horowitz, F. G., Stedinger, J. R., Tester, J. W., Richards, M., Frone, Z., Bolat, R., Hornbach, M., Chickering Pace, C., Magnani, B., Anderson, B., He, X., and Welcker, K., 2016, Low-Temperature Geothermal Play Fairway Analysis for the Appalachian Basin , in Proceedings, 41st Workshop on Geothermal Reservoir Engineering: Stanford, California, Stanford University, 11 p.

Kolkas, M. M., 1998, Subsurface brine disposal in the Sauk Sequence of central and western New York: Implications for new salt cavern gas-storage reservoirs. PhD dissertation. The City University of New York, New York City, New York.

Knoll A.H., Bambach R.K., Canfield D.E., Grotzinger J.P., 1997, Comparative Earth history and Late Permian mass extinction. Science, Volume 273, p. 452–457

Kreidler, W.L., 1975, Underground Disposal of Liquid Wastes in New York. New York State Museum and Science Service, Map and Chart Series, no. 26.

Landing, E., 2007, Ediacaran-Ordovician of East Laurentia-Geologic setting and Controls on Deposition Along the New York Promontory Region, New York State Museum Bulletin 510, p. 5-24.

Landing, E., 2012, The Great American Carbonate Bank in Eastern Laurentia: Its Births, Deaths, and Linkage to Paleooceanic Oxygenation (Early Cambrian-Late Ordovician), *in* J. R. Derby, R. D. Fritz, S. D. Longacre, W. A. Morgan, and C. A. Sternbach (Eds.), The Great American Carbonate Bank: The Geology and Economic Resources of the Cambrian: AAPG Memoir 98, p. 451-492.

Lugert, C., Smith, L., and Nyahay, R., 2006, Systematic technical innovations initiative: Brine disposal in the Northeast. Final Report. Albany, NY, New York State Energy Research and Development Authority, 269 p.

McCann, T.P., Privrasky, N.C., Stead, F.L., Wilson, J. E., 1968, Possibilities of disposal of industrial wastes in the subsurface rocks on north flank of Appalachian Basin in New York: AAPG Special Volumes, no.10, p. 43-92

Miller, D., 1989, Early Cretaceous uplift and erosion of the northern Appalachian Basin, New York, based on apatite fission track analysis, Earth and Planetary Science Letters, Volume 93, no.1, p. 35

O'Brien, T.M., and van der Pluijm, B.A., 2012, Timing of Iapetus Ocean rifting from Ar geochronology of psuedotachylytes in the St. Lawrence rift system of southern Quebec: Geology, v. 40, p. 443-446

Rasmussen, J.C., Keith, S.B., Swan, M.M., Laux, D.P., and Caprara, J., 2003, Strikeslip faulting and reservoir development in New York State: Albany, New York, New York State Energy Research and Development Authority.

Rickard, L. V., 1973, Stratigraphy and structure of the subsurface Cambrian and Ordovician carbonates of New York : New York State Museum and Science Service, Map and Chart Series 18, 26 p.

Selleck, B., 1997, Fluid-basement interaction at the Proterozoic-Paleozoic unconformity, Adirondack periphery, New York State; Abstracts with Programs, Geological Society of America, 29, 1, p. 48

Shope, E.N., 2012, A detailed approach to low-grade geothermal resources in the Appalachian Basin of New York and Pennsylvania: Heterogeneities within the geologic model and their effect on geothermal resource assessment. MS Thesis. Cornell University, Ithaca, NY.

Smith, L., Lugert, C., Bauer, S., Ehgartner, B., and Nyahay, R., 2005, Systematic technical innovations initiative brine disposal in the Northeast: Final report: Albany, NY, New York State Energy Research and Development Authority, 271 p.

Smith, L., 2006, Origin and Reservoir Characteristics of Upper Ordovician Trenton-Black River Hydrothermal Dolomite Reservoirs in New York, USA: AAPG Bulletin 90, no.11, p. 1691 - 1718.

Smith, L., Nyahay, R., and Slater, B., 2010, Integrated Reservoir Characterization of the Subsurface Cambrian and Lower Ordovician Potsdam, Galway and Theresa Formations in New York: Albany, NY, New York State Energy Research and Development Authority, 69 p.

Smith Jr., L.B., 2012, Great American carbonate bank subsurface stratigraphy in the northern Appalachian Basin, New York state, *in* J. R. Derby, R. D. Fritz, S. A Longacre, W. A. Morgan, and C. A. Sternbach, eds., The great American carbonate bank: The geology and economic resources of the Cambrian–Ordovician Sauk megasequence of Laurentia: AAPG Memoir 98, p. 1195–1206.

Smith, J.S., 2016, Repurposing petroleum reservoirs for geothermal energy: a case study of the Appalachian basin. M.S. Thesis. Cornell University, N.Y.

Slater, B.E., 2007, Outcrop analog for lower Paleozoic hydrothermal dolomite reservoirs, Mohawk Valley, NY, 105 p.

Sloss, L.L., 1963, Sequences of the Cratonic Interior of North America: Geological Society of America Bulletin, v. 74, p. 93-114.

Stutz, G., Shope, E., Aguirre,G., Batir, J., Frone,Z., Williams, M., Reber, T., Whealton, C., Smith, J., Richards, M., Blackwell, D., Tester, J., Stedinger, J., and Jordan, T., 2015,

Geothermal energy characterization in the Appalachian Basin of New York and Pennsylvania. Geosphere 11(5). p. 1291 - 1304.

Thomas, W.A., 2006, Tectonic inheritance at a continental margin: GSA Today, v. 16, no. 2, p. 4–11, doi: 10.1130/1052-5173(2006)016[4:TIAACM]2.0.CO;2

Wise, D.U., and Ganis, G.R., 2009, Taconic orogeny in Pennsylvania: A~ 15–20 my Apennine-style Ordovician event viewed from its Martic hinterland: Journal of Structural Geology, v. 31, p. 887–899

Whitney, P., and Davin, M., 1987, Taconic deformation and metasomatism in Proterozoic rocks of the easternmost Adirondacks; Geology, 15; p. 500-503.

CHAPTER 2:

DATA AND METHODS

2.1 Log Data Acquisition

Most data from the 78 wells examined in this study were collected from the New York State Museum and its ESOGIS online database (ESOGIS, New York State Museum, 2019). These 78 wells are chosen because they reach depths that penetrate the formations that subcrop the Knox Unconformity, and because a raster image or digital Gamma Ray (GR) log well cuttings used for petrophysical analysis is available. The logs and cuttings were either provided by the New York State Museum or donated by Gerald M. Friedman. Since wells are usually named for the landowner, several wells can have the same names and/or change their names, and an industry standard was created in the United States to assign wells an American Petroleum Institute (API) number. The API well number is a unique identifier with up to 14 digits divided by dashes. For example, an imaginary well in Tompkins County, New York can be identified with the imaginary API '31-109-11111-0000'. The first two digits, '31', refer to the state code for NY. The next three digits '109,' mean that the well is located in 'County Code' 109, or Tompkins County. The following five digits are referred to as a 'Unique Well Identifier,' and the final four digits refer to whether the well has been sidetracked and the amount of operations that took place (American Petroleum Institute, 1979).

The digital well data available in ESOGIS include well API numbers, well names, surface longitudes and latitudes, total vertical depths, producing formations, and digitized and raster well logs.

2.2 Well Logs

Logging tools record the magnitude of physical, chemical, electrical and other properties of the subsurface as they traverse the borehole. They are presented as detailed plots of parameters of rocks versus depth. Individual logging tools record specific properties of the subsurface as they run down the wireline. From these logs, interpretations are made to identify lithologies, porosity amount, fluid compositions, and pay zones, in addition to specialized information**.** In an ideal situation, myriad well logs are used in conjunction with each other to lower the uncertainty of the geologists' interpretations. However, because these tools are very expensive it is common that a well will only have one or very few logging tools used. For this thesis, the four important well logs used for identifying lithological changes and porosity analysis are the Gamma Ray (GR), Neutron Porosity Hydrogen Index (NPHI), Density (RHOB), and Photoelectric Factor (PEF) logs.

The GR log, which is the most common logging tool used in New York, is used to passively measure the natural radioactive decay of uranium (U), thorium (Th), and potassium (K); from the GR values lithologies are identified and boundaries between intervals of differing lithologies are recognized. Elevated levels of radioactive decay of these elements indicate zones of clays, volcanic ashes, igneous and metamorphic rocks, and feldspathic sandstones. As the amount of radioactive decay of U, Th, and K increases, the GR log response increases. Due to the range of different types of tools used to measure GR, the numerical values of radioactive decay recorded may differ. For example, one log may measure radioactive decay on a scale from 0-200, while another may measure it from 0-150. For wells in western and central NY, "clean" (shale-free) formations typically are represented by very low GR readings, while shaly formations or sandstone with feldspars have the highest GR readings. A weakness of the typical

GR log is the inability to separate whether the increase in radioactivity is due to the presence of U, Th, or K. A Spectral GR log, which is much less commonly deployed than a GR log in NY, divides the gamma wavelengths into different bins, and is able to differentiate the source of radioactivity.

The NPHI log is one of three log types used to determine porosity, the others being sonic-porosity and density-porosity logs. Of importance to this study are the neutron-porosity (NPHI) and density-porosity logs, since the sonic-porosity log is not as commonly used in NY's deep subsurface. Density-porosity logs are also uncommon, but a conversion can be made of the more readily available density logs (RHOB) to calculate density-porosity. This conversion is further discussed in Chapter 2.3.

NPHI logs bombard formations with high-energy neutrons and measure the neutron's energy loss. Since the hydrogen atom is almost equal in size to a neutron, maximum energy loss occurs when a neutron collides with a hydrogen atom. Neutron loss is used as a proxy for porosity on the assumption that fluids in pores contain hydrogen whereas minerals do not. The NPHI log is calibrated to the specific amount of neutron energy loss that would occur if water is the pore fluid. Thus, in a case where gas is encountered, porosity is misrepresented as a lower number, and can often be negative due to the inappropriate calibration. Contrarily, the hydrogen-oxygen bonds found between layers of shale result in an inflated report of neutron porosity. Corrections for the effect of gas and shale on the NPHI log require the use of other logs such as the GR and density logs and are discussed in greater detail in Chapter 2.5.

RHOB logs measure the density of electrons in a formation. The tool actively emits gamma rays that collide with electrons in the formation and scatter. A detector located at a fixed

distance from the gamma ray source then counts the loss of energy of gamma rays that return and uses the amount as a proxy for density (Asquith, 1982).

The PEF tool, sometimes known as the litho-density tool, measures the photoelectric factor, P_e, from the photoelectric absorption of gamma rays. This tool is used to identify lithologies more precisely than is possible with natural gamma ray measurements (Bassiouni, 1994). Sandstone corresponds to PEF of around 2 barns/electrons or less, limestones are determined by PEF of around 4 barns/electrons or more, and dolomites correspond to around 3 barns/electrons. Shale, gases, or anhydrite are difficult to identify with this log because of their high range of possible PEF readings, so the PEF log is not used for them.

Resistivity logs examined in this study (LLS - shallow laterlog, and LLD – deep laterolog) measure the formation's resistivity in ohm.m^2/m. Typically, rocks are insulators, while gas and water are not. Therefore, formations with no fluids will have no resistivity, and hydrocarbons have high resistivity. Water presence is indicated by low resistivity.

The most important of the logs are the GR log for picking formation boundaries, and the NPHI log for porosity calculations. However, both logs require modifications to decrease uncertainty and the effect of gas or shales on the measurements.

2.3 Gamma Ray Log Normalization

A normalized GR range is necessary for assessments of radioactivity levels or shale content across multiple wells. This is especially important when the ranges used by operators during the recording of these GR logs differ. Digitized GR logs are normalized to a range of 0 – 200, in which the well-specific minimum recorded radioactivity is normalized to 0 and maximum values are normalized to 200. This is done using the IHS Markit Petra Software: GR logs from

all wells are normalized on a high-low scale range, which stretches or compresses the GR log curves to a common range. Thus, the maximum and minimum level of radioactive decay has been standardized across all wells. The normalization of the GR logs makes it possible to calculate the shale index and shale volume, which are necessary for correcting NPHI logs. In the case when the GR log is not digitized, and therefore not normalized, the patterns of the GR log deflections are observed in raster images. Teresa E. Jordan provided the digitized image of the Shepard 1 well log for normalization and top picking conducted in this study.

2.4 Picking Formation Tops and True Vertical Depth

The normalized GR logs make it possible to analyze GR patterns of multiple wells at various locations in NY. The GR log is often used for the interpretation of stratigraphic tops. The tops of formations picked in this study follow the GR signals for formation tops picked by Rickard (1973) and Smith et al. (2010).

Some top picks in this thesis do not conform to those picked by previous geologists. This is the case when tops picked in this study differ due to observations from well cuttings. An example of such a situation is when observing the top of the Potsdam Formation sandstones, which is often difficult to separate using GR from the overlying Galway's basal sandstone member. This is explored in Chapter 4 with the Shepard 1 well.

To increase the accuracy of the top picks, measurements at wells that are not vertical are corrected and depths are reported in True Vertical Depth (TVD). These deviated wells are indicated on the ESOGIS database, as well as from reports conducted by the drillers. A log of deviations, the depth at which the well is deviated and often the amount of deviation is typically available from ESOGIS. Any deviated wells are corrected via the Petra software, which corrects

for TVD using this information from the drillers and displays the deviation of the wellbore as a visualization of how deviated the well is. Using Petra, data points are adjusted from measured depth to TVD. Surface elevation is variable across the study area. Since the elevation of each well's location is also known, the Sub-Sea True Vertical Depth (SSTVD) is also calculated to account for the effect of the altitude. With TVD or SSTVD, stratigraphic tops are more accurately picked across all of western and central NY. All top picks for the wells observed are attached in Appendix A**.**

2.5 Corrections for Shale and Gas Effects in Neutron Logs

GR, NPHI, and density logs are used to correct the porosity log of each well for lithology and presence of gas and shale (Figure 2.1). If the PEF log is also available, the uncertainty associated with lithology determination is decreased. The lithology type has a large effect on the calculations, as matrix densities are central to several key components of the corrections and recorded porosity. The MATLAB code (Appendix B) for the calculations below is modified from Camp (2017) and uses equations from Bassiouni (1994). A weakness of the correction is in the assumption that increased radioactivity recorded by the GR log corresponds to shales. When examining the porosity of a feldspathic sandstone, for example, the shale correction does not work, because the GR log does not differentiate whether the increase in radioactivity due to the presence of shale or orthoclase. Treatment of orthoclase as if it is shale causes erroneous results. Therefore, when any indication of potassium is observed, shale corrections are either not employed or the entire unit is removed from calculation.

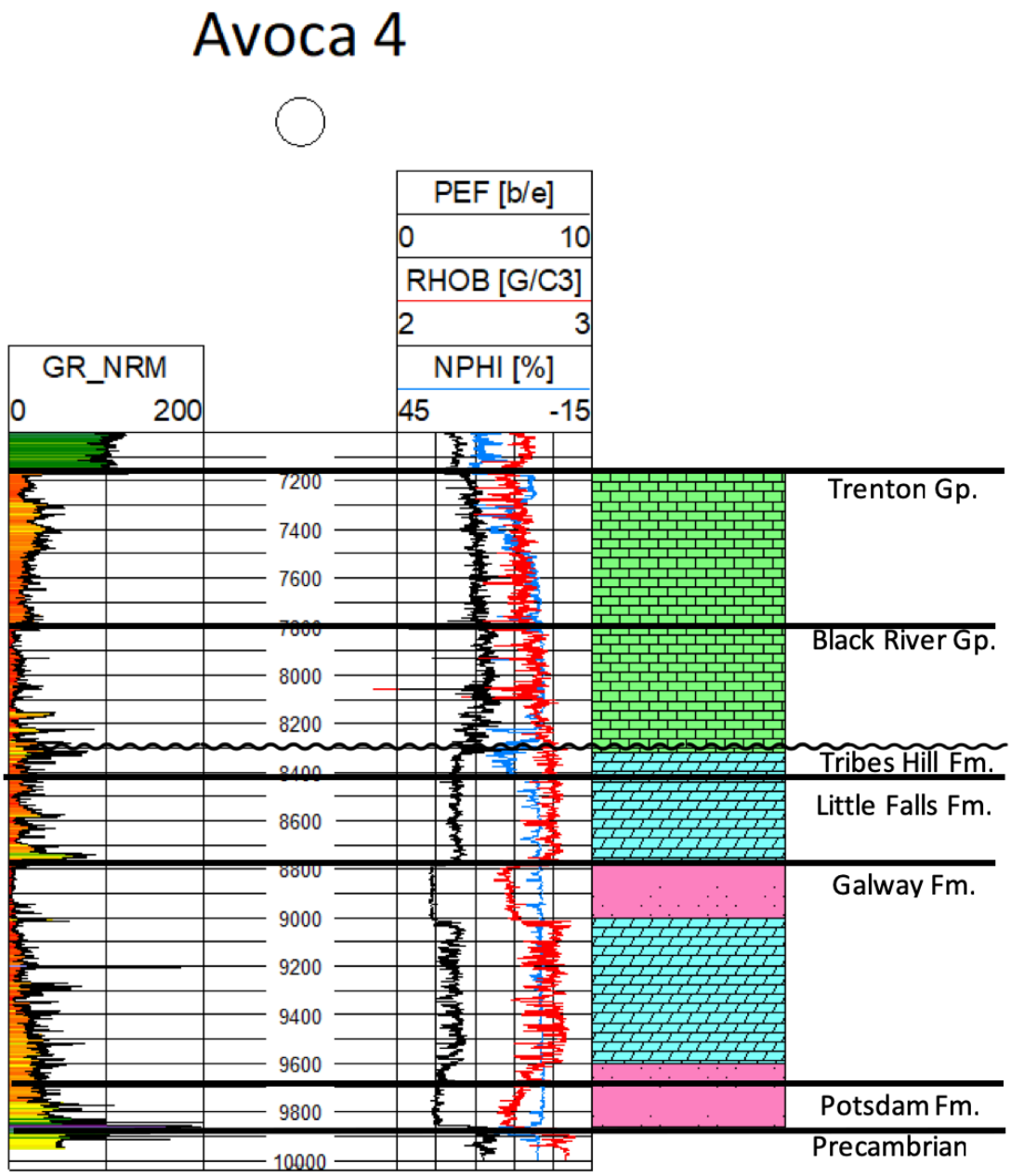

Figure 2.1: A well log example, utilizing the Avoca 4 well in central NY (Figure 2.3). The GR, NPHI, density, and PEF logs are required to correct the NPHI log for gas and shale presence. On the first (leftmost) track is the GR log normalized to a range of 0-200. Measured depths below surface are in feet. The second log track displays the NPHI log in blue, RHOB log in red, and PEF log in black. Porosity values increase to the left, which is conventionally done to find gas (NPHI is to right of RHOB) or oil (NPHI is to the left of RHOB) .Inferred lithologies from the logs are displayed next to them, where limestone is in green brick, dolomite is in blue slanted brick pattern, and sandstone is in speckled pink. Picked tops are represented by colored horizontal lines, with formation name labels below the lines.

To correct the porosity log for the effects of natural gas in the pores and hydrogen bound in clays, several parameters are assumed. Among the assumptions is the average neutron porosity of the closest shale formation, Φ_{sh}. In NY, this would be the average neutron porosity of the Ordovician Utica Shale that overlies the Trenton Group. According to Martin et al. (2008), the Utica Shale neutron porosity ranges from 3-6%, so the value used for Φ_{sh} is 4.5%. Another parameter of importance is the density of the gas or water in the pores, ρ_f. The naturally occurring fluid in NY's subsurface is assumed to be brine, which is assumed here to be a ρ_f of ~1.19 g/cm^3 (Kolkas, 1998). Finally, the matrix densities of dolostone (ρ_d), limestone, (ρ_l) and sandstone (ρ_s) are assumed. These lithologic density assumptions are based on RHOB log readings corresponding to lithologies identified by the P_e of the wells used for this study.

With these assumptions established, the gas and shale corrections can be calculated. First, the GR log is used to calculate the shale content, V_{sh}, which is a measure of the fractional amount of shale in a formation from 0-1. The calculation of V_{sh} is linear. It is therefore an exaggeration of the true volume of shale and requires a correction, so until the correction is applied it is called shale index, or I_{sh}:

$$I_{sh} = (\gamma_{log} - \gamma_0) / (\gamma_{100} - \gamma_0)$$

…where γlog is the GR response in the zone of interest, γ_0 is the minimum GR response, and γ_{100} is the maximum GR response. Empirical relationships are used to correct for exaggerated GR response when using *Ish*. For the Paleozoic rocks in this study, the Larionov equation is used:

$$V_{sh} = 0.083(2^{3.7I_{sh}} - 1)$$

By comparing V_{sh} to the GR for each data point, the V_{sh} corresponding to shale or highly radioactive layers was determined to be 20% or above. Thus, any points with a V_{sh} greater than 20% was assumed to be shale or to contain high amounts of clay, and was removed from the data.

Next, to determine the presence of gas in a formation, density-porosity (Φ_d) is calculated from the RHOB log. RHOB and PEF logs are used to determine lithology, and based on the lithology, the following equation is used:

$$\Phi_d = (\rho_{ma} - \rho_b) / (\rho_{ma} - \rho_f)$$

...where ρ_b is bulk density, or density recorded on the RHOB log, and ρ_{ma} is matrix density.

For each data point, the Φ_d is compared to neutron porosity, Φ_n. If $\Phi_d > \Phi_n$, gas is present. When this is the case, the equation for gas correction is used:

$$\Phi_{cn} = \sqrt{\frac{(\Phi n^2 + + \Phi d^2)}{2}}$$

Finally, the effective porosity equation is calculated to find pores large enough for fluid flow. This uses the value of Φ_n that has been corrected by the previous equations:

$$\Phi_{cn} = \Phi_n - (V_{sh} * I_{sh})$$

With this final correction, the NPHI log is corrected for the presence of both shale and gas, and effective porosity is found (Figure 2.2).

2.6 Well Cuttings

Well cuttings of three wells in western and central NY were used to further improve certainty on lithologies determined via well logs: Mitchell 1 in Steuben County, Robert Olin 1 in Steuben County, and Shepard 1 in Tompkins County (Appendix C) (Figure 2.3). The sample interval of packets examined was at 100 feet intervals or less. Percentages of dominating lithologies were reported, and the presence of grains of minor minerals were noted as well.

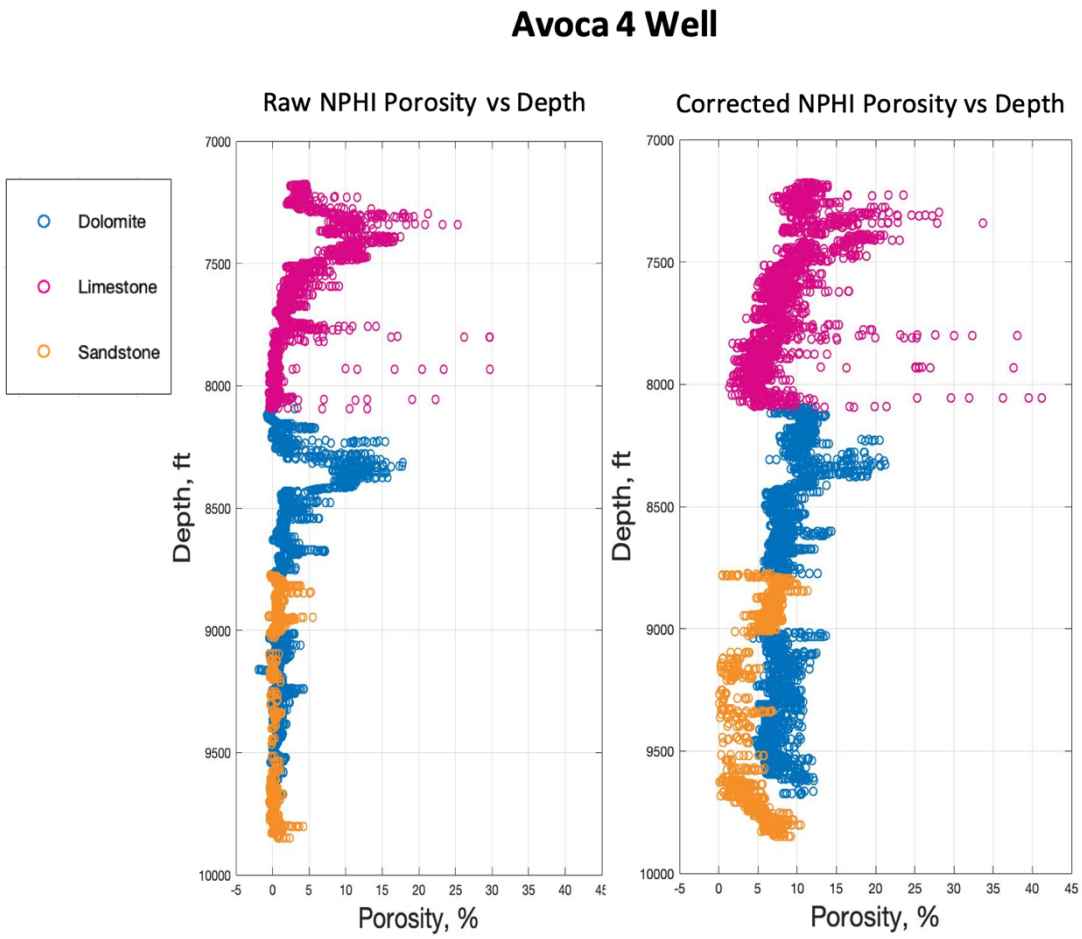

Figure 2.2: Charts of NPHI Φ_n values, in percentage, versus depth in feet for the Avoca 4 well in Central NY. To the left is the chart displaying uncorrected NPHI porosity values recorded by the logging tools. Due to the gas effect, some Φ_n values are negative. Due to shale effects, some horizons report overly high Φ_n values. To the right are Φ_n values corrected for gas and shale.

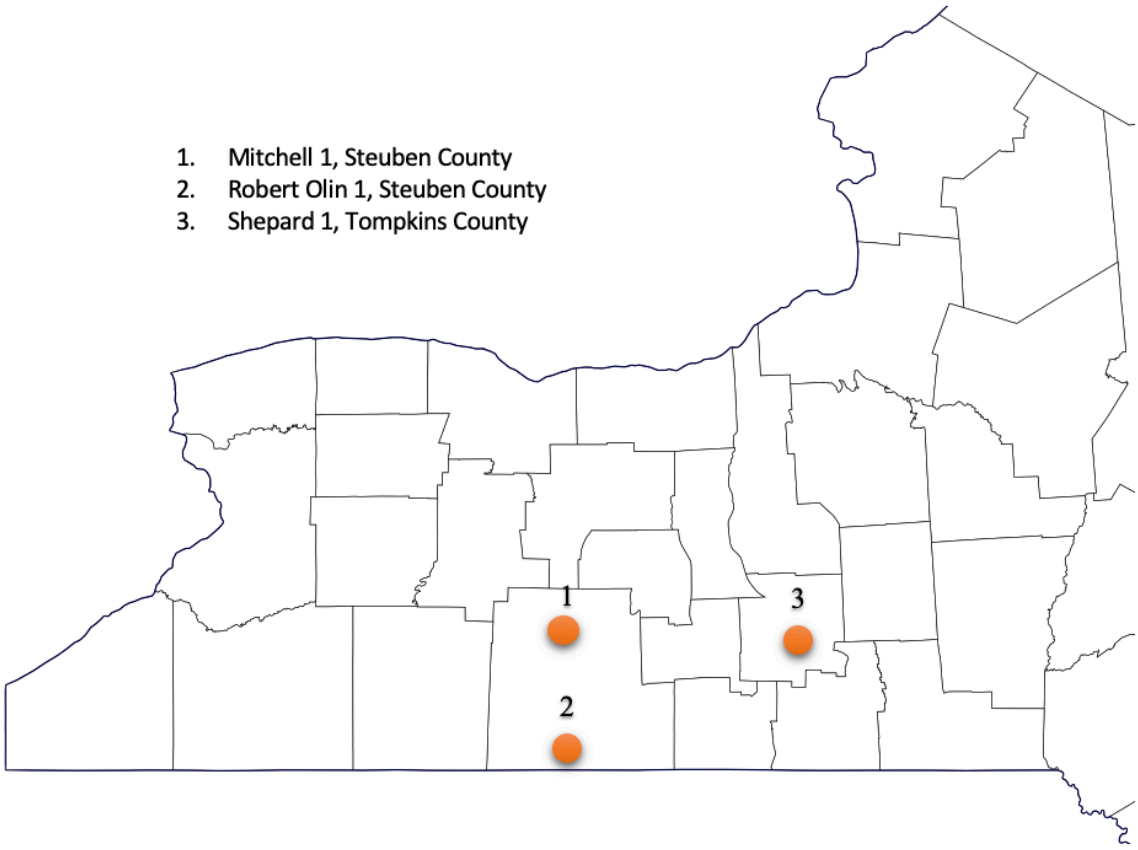

Figure 2.3: Map of several counties in central and western New York with county lines. Well cuttings locations are marked with orange circles and labeled with numbers. Label names and counties are listed with their corresponding numbers.

REFERENCES

American Petroleum Institute (API), 1979, The API well number and standard state and county numeric coded including offshore waters, Dallas, TX, American Petroleum Institute, API Bulletin D12A, 136.

Asquith, G.B., 1982. Methods in Exploration Series: Basic Well Log Analysis for Geologists. The American Association of Petroleum Geologists. Tulsa, Oklahoma.

Bassiouni, Z.B., 1994, Theory, measurement, and interpretation of well logs: Richardson, TX, Henry L. Doherty Memorial Fund of AIME, Society of Petroleum Engineers

Camp, E.,R. 2017, Repurposing petroleum reservoirs for geothermal energy: a case study of the Appalachian basin. PhD Dissertation. Cornell University, Ithaca, NY.

Empire State Organized Geologic Information System (ESOGIS), 2014, New York State Museum, http://esogis.nysm.nysed.gov/

Kolkas, M. M., 1998, Subsurface brine disposal in the Sauk Sequence of central and western New York: Implications for new salt cavern gas-storage reservoirs. PhD dissertation. The City University of New York, New York City, New York.

Martin, J. P., Nyahay, R., Leone, J., and Smith, L. B, 2008, Developing a new gas resource in the heart of the Northeastern US Market: New York's Utica Shale play. Annual Meeting of the American Association of Petroleum Geologists, San Antonio, TX, April 20-23.

Rickard, L.V. 1973, Stratigraphy and the structure of the subsurface Cambrian and Ordovician carbonates of New York. New York State Museum Map and Chart 12. 55 pp., 14 plates.

Smith, L., Nyahay, R., and Slater, B., 2010, Integrated Reservoir Characterization of the Subsurface Cambrian and Lower Ordovician Potsdam, Galway and Theresa Formations

in New York: Albany, NY, New York State Energy Research and Development Authority, 69 p.

CHAPTER 3:

OVERALL PETROPHYSICAL AND STRATIGRAPHIC ANALYSIS OF THE SUBSURFACE CAMBRO-ORDOVICIAN UNITS OF CENTRAL NEW YORK

3.1 Abstract

The Cambro-Ordovician subsurface strata below Cornell University, referred to here as the Beekmantown Group, are analyzed for their reservoir quality using well logs, cuttings, cutting reports and permeability reports. No well has been drilled at Cornell University to date. Therefore, depths and thicknesses of formations are interpolated from 78 wells drilled in central and western NY for an estimation of the stratigraphy encountered beneath Cornell. The stratigraphic units examined include everything below the Knox Unconformity and above the Precambrian basement at Cornell's location: from the top, they are the Tribes Hill Formation dolomites and limestones, the Little Falls Formation limestones and dolomites, the Galway Formation interbedded dolostones and sandstones and the Potsdam Formation sandstones. Alongside this stratigraphic study is an analysis of the porosity and permeability reports of wells near Cornell, within central and western New York. Results indicate little to no permeability at the Tribes Hill Formation, with greater potential porosity and permeability at the basal Little Falls Formation, the Galway Formation Rose Run member, the Galway Formation informal Yellowjacket member, and the Potsdam Formation, which are listed in order of higher potential. The top of the Beekmantown Group at Cornell's location is estimated to be at ~7,800 feet or 2,375 meters below the surface, and the thickness of the Group is estimated to be ~4,900 feet or ~1,500 meters.

3.2 Introduction

As was discussed in Chapter 1.1**,** because no wells have been drilled at the campus to date, the stratigraphy and petrophysical qualities of the subsurface sedimentary layers directly beneath Cornell University are currently unknown. Therefore, the interpolation of stratigraphic and petrophysical data from wells nearby the Cornell University campus at Ithaca, Tompkins County, central NY are used to estimate the reservoir qualities of these layers, and to find potential intervals that may be suitable for geothermal production.

3.3 Top Picking Criteria from Well Logs

The stratigraphy of the layers examined in this chapter is discussed in Chapter 1.4. For the sedimentary layers below the Knox Unconformity, the following criteria are used to determine the tops of formations: first, top picks from Rickard (1973), Smith et al. (2005), and Smith et al. (2010), are consulted as a foundational basis based on reference well logs (GR) with picks. Next, well logs across several wells are analyzed alongside lithological descriptions of the formations. When well logs and cuttings analyses indicate a deviation from the tops picked by the references above, they are adjusted based on what is displayed by the data.

The selection of the location of the tops of many formations can be ambiguous. Often, different geologists choose different depths as the tops of the same formation at the same borehole based on their individualized reasoning and criteria. In this study, the pattern of the GR log is the primary distinguishing log used to determine tops. An example of the tops and associated log readings is shown in Figure 2.1. When the deflections of the GR log are not distinguishable enough to pick consistently a formation top, the accompanying density and/or photoelectric factor logs are used. This is the case, for example, with the contact between the Galway Formation and the units that both underlie and overlie it. Below, because the Potsdam

sandstones are overlain by the basal sandstone of the Galway Formation, it is often difficult to distinguish the top of the Potsdam in the GR log. Therefore, as a second criteria, the top of the Potsdam Formation sandstone occurs at a marked decrease in density recorded by the density log, and relative decrease in photoelectric factor in the PEF log. Due to the gradual transition of the top of the Galway Formation's sandstone to the basal Little Falls limestones or dolomite, the top of the Galway Formation can be placed either at the top of the Galway sandstone, or include the interval of gradation. The top of the sandy layer of the Galway is much easier to distinguish from well logs. Thus, in this study, the intergradational interval of dolomites and sandstones is at the bottom of the Little Falls.

3.4 Depth and Thickness of the Sedimentary Strata Beneath the Knox Unconformity

For decades, geologists have generated isopach and structural maps of the Beekmantown Group from well data such as logs and cuttings (e.g. Rickard, 1973, Lugert et al., 2006, and Smith et al., 2010). However, these maps have not yet been generated with corrections for well deviations – in other words, current maps show tops in measured depth (MD), which is the length of the borehole when it reached X formation regardless of any azimuthal change in direction as the well was drilled, rather than TVD, which accounts for the true vertical depth from the surface. In this section, isopach and structural maps are generated with those corrections included, and compared to maps generated without the correction.

In this study, the tops of all formations beneath the Knox Unconformity and top of the crystalline basement are picked across 78 wells, all of which have been corrected for TVD and SSTVD where applicable and/or possible (Appendix A) (Figure 3. 1). As is discussed in Chapter 1.4, the Knox Unconformity cuts progressively deeper into strata toward the northwest. For

example, the unconformity directly overlies the Tribes Hill Formation at Cornell's area in central NY, but erodes further into strata to the northwest so that it overlies the Galway Formation in Chautauqua County (Figure 1.4). Thus, for the purpose of the overall examination of these sedimentary layers, the top of the sedimentary layers examined for the entire interval includes all formations above the Galway that directly subcrop the Knox Unconformity in central and western New York (Figure 3.1). Later, when the formations are examined individually, the Tribes Hill and Little Falls formations and their depths and thicknesses are examined separately.

An isopach map is generated for the thickness of the interval spanning the top of the formation directly beneath the Knox Unconformity (the Tribes Hill Formation at Cornell's location) to the top of the basement for all wells where such information is available (Figure 3.2). The top of the strata examined in this study is determined to be at ~7,800 feet, or ~2,375 meters TVD at Cornell's location. The isopach map indicates that the thickness of the interval studied in this thesis for potential reservoir properties is about 1,430 feet, or 435 meters TVD at Cornell.

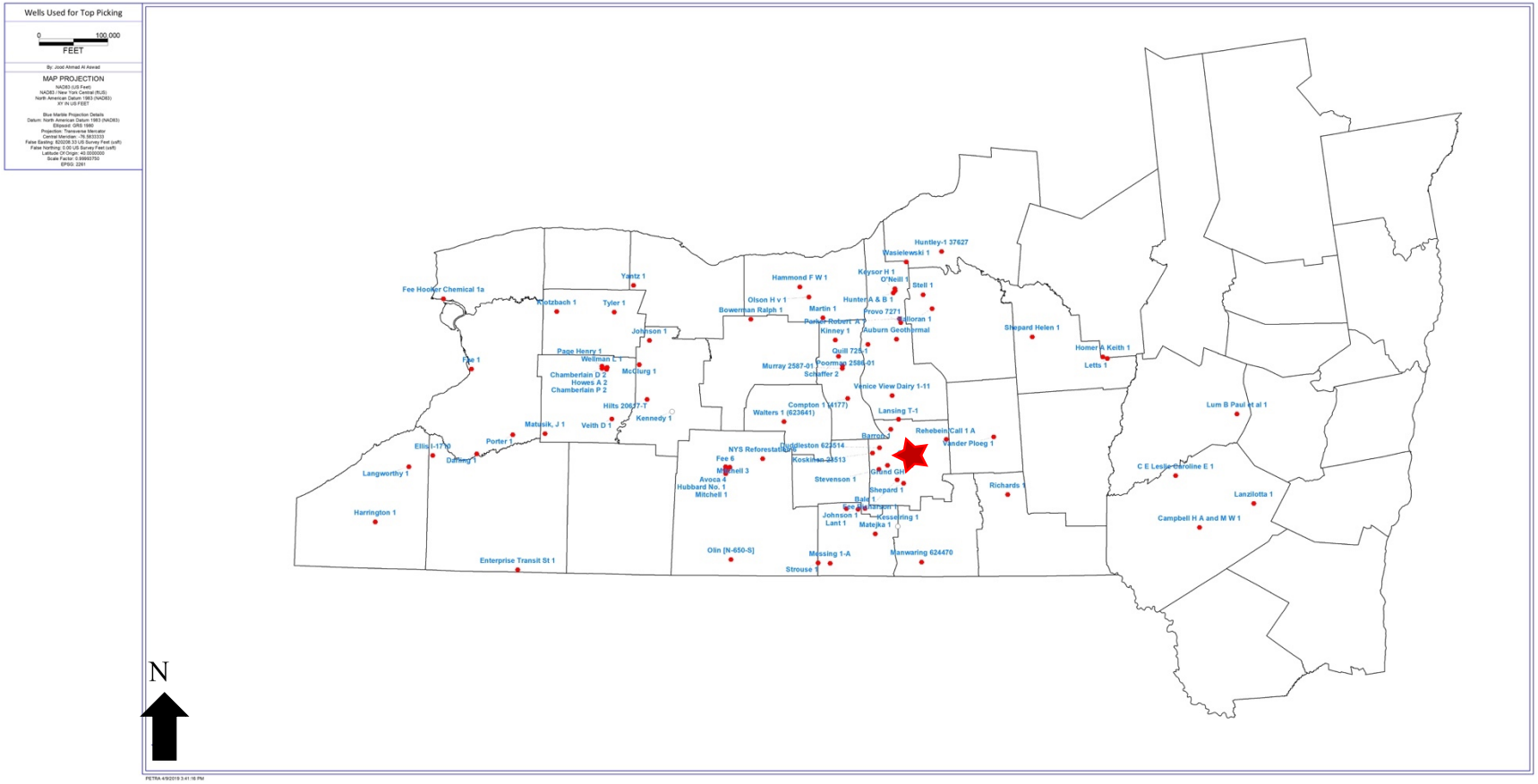

Figure 3.1: Map of all wells evaluated for stratigraphic top picks in central and western New York. Wells are depicted in red circle. The red star symbolizes Cornell University. Well names are in blue. API numbers corresponding to well names, as well as the exact location of the wells, can be found in Appendix A. Projected in NAD83.

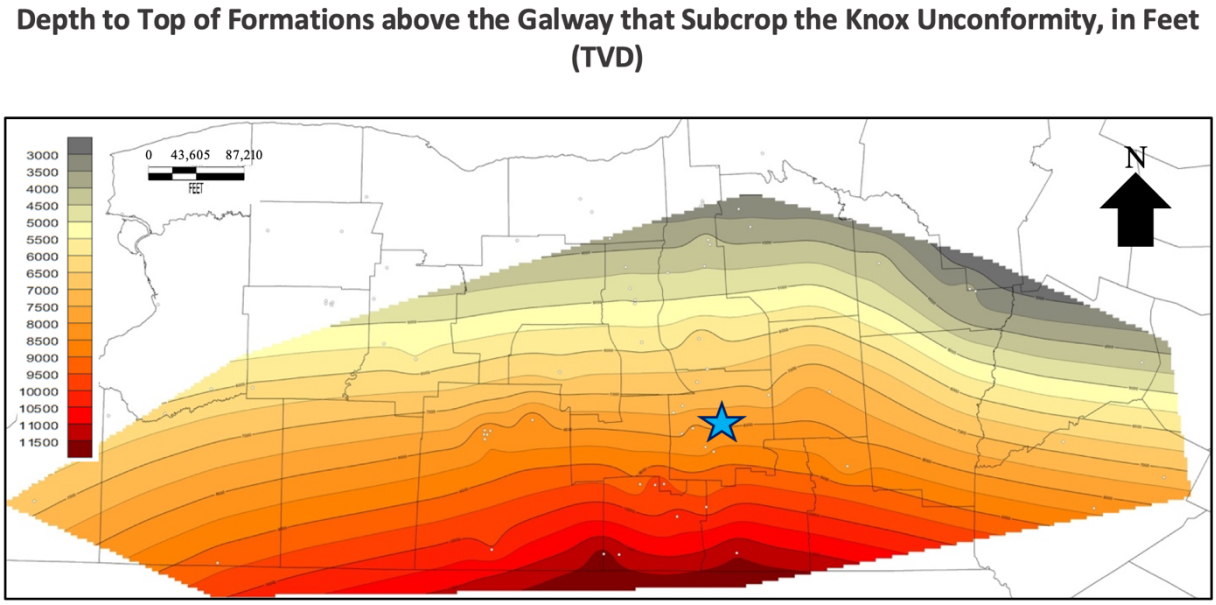

Figure 3.2: Structural map of the depth to the top of the shallowest formations above the Galway that directly subcrops the Knox Unconformity. The location of Cornell University is denoted by the blue star. Wells used for the generation of this map are symbolized by circles inside the colored portion of the map. Contour lines are in feet below the surface, True Vertical Depth. At the location of Cornell University, the formation that subcrops the unconformity is ~7,800 feet/ 2,375 meters below the surface and considered to be the top of the Cambro-Ordovician section examined in this study. Map projection is NAD 1983.

Additionally, an isopach map is created to analyze the thickness of the entire Beekmantown Group across western and central NY in meters TVD, and compared to an isopach map by Smith et al. (2010) that was generated in meters MD (Figure 3.3). In general, the depths contours match pretty well between the two maps. For example, at Cornell's location, the thickness of the Beekmantown is ~1,500 meters or ~4,900 feet at both maps. However, the isopach map generated in this thesis reveals a thickening of the Beekmantown Group to the east and west, while the map by Smith et al. is more uniform in those directions. Additionally, the isopach map generated in this study includes data from several wells around Cornell and in central NY that were not used in the other map. It is expected that, regardless of the difference in picks, maps generated using corrections to deviated wells will likely yield a more accurate prediction to depths and thicknesses of formations in central NY.

Isopach Thickness Map for Beekmantown Group in Central and Western New York from Wells Measured in Meters TVD (above) and meters MD (below)

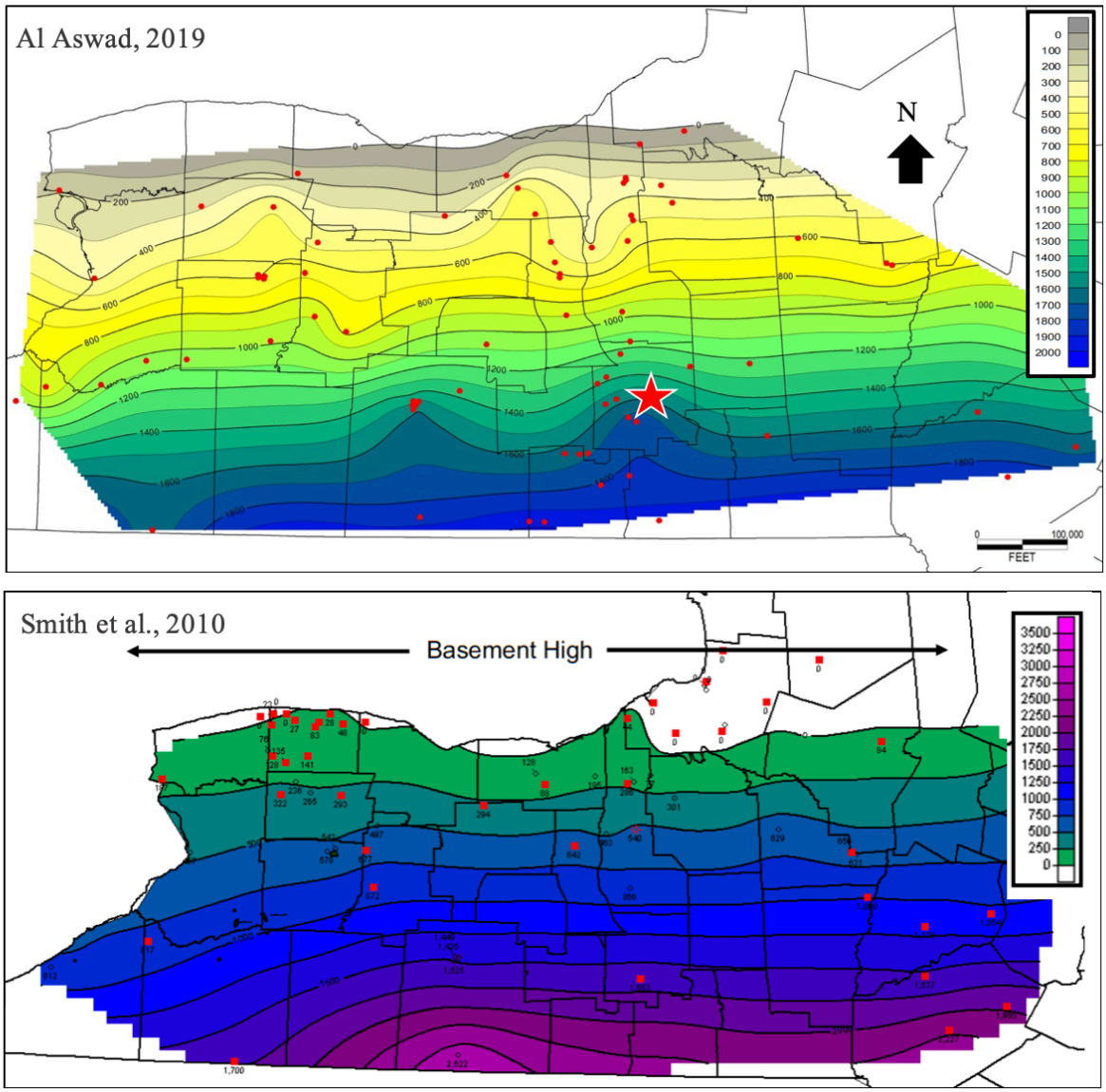

Figure 3.3: Above: Isopach map of the thickness of the entire sedimentary section from the strata deposited after the Galway to the top of the Precambrian basement. Wells used to generate map are in red circles. Thickness is in metersof True Vertical Depth. Projected in NAD83. The location of Cornell University is marked by a blue star. Below: Isopach map of the entire Beekmantown Group, in meters MD. Cornell's location is marked as a red star. Wells used to generate the map are depicted in red squares. Lower figure from Smith et al., 2010.

3.5 Wells Used for NPHI Log Corrections

Thirteen wells are corrected for the presence of gas and shale. These wells are chosen based on their locations at central or western NY, and the presence of at least part of the Beekmantown Group. These corrected logs are used primarily to compare and analyze porosity across formations or intervals of the Beekmantown Group. The compilation of the results of this correction are found at Appendix D. The location and names of the wells used for the study can be seen in Figure 3.4.

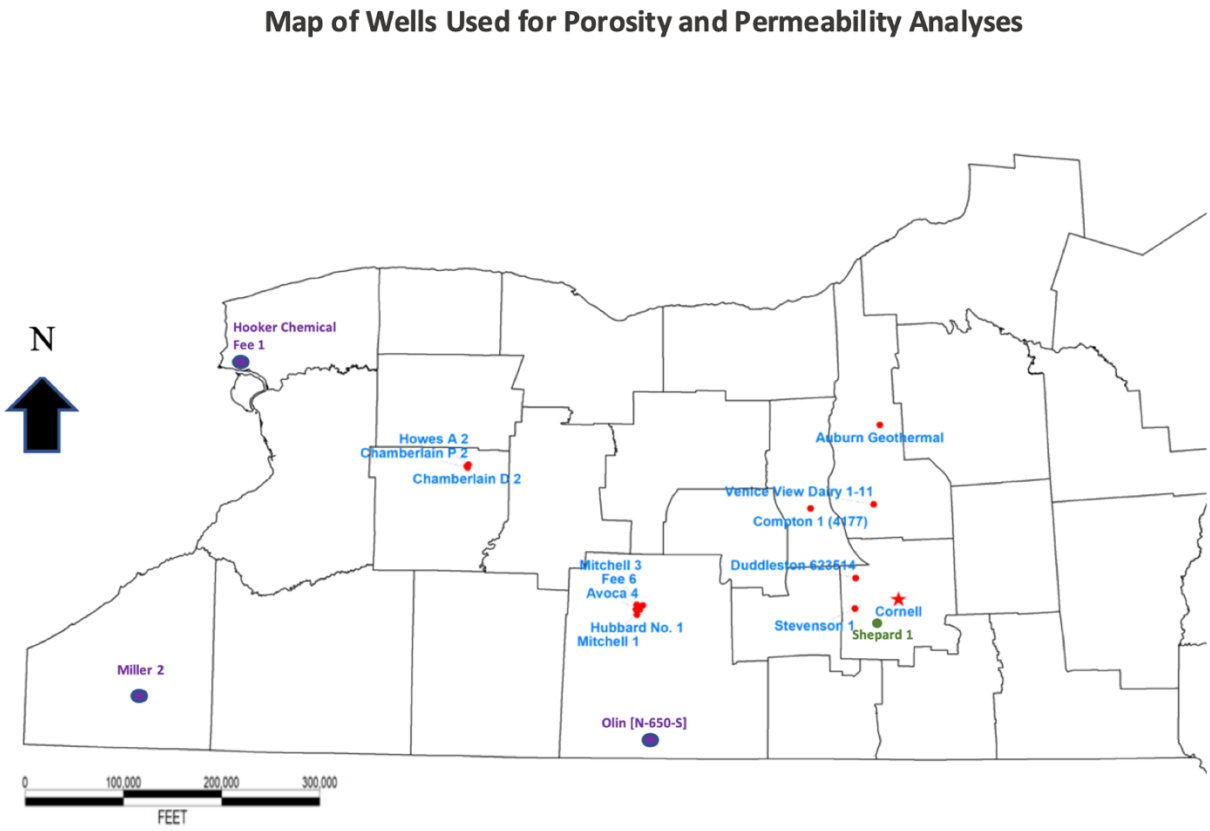

Figure 3.4: Symbolized by red circles are locations of wells used for corrections of NPHI logs affected by presence of gas or shale. Of these wells, nine are located in central New York. Cornell's location is symbolized by a red star. General locations of reported porosity and/or permeability tests are denoted by purple circles. The approximate location of the Shepard 1 well, which was used for cuttings analysis, is included and symbolized by a green circle.

3.6 Tribes Hill: Porosity and Permeability

The Tribes Hill Formation is expected to be the uppermost formation encountered beneath the Knox Unconformity at Cornell's location (see Figure 1.4). This is assumed not only because of previous studies conducted on the formations that subcrop the unconformity, but also from cuttings reports archived by ESOGIS and cuttings from the Shepard 1 well (API: 31-109-03973-0000), which is ~ 6 miles (10 km) away from Cornell University (see Appendix C), that were examined for the purpose of this thesis (Figure 3.5). The Tribes Hill Formation is lithologically distinct from the overlying Rochdale Formation found in eastern New York due to the presence of a conglomerate unit at the base of the Rochdale Formation (Landing, 2012).

Based on facies studies of outcrops and thin sections, the Early Ordovician Tribes Hill Formation has been divided into ten lithofacies that represent peritidal to subtidal environments (e.g. Fisher, 1954; Braun and Friedman, 1969; Harris and Friedman, 1982; Curl et al., 1984; Kolkas, 1998). Based on cuttings from nearby wells, it is a light to dark grey, shaly, argillaceous limestone that is variably dolomitic. No gas production or permeability reports been documented for this formation.

One well in central NY contains the logs necessary to estimate porosity: the Stevenson 1 well (API: 31-109-22998-0000), in Tompkins County about 9 miles away from Cornell University. From this well, maximum Φ_{cn} is 12%, and the average Φ_{cn} is 6% (Figure 3.5a). The availability of the PEF log has allowed for the determination that the entire interval of the Tribes Hill at Stevenson 1 is dolomitic. Visually, there appear to be some small zones (~5 foot thickness) of Φ_{cn} near 10%, and some zones (~10 foot thickness) of Φ_{cn} from 5-10%. The GR API values and Φ_{cn} values were plotted to compare the relationship of radioactivity to porosity

quantitatively (Figure 3.5b). The regression of the data has the strongest fit (highest R^2) of 0.264 when regressed with a power law:

$$y = 7.3251x^{0.75}$$

The regression confirms that there is no clear relationship between radioactivity and porosity. Furthermore, as the entire formation is dolomitic at Stevenson 1, a relationship of variable lithology to porosity could not be observed. Hence there is no independent information with which to explain the vertical porosity trends displayed in Figure 3.5a.

A.

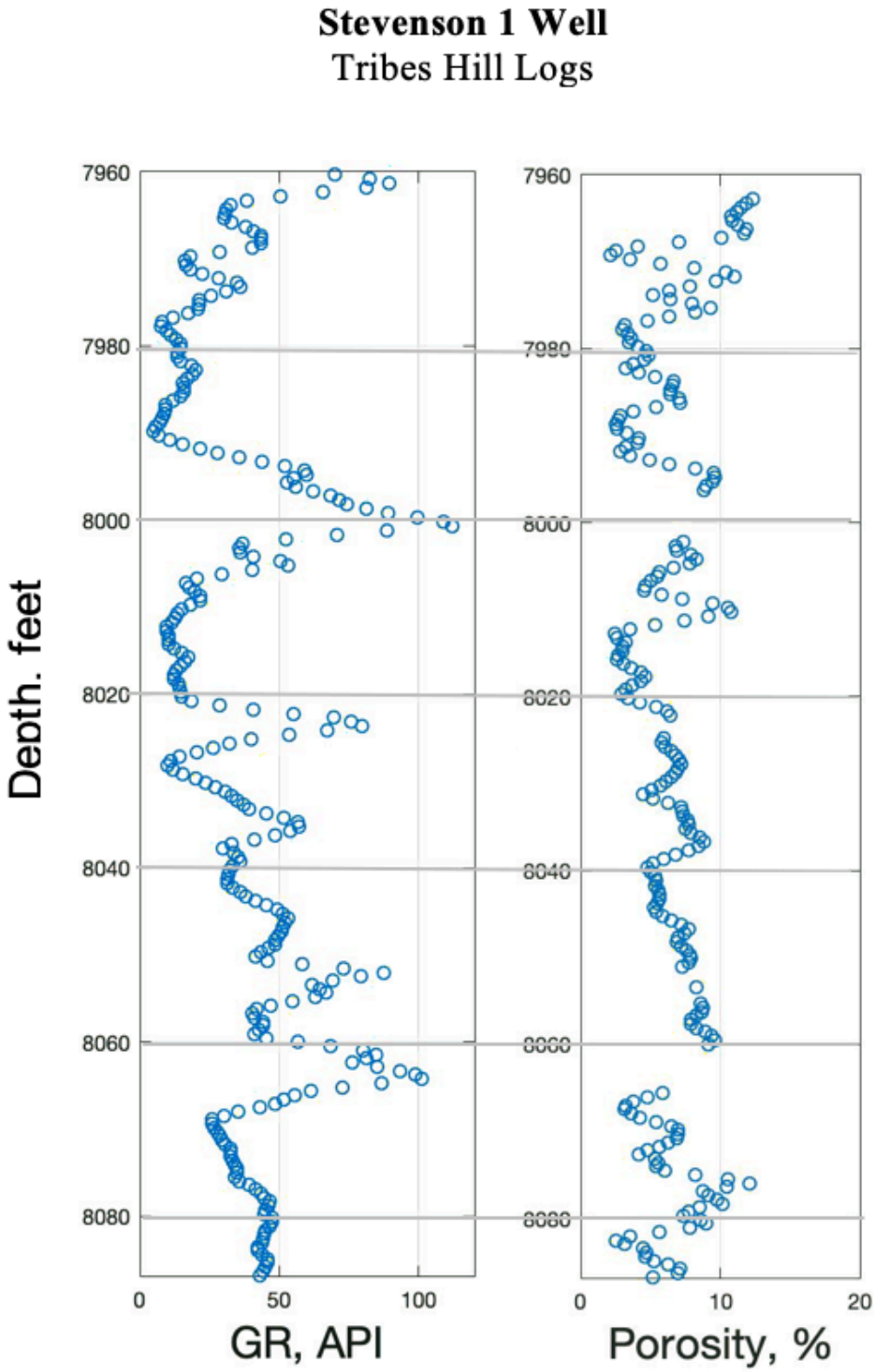
Stevenson 1 Well
Tribes Hill Logs
Depth. feet
7960
7980
8000
8020
8040
8060
8080
0
50
100
GR, API
0
10
20
Porosity, %

B.

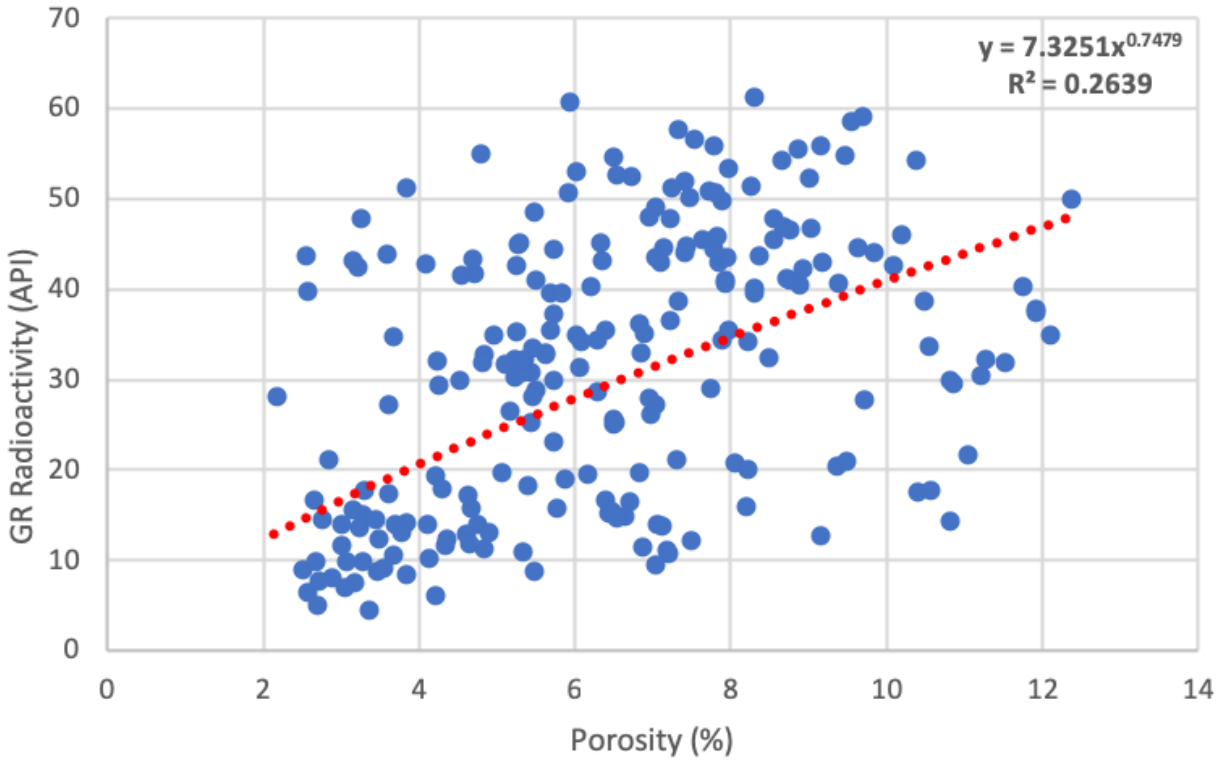

Figure 3.5: a) Gamma Ray log (left) and corrected NPHI Porosity log (right) of the Stevenson 1 well, with depth of the Tribes Hill formation, in feet, as the vertical scale. There appears to be no pattern that ties radioactivity to trends in porosity. Blank spaces in the porosity log denote data points that were identified as shale and have been removed. b) Relationship of porosity, on x-axis, with radioactivity recorded from the normalized GR log, on y-axis. Data are illustrated as blue dots. The red dotted line is the power-law fit of the regressed data. The relationship and R^2 of the power law are displayed in the upper right corner of the graph.

3.7 Little Falls: Porosity and Permeability

The Upper Cambrian Little Falls Formation underlies the Tribes Hill Formation in New York. It is typically a dolomite that has some interbedded sandstone at its base, and it was deposited in a proximal shelf environment (Fisher, 1977). Cuttings analyses indicate a light-to-dark grey dolomite with some pyrite and chert. The base of the Little Falls can be ambiguous to pick. Cuttings reports occasionally indicate some shale present as well. In this study, the base of the Little Falls is distinguished from the top of the underlying Galway Formation by the presence of dolomite within the basal Little Falls. The top of the Galway has no dolomite at all.

The interpolated depth of the Little Falls at Cornell University is 8,000 feet or roughly 2,440 meters TVD. Permeability studies were conducted on the Miller # 2 well in Jamestown in western New York by the Battelle Memorial Institute in 2009 (Figure 3.6) (New York State Energy Research and Development Authority, 2011). At the Miller #2 well, a full core with the Little Falls dolomite was studied for porosity and permeability. Reports indicate a mean of 0.0347 millidarcys (md) permeability to air and 0.2 md Klinkerberg permeability. The report indicates that zones with high porosity are typically in the middle and lower portion of Little Falls, and may be related to dolomite grain size. In 1968, McCann and others noted numerous porous intervals that yielded salt water in the subsurface in western and central New York.

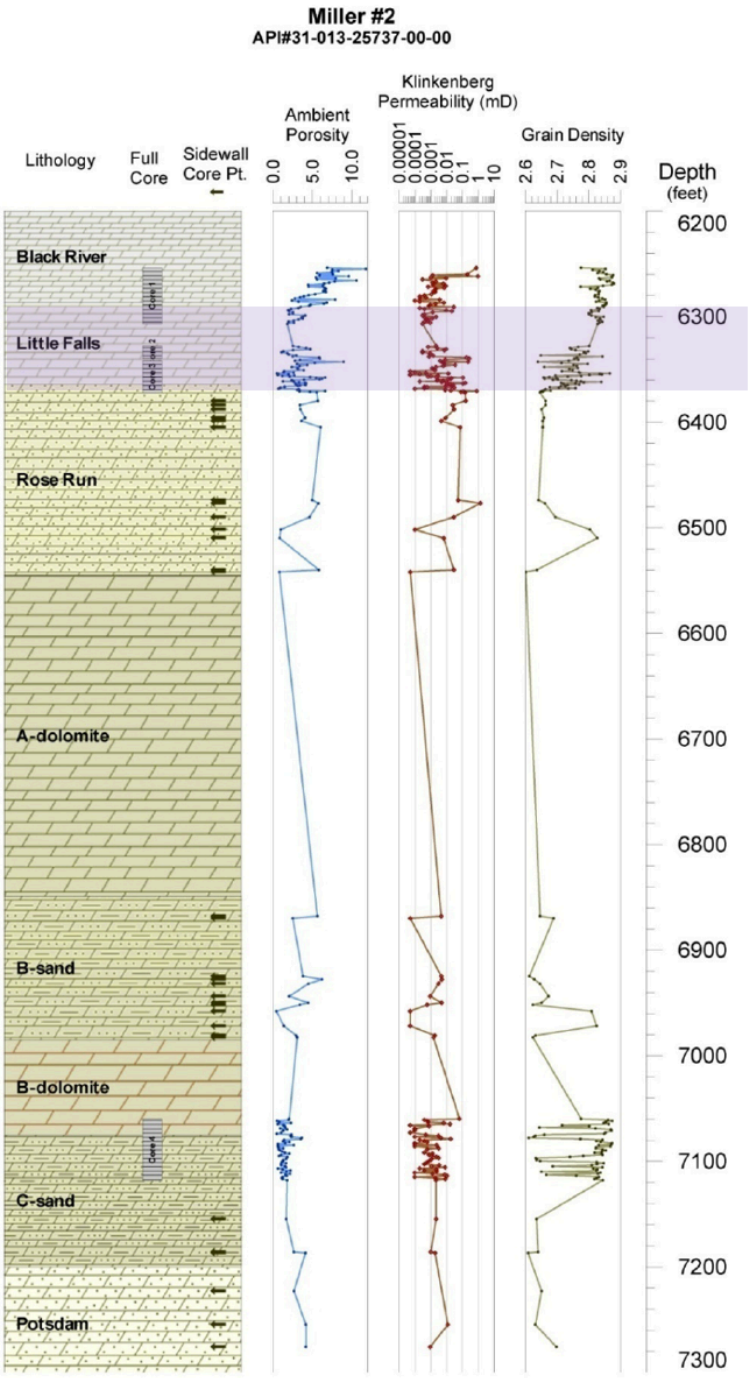

Figure 3.6: Porosity, permeability, and density of core data for the strata encountered in the subsurface at the Miller # 2 well in Jamestown, western NY. Full cores are symbolized by grey rectangles. The Little Falls Formation is highlighted in purple (Image modified from New York State Energy Research and Development Authority, 2011).

The average well log porosity of this formation is approximately 8-16% with maximum porosities of ~18 - 39% (Appendix D). While most wells have maximum porosities closer to 18-22%, two wells exhibit exceptionally high porosity maximums of ~39%: the Mitchell 3 well in Steuben County, central NY (API: 31-101-21633-0000), and the Compton 1 (4177) well in Seneca County, central NY (API: 31-099-20446-0000) (locations shown in Figures 2.3). The Mitchell 3 well has exceptionally high average and maximum porosities relative to all the other wells. These intervals of maximum porosity appear to be isolated spikes representing just a few feet of very high Φ_{cn}, while the rest of the formation has Φ_{cn} values that more closely align with the average porosity. This suggests that these small intervals of high porosity may be due to the presence of vugs, fractures, or other features of secondary porosity commonly found in dolomite. Higher porosity appears to be concentrated in the basal Little Falls, in which the dolomites are interbedded with some sandstone.

3.8 Galway: Porosity and Permeability

In 1998, Kolkas conducted petrographic studies of strata from the Cambro-Ordovician from two other wells in western and central New York: Olin (N-650-S) (referred to as Robert Olin #1 by Kolkas) in Steuben County, central New York (API: 31-101-03924-0000), and Mitchell #1 in Steuben County, central New Yok (API: 31-101-21468-0000). The study on the Mitchell 1 well analyzes porosity and permeability of well cuttings, while the Robert Olin well has analysis of part of the Galway Formation from core samples. Reported results analyzed in this thesis are based on air permeability.

Although the Galway Formation is sometimes referred to as the Theresa Formation, it has been discovered through various studies that the type Theresa Formation previously described by oil, gas and other companies in central NY is stratigraphically Ordovician in age and does not

occur in the subsurface in NY, whereas the Galway Formation is Late Cambrian and exists in New York (Rickard, 1973; Landing, 2007). Therefore, the formation underlying the Little Falls Formation in New York is referred to in this study as the Galway Formation.

The Galway Formation in central NY consists of interbedded dolomite and sandstone, and the thickness of these beds varies from location to location. An informal classification of members of the Galway Formation is presented by Smith et al. (2010) based on identification from well logs (Figure 3.7): from the top down these members are the Rose Run sandstone member (analogous to the Rose Run sandstone Formation of Ohio), A Dolomite member, B Sand member, B Dolomite member, B Interbedded, C Sand and Clean Sand members.

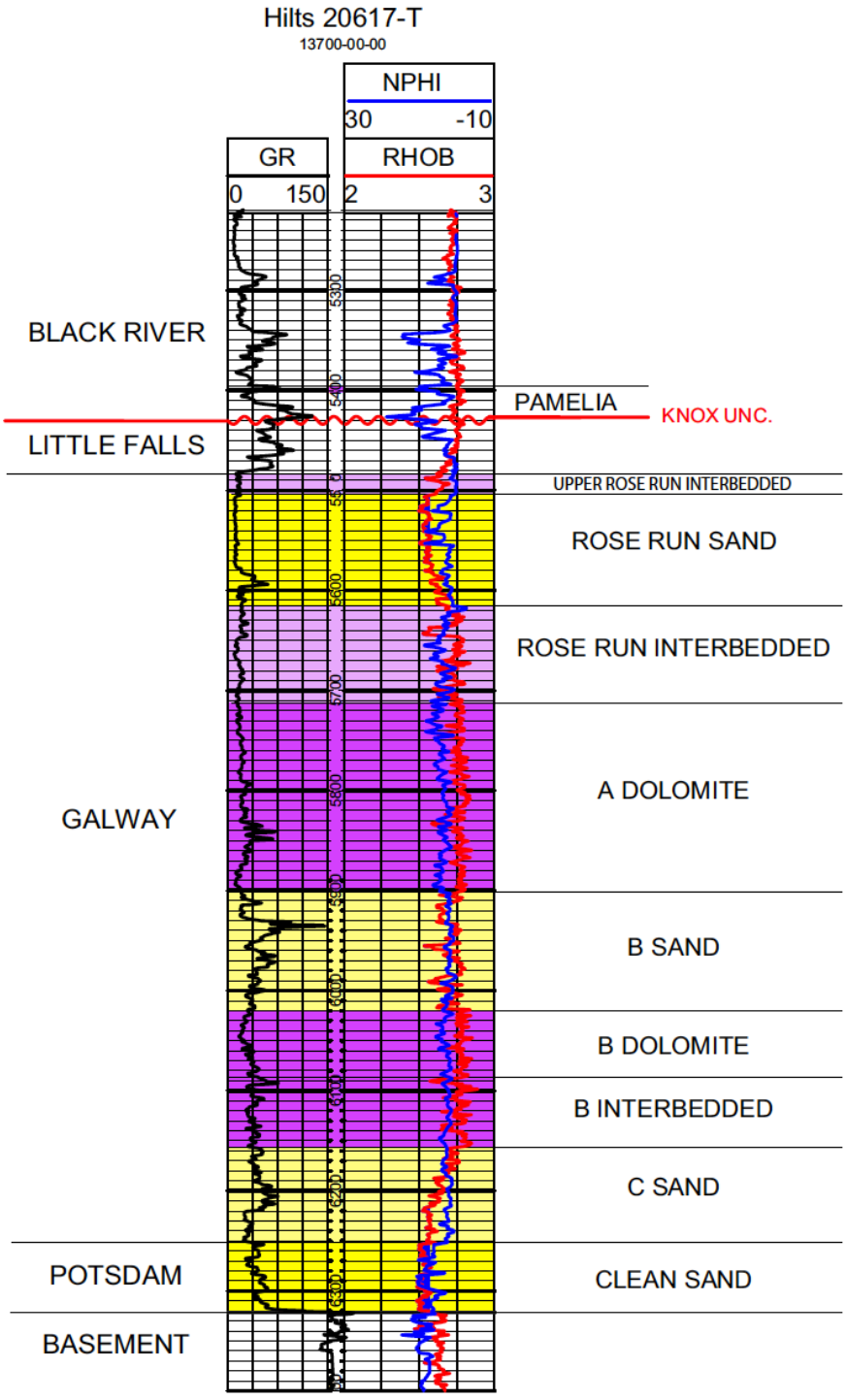

Figure 3.7: Type log of a well (API: 31-051-13700-0000) with the Galway Formation informal member names, and log patterns corresponding to those informal members Horizontal lines are stratigraphic tops, and the red horizontal line indicates an unconformity. Here, porosity values increase to the left. Figure from Smith et al., 2010.

The informal nomenclature designed by Smith et al. in 2010 correspond with interpreted lithologies. For example, the A Dolomite member is mostly made up of dolomites, B Sand member is a member interpreted to be comprised mostly of sandstone, and the B Interbedded member consists of interbedded dolomites and sands.

Informal members of the Galway Formation are assigned in a similar manner in this study: based on well log interpretation of the GR and RHOB logs, informal member names are assigned to zones in the Galway Formation based on lithology. The subdivision of many of the lower members differs in this study from those identified by Smith et al. in 2010 because changes in composition are difficult to interpret in many of the wells. In several wells, the thicknesses of beds, as well as many of the RHOB and GR logs which are used to identify lithologies, vary: intervals that are mostly dolomitic, like the Smith et al. (2010) B Dolomite member, are difficult to distinguish from intervals that are made up of interbedded dolomites and sands, like the B Interbedded member that underlies B Dolomite, because of the fluctuations in the GR and RHOB logs that occur almost every 10 feet (Figure 3.8). As such, the only distinguishable members of the Galway Formation are those that are mostly made of sands with a consistently low RHOB logs (< 2.7 g/cm^3).

This study adopts the nomenclature of the upper sandstone member of the Galway Formation as the Rose Run member. This study differs in that all members underlying the Rose Run sands, from Rose Run Interbedded to B Interbedded, are assembled together as one member, referred to here informally as the Yellowjacket member, which is interpreted to be interbedded dolomites and sands. Below this member is what this thesis refers to as the informal Vespa member, which was referred to as the informal Clean Sand member by Smith et al. in 2010 (Figure 3.9).

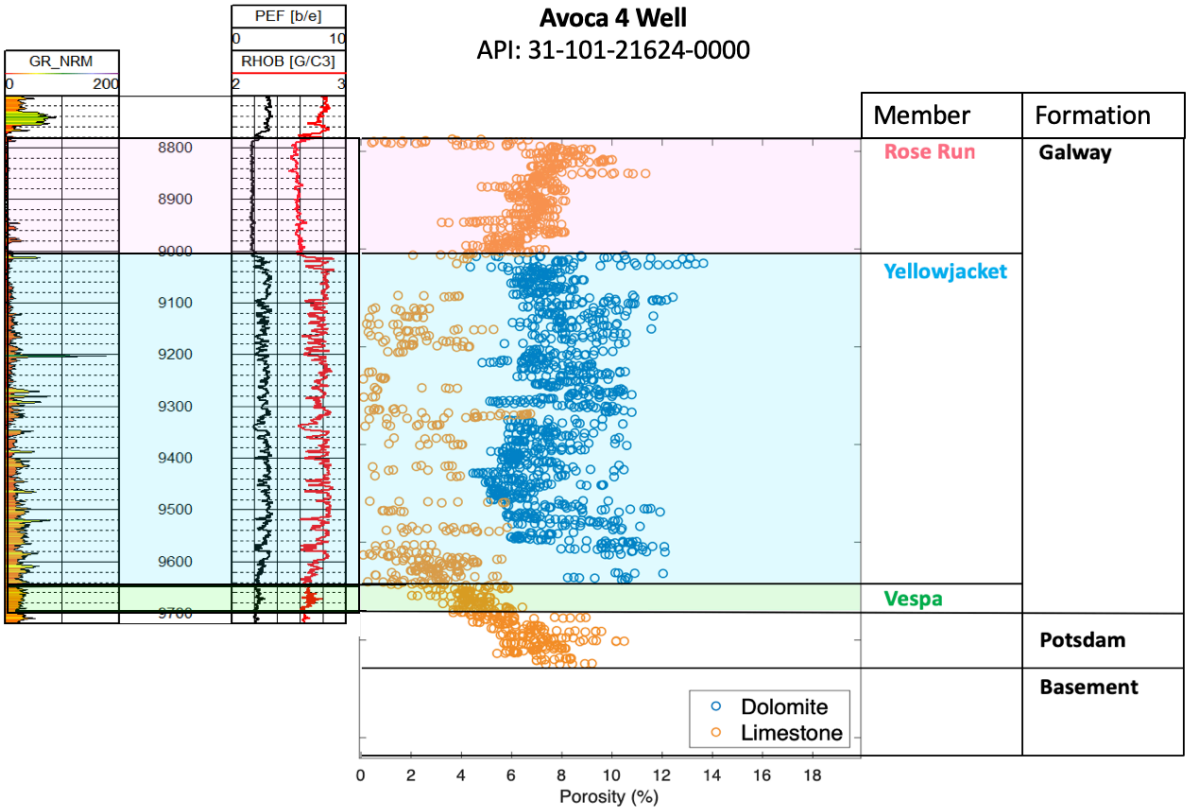

Figure 3.8: Logs and lithology patterns corresponding to the informal members of the Galway Formation referred to in this study: the Rose Run (in pink), Yellowjacket (in blue) and Vespa (in green) members. The left column shows type logs with depth, in MD, used to identify each member: low GR, low RHOB (<2.65 g/cm^3), and low PEF (≤ 2 b/e) logs for Rose Run, varying GR, RHOB and PEF logs for Yellowjacket, and decreasing RHOB and PEF logs correspond to Vespa. The middle column includes corrected NPHI porosity and interpreted lithologies.

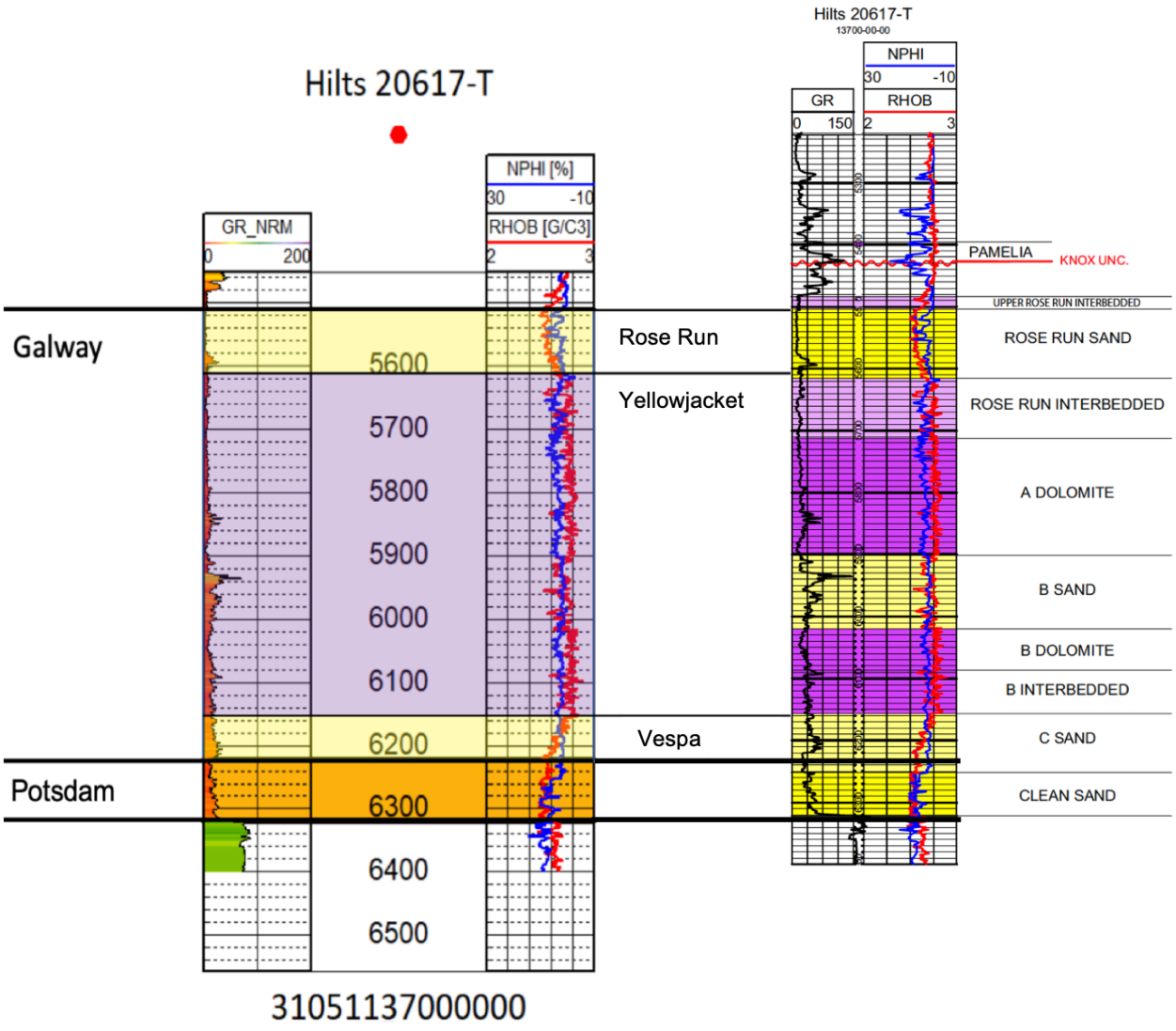

Figure 3.9: Comparison of the Galway Formation member divisions and their associated type logs of this study (left) and Smith et al.'s 2010 study (right) for the Hilts 20617-T well (API: 31-051-13700-0000) in western NY. Formation names are at the middle and far right, informal member names used in this study are in the middle, and informal names used by Smith et al. in 2010 are to the far left. Depths are in MD. Porosity values increase to the left. Image modified from Smith et al., 2010.

The top of the Galway Formation is estimated to be at about 8,550 feet, or 2606 m TVD at Cornell University. The Rose Run sandstone member of the Galway Formation in New York is a clean, fine-to-coarse grained quartz arenite. It is the topmost member of the Galway that is ubiquitously found across western and central NY in areas where it has not been eroded away by the Knox Unconformity. The Rose Run grades upward to the Little Falls limestones and dolostones.

The Rose Run member of the Galway formation equivalent has been established as a prolific gas reservoir in Ohio and Pennsylvania since 1965: hundreds of wells in Ohio were drilled to the Rose Run Sandstone reservoir alone (Riley, 1995). The Rose Run has also been of interest in studies regarding the reservoir quality of the Galway Formation in western and central New York (Smith et al., 2010). The entirety of the Galway Formation has been investigated by others much more thoroughly than the overlying Tribes Hill and Little Falls formations due to its history as a prolific gas producer. Along with the Miller #2 well in Jamestown, Chautauqua County, western NY, one other well has been investigated for the permeability of the entire Galway Formation: the Hooker Chemical Fee #1 (API : 31-063-06669-0000) well in Erie County, Niagara, western NY (Smith et al., 2010).

A core from the Kennedy # 1 well (API: 31-051-04630-0000) in Livingston County, western NY contains the clean sands of the Rose Run member. Reports on this core indicate that the Rose Run is composed of fine to coarse-sized quartz sand, and porosity is almost entirely secondary in nature, with average porosity of the core being about 6%.

Besides the Rose Run member, both other members in the Galway Formation are also of interest. The Auburn Geothermal well at Auburn, Cayuga County, central NY, has a particularly informative suite of logs that were deployed down to the basement (Figure 3.10). The flowmeter

(FLOW) log reports the rate of flow from low flow-rate pumping from hydraulic fracturing tests conducted at ~1600 pounds per square inch. From 4800'- 4950' (the depth range of the Yellowjacket member of the Galway), the FLOW log indicates relatively high flow of water pumped into the well at this interval (Martin, 2010). Although the units for the flow log of this well is unknown, it is assumed to be in gallons/min. This may be indicative of a zone with relatively high porosity and permeability. Complementary to the flowmeter log is a pair of shallow and deep resistivity logs, whose measurements also spike within the depth range of this member. Resistivity logs measure amount of conductivity, which does not increase unless water or hydrocarbon is encountered. A high resistivity log reading at this zone indicates the presence of gas within this interval, which may also be an indication of exceptional reservoir quality. A lower resistivity log reading typically indicated the presence of water, which may be the case for the informal Vespa member of the Galway Formation.

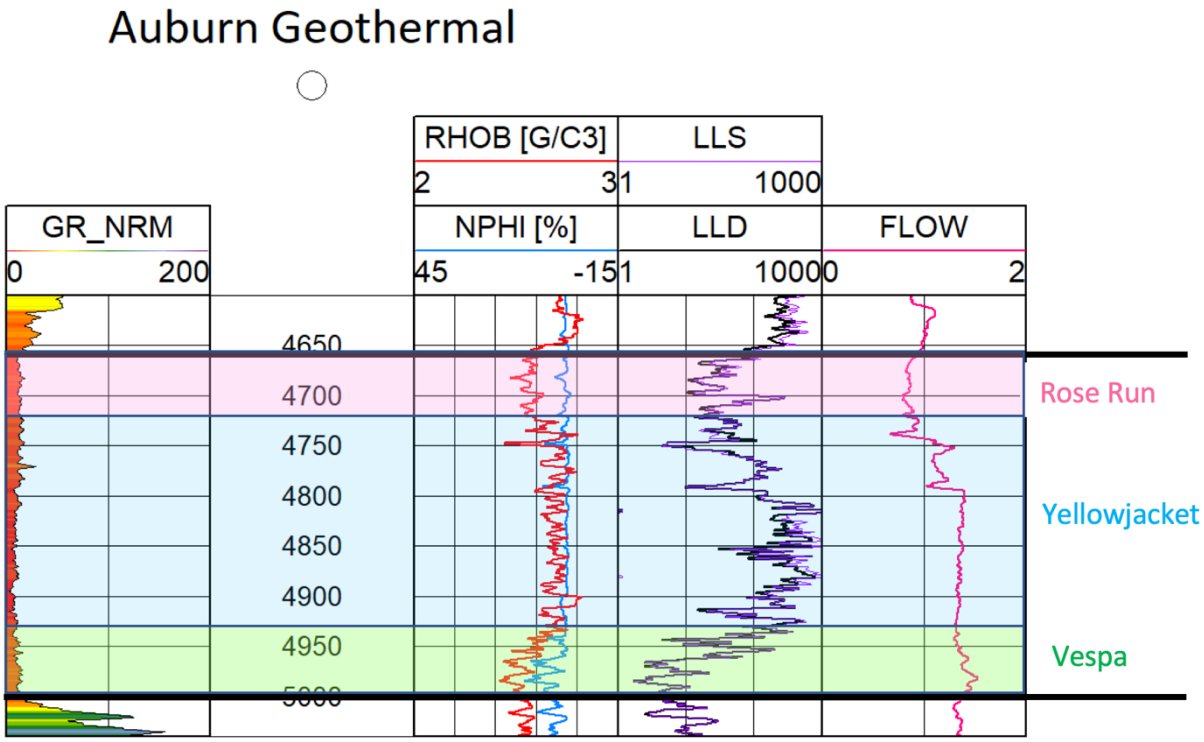

Figure 3.10: Well logs associated with the Galway Formation at the Auburn Geothermal well. Bolded black lines denote the upper and lower bounds of the formation. Depths are in feet TVD. Flowmeter log readings (FLOW) , which are assumed to be in gallons/min, are exceptionally high throughout most of the Yellowjacket and Vespa members, indicating a possibility of higher permeability. The Yellowjacket member is of special interest because of the coupling of this high flowmeter reading with high resistivity log readings (LLS and LLD), indicating higher hydrocarbon saturation. Vespa indicates continuously high flow, but low LLS and LLD log readings, indicating the presence of water. Porosity values increase to the left.

Raw density and NPHI logs, when observed concurrently, also deflect in a pattern that typically indicates the presence of gas: the density log deflects to the left of the NPHI log. The member below the Yellowjacket member is the Vespa member, which is about 50 feet in thickness. This zone at Auburn not only has the highest range and maximum of corrected porosity in the entire stratigraphic interval below the Knox Unconformity (about 4-14% Φ_{cn} range, and 9% on average), but also has the highest flow. However, the resistivity logs begin to decline at this interval, indicating less gas or water present than in the Yellowjacket member.

At Miller # 2, the Rose Run member spans from ~6,360 – 6540 feet or 1,940-1990 meter, the Yellowjacket member is from 6,540-7,180 feet or 1,990-2,190 meters, and the Vespa member is approximately 7,180 – 7,200 feet or 2,190-2,195 meters.

Permeability studies conducted on the Miller # 2 report a core at the Vespa interval below the surface. The Vespa member has an average klinkenberg permeability that is low, 0.0067 md, which is lower than the Yellowjacket member's average permeability of 0.0138 md (Figure 3.6). The member of the Galway Formation with the highest permeability is the Rose Run, which has 0.15 md permeability on average (New York State Energy Research and Development Authority, 2011).

It is important to note that this study is not a complete overview of permeability within the Galway, as a great portion of the Galway was not cored at the Miller #2 well (Figure 3.6). The Fee Hooker Chemical 1a well (API: 31-063-06669-0000) in Erie County, western NY has a core that represents a large portion of the Yellowjacket member. Two separate studies on porosity and permeability of this section were conducted: porosity and air permeability tests on well cuttings and core done by Kolkas in 1998, and separate thin section and core plug studies were reported by Smith et al. in 2010 (Figure 3.11).

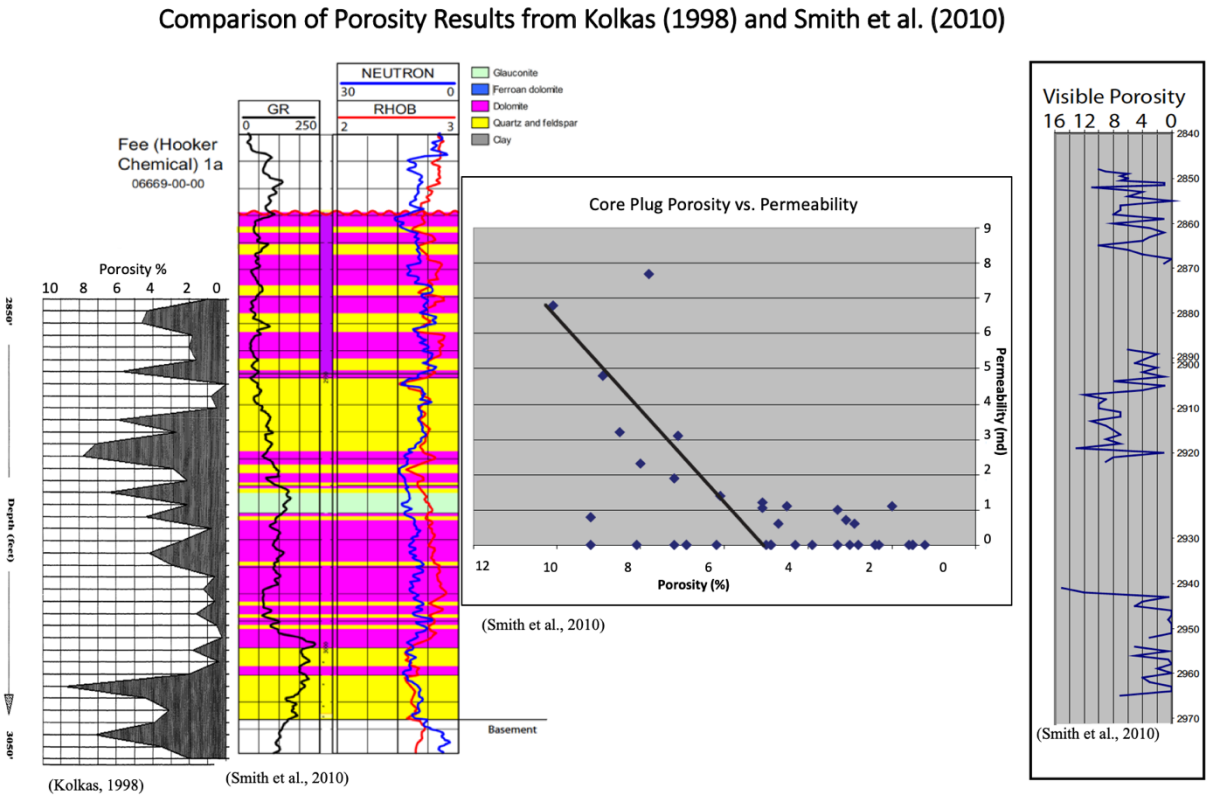

Figure 3.11: Comparison of porosity results for a portion of the Yellowjacket member of the Galway formation from the analyses conducted by Kolkas (far left, figure from Kolkas, 1998), and Smith et al. (middle, right and far right, figures from Smith et al., 2010) at the Hooker Chemical 1a well. The analysis that is to the far left depicts porosity from a portion of the Yellowjacket in this well, taken from a core section. Depths are ~2,840-~3,050 feet or ~865 – 930 meters MD. The figure that is second from the left depicts lithology determined by Smith and others, in colors, which are overlaid on GR, NPHI, and RHOB logs. Depths here are at the same interval of the Yellowjacket, from ~2,840 - 2,970 feet or ~865 - 905 meters. Yellow represents quartz and feldspar, purple represents dolomite, and green represents glauconite. Visible porosity from thin sections of the same depth interval is shown in the image that is to the far right. Second from the right is a chart of porosity versus permeability of a core plug from the Yellowjacket. Porosity values shown here increase to the left.

Kolkas's examination of a core section from the well yielded a maximum porosity of around 8.5%. Smith and others (2010) reported a maximum porosity from thin sections and core plugs that was slightly higher, at about 15% and 11%, respectively. Overall, both studies indicate an average porosity of around 5%.

Core plug values of this interval, reported by Smith and others (2010), have permeabilities that range up to 7 md with varying porosity. The portion of the core that has this high permeability is a bed of quartzose and feldspathic sandstone. It is suggested that the feldspathic sandstones in this interval are responsible for any intervals of visibly high porosity, since feldspars are easily dissolved. Since this well is located in westernmost NY, it is also suggested that the proximity of the Galway to the source rock (basement rocks) accounts for the high abundance of feldspars in the Yellowjacket member of the core (Smith et al., 2010). If so, it is probable that along with the Rose Run member, the lower portion of the Yellowjacket member has good reservoir quality.

However, air permeability tests on core plugs that were conducted by Kolkas indicate very low permeability in comparison, at a maximum of almost 0.1 md. The discrepancy in results may have stemmed from unknown variance in methods used to estimate permeability.

The Olin well core, which was analyzed by Kolkas in 1998, is examined stratigraphically to see which layers have the most favorable permeability (Figure 3.12). The Yellowjacket and Vespa member picks were based on Smith et al.'s (2010) top picks of the same well, as well as cutting analyses (Appendix C). No suitable RHOB or NPHI logs exist at this well for comparison of porosity tests.

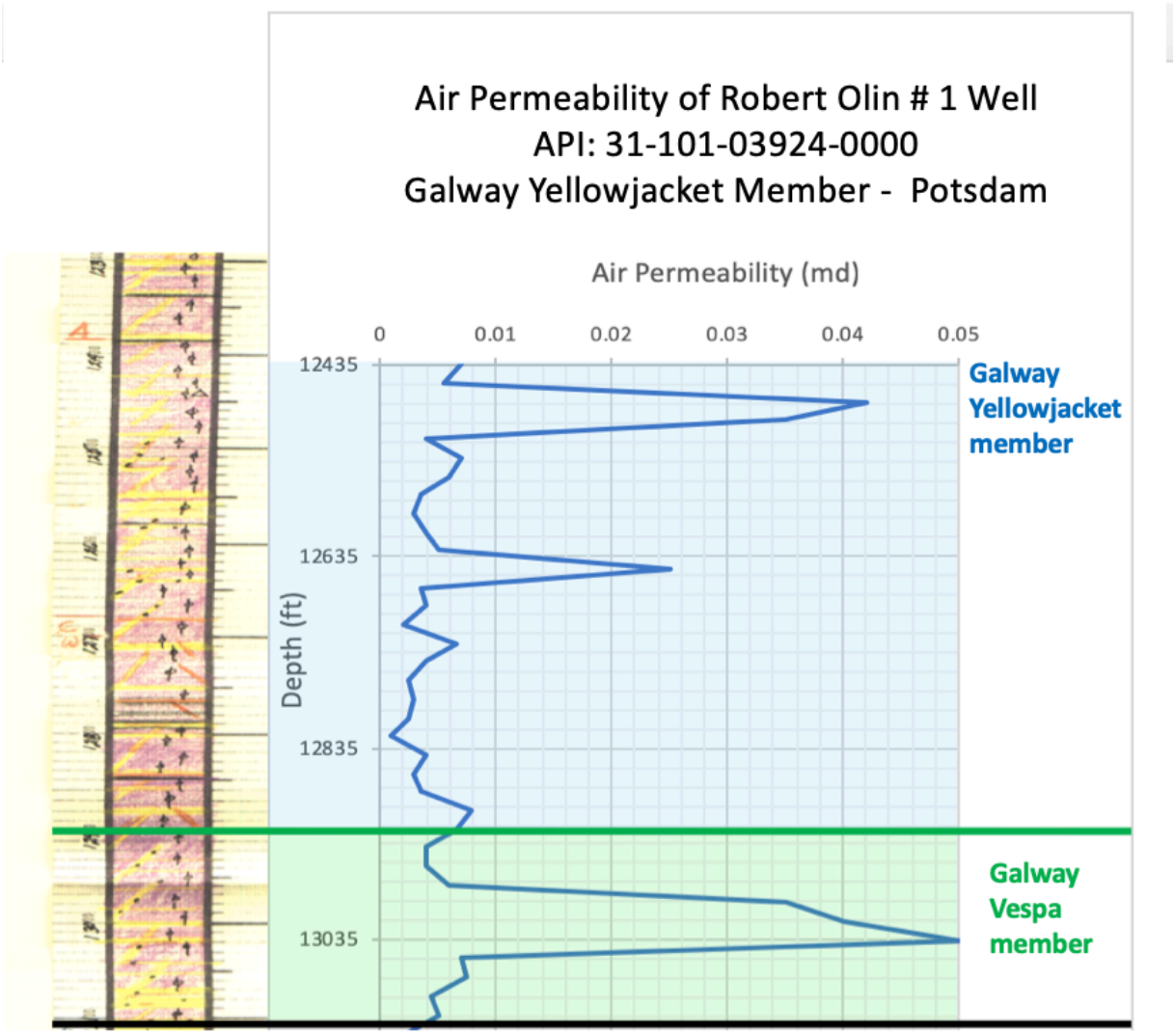

Figure 3.12: Air Permeability results of a core from the Olin [N-650-S] well conducted by Kolkas in 1998. The portion of the chart in blue represents the informal Galway Yellowjacket member, and in green is the informal Galway Vespa member. Figure modified from Kolkas, 1998. The figure is aligned with cuttings reports from the ESOGIS database (2019) as a visualization of lithological changes and reasoning for stratigraphic picks. Overall, air permeability is uniformly low throughout. Lithologies in the cuttings report use yellow to symbolize sands, and pink to symb olize dolomites. Depths are in MD.

Throughout the Olin well, reported porosity is low (up to 4% in thin sections). Air permeability at this interval is also low, with a range of 0 - 0.05 millidarcys across the section of the Galway Formation. Air permeability maxima are ~ 0.042 md at about 12,475 feet TVD, ~ 0.025 md at about 12,550 feet TVD, and ~ 0.05 md at approximately 13,035 TVD. The first two maxima are at the Yellowjacket member, and the third maximum is at the Galway Vespa member. From this well, the Vespa member seems to have the best air permeability at 0.05 md, which is still very low.

Kolkas' study on well cuttings porosity is compared to corrected NPHI well log porosity at the Mitchell 1 well (Figure 3.13). The results differ greatly: physical sample porosity is low, with an average porosity of about 4% and maximum of 7%. Corrected NPHI porosities, on the other hand, have an average porosity of about 10% and maximum porosity of about 22%. There do not appear to be any clear similarities in patterns of increasing or decreasing porosity across the two methods. Because the physical sample was neither a full core nor a core sample, error in porosity occurs often when analyzing unconsolidated pieces instead of a core or core plug (American Petroleum Institute, 1998). This study assumes well log porosity to be a more suitable indication of formation porosity at Mitchell 1. As a result, it is assumed that the average porosity of the Beekmantown Group at Mitchell 1 is about 10%.

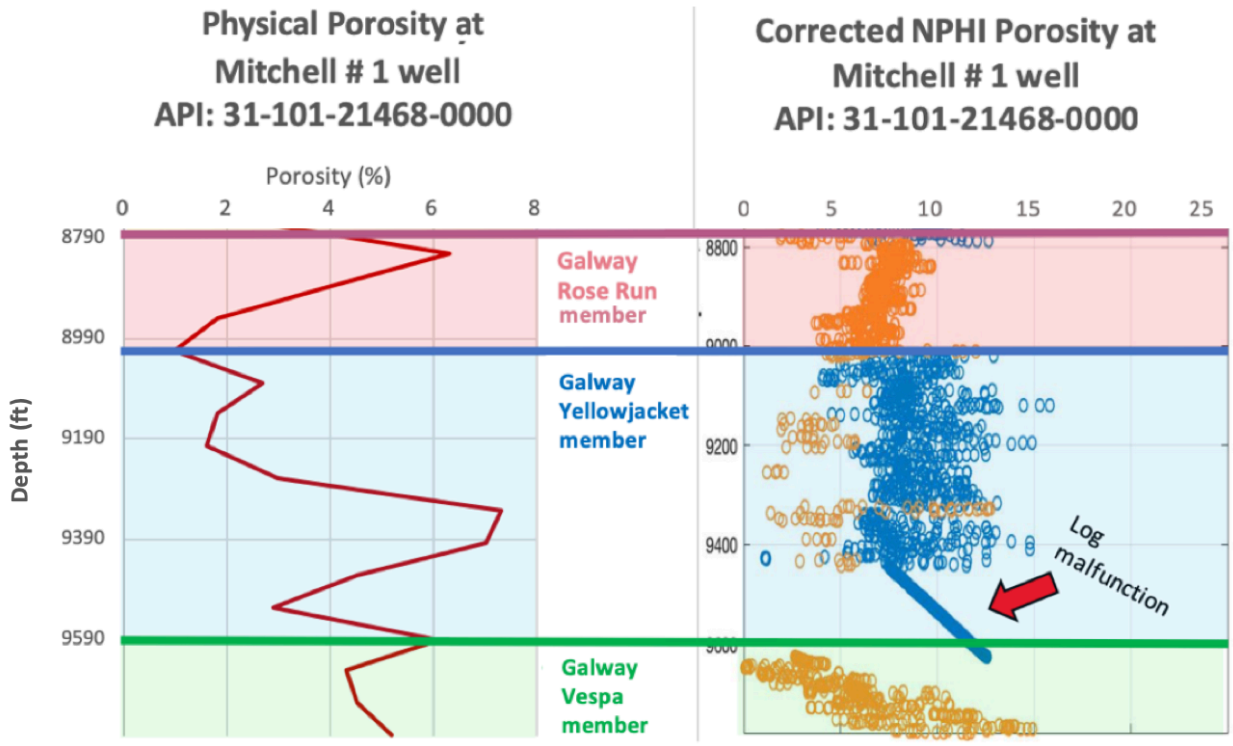

Figure 3.13: Comparison of cuttings porosity analysis conducted by Kolkas (1998) and corrected porosity log at the Mitchell # 1 well. The NPHI values are displayed as blue circles or dolomite, and orange for sandstone. Porosity from roughly 9,420 feet to 9,500 feet are an error from the NPHI log malfunction. Depths in feet TVD.

3.9: Potsdam: Porosity and Permeability

Approximately 47 miles (75 kilometers) southwest from Cornell, in Avoca, Steuben County, central NY, exists a cluster of wells that provide valuable insight on the Potsdam Formation and its properties. They are spaced up to 2 miles (3 kilometers) apart from each other, and were drilled for the purpose of exploring the Beekmantown Group as a candidate for gas storage. From north to south, these wells are the Fee 6 (API: 31-101-21636-0000), Mitchell 3 (API: 31-101-21633-0000), Avoca 4 (API: 31-101-21624-0000),), Mitchell 1 (API: 31-101-21468-0000), and Hubbard No.1 (API: 31-101-21496-0000) wells (Figure 3.14). Because of the similarity of the names Mitchell 1 and Mitchell 3, they are referred to here as the M1 and M3 wells, respectively. At this location, the Potsdam Formation is approximately 200 feet, or 60 meters, thick. Each of these wells contain GR, NPHI and RHOB logs which make finding true porosity possible. Two wells (M1 and Avoca 4) have PEF logs used to better identify lithologies, and a spectral GR log that also better identifies the composition of the Potsdam, which becomes an important identifier for one of its members later in this section. Also,

Kolkas (1998) measured porosity and air permeability for cuttings samples from M1.

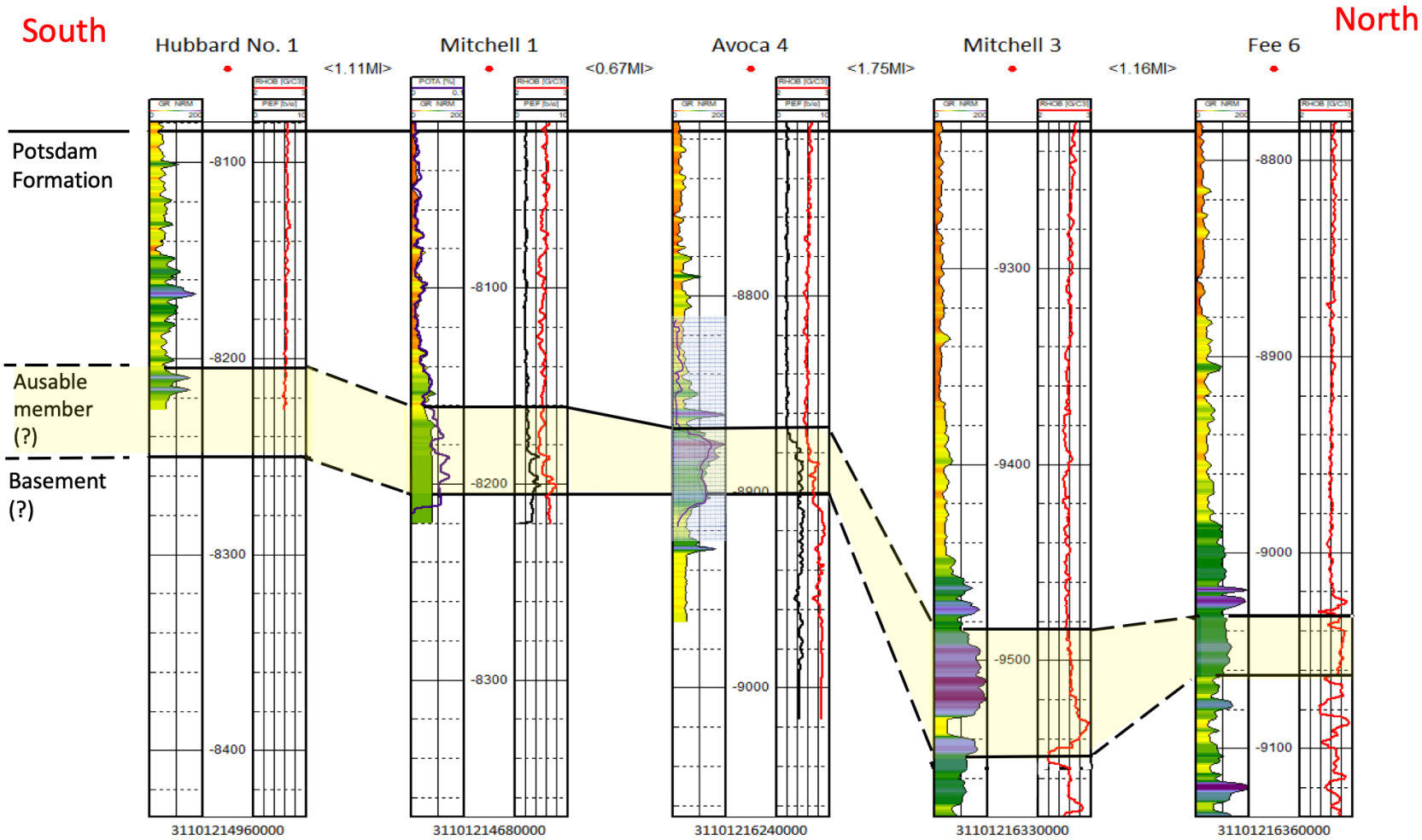

Figure 3.14: N-S cross-section of wells at Avoca, Steuben Country, central NY, flattened at the top of the Potsdam Formation. Depths are in SSTVD. The Potsdam Formation in the Mitchell 3 (M3) well appears to be both thicker and deeper than in the rest of the wells. GR and RHOB logs are used to pick tops. Dashed lines indicate uncertain top picks. The Ausable member is identified using the Spectral GR log, which is depicted in a bold purple line overlaying the GR log. Due to the absence of the Spectral GR log, the top of the Ausable member is interpolated at the other wells using the GR and RHOB logs. Stratigraphic top names is shown in the far left.

The Potsdam sandstone has two members: the basal Ausable member and overlying Keenesville member. The basal Ausable member is characterized in outcrop by four non-marine facies that include massive conglomerate, bedded conglomerate, conglomerate-arkose fining upward sequences, and conglomerate arkose. These facies are interpreted as representative of debris flows and braided-stream deposits. The arkosic composition in outcrop is the basis for attributing "feldspar wash" reported in boreholes to the Ausable member. The Keeneseville member represents the first marine onlap over the Proterozoic basement, and is composed of bedded fine-to-medium grained quartz arenite, and represents subaqueous, nearshore, tidal deposition (Husinec and Donaldson, 2014). The top of the Potsdam Formation is interpolated to be at about 9,450 feet, or 2,880 meters TVD at Cornell's location, and is roughly 200 feet (60 meters) in thickness in central NY.

The Potsdam has acted as an aquifer for hydrothermal fluid expelled from the basement to the Cambrian and Ordovician strata during the Taconic Orogeny. Evidence of this can be seen in the Late Ordovician (450 Ma) overgrowths of monzonite in the Potsdam, as well as the dolomitization of the Proterozoic marble (Selleck, 1997; Allaz et al., 2013).

In 1998, Kolkas conducted a study on the porosity and air permeability of core plugs at the Robert Olin #1 (N-650-S) well in Steuben County, central New York (API: 31-101-03924-0000) (Figure 3.15). Air permeability at the Potsdam is low, at less than 0.01 md.

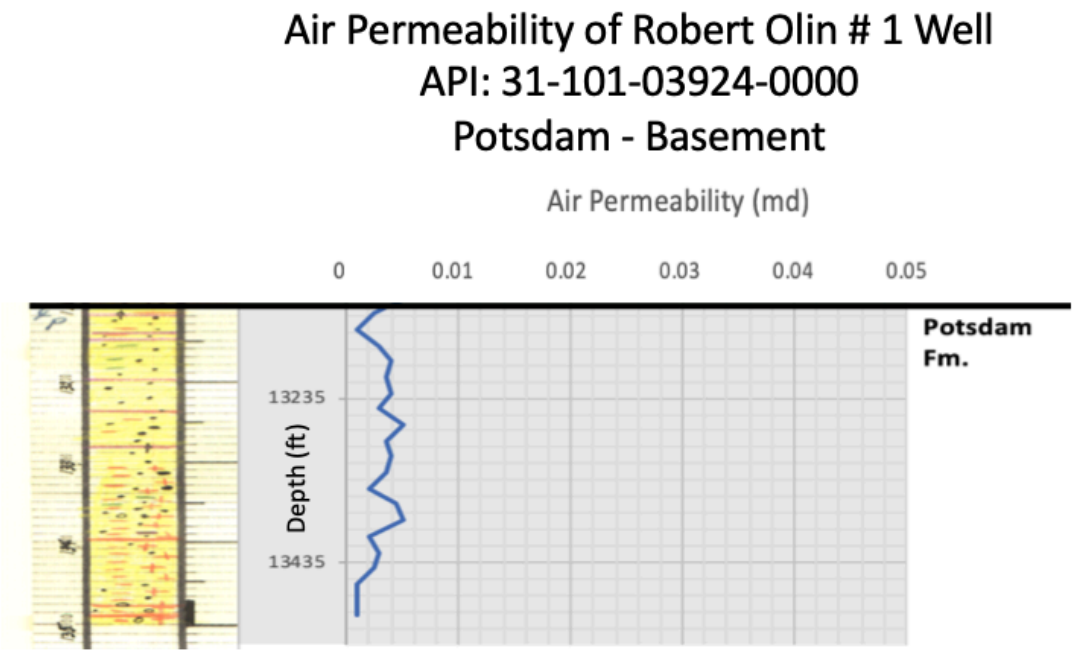

Figure 3.15: Core plug air permeability of the Potsdam Formation at the Robert Olin 1 (N-650-S) well (API: 31-101-03924-0000), conducted by Kolkas in 1998. The figure is aligned with cuttings reports from the ESOGIS database (2019) as a visualization of lithological changes and reasoning for stratigraphic picks, in which yellow stands for sandstone and pink stands for dolomite. Figure modified from Kolkas, 1998.

The zone of interest to this study is the basal Ausable member. This is because it has been reported that stratigraphic tests of the Potsdam Formation indicated exceptionally high permeability of 200-960 md at the Mitchell 1 well (API: 31-101-21468-0000) in Steuben County, central NY (Guo et al., 1996). However, when other wells were drilled within 2 miles of Mitchell 1, none of them had any intervals that were particularly porous or permeable. (Lugert et al, 2006). It is unknown why the Mitchell 1 had such high permeability, and the particular depths and thicknesses of this permeable zone within the Cambrian have not been reported. Additionally, the study conducted by Kolkas (1998) in this well indicates very low air permeability at the Potsdam (Figure 3.15).

In western NY the basal Ausable member is a prolific gas reservoir wherever there exists a structural closure or fracture system to serve as a trap (Bastedo and Van Tyne, 1990). However, porosity and permeability studies conducted on the Avoca 4 well less than a mile west of the Mitchell 1 well document low porosity and permeability (Lugert et al., 2006).

At Avoca 4 (API: 31-101-21624-0000), which is less than a mile away from Mitchell 1, the Φ_{cn} of the Potsdam within the Ausable increases slightly with depth by about 1% per 50 feet over a distance of around 200 feet. The porosity was a modest amount and ranged from ~0% at the top of the Potsdam to about 11% near the bottom. Minimum, maximum, and average Φ_{cn} are approximately 5%, 7% and 11% within the bottom 50 feet (TVD) of the Potsdam analyzed at Avoca 4. Cuttings analysis of the Mitchell 1 well indicate an ambiguity of the presence of the basal Ausable member or feldspars at these depths. At both wells, the Potsdam decreases in density and increases in porosity with increasing depth. The presence of potassium feldspars are confirmed to be present at Avoca 4 by a spectral GR potassium log, which is available as a raster image. At both M1 and Avoca 4, when potassium content increases, the GR and spectral gamma

log also increase, as expected (Figure 3.16). Although the cuttings indicate no conclusive evidence of the basement, the PEFZ and density logs show with more certainty that the top of the basement is probably at the point when both logs begin to substantially increase. If this is so, the Ausable member is only about 40 feet (~12 meters) thick at both M1 and Avoca 4, from ~9,840 - 9,880 feet or ~3,000 – 3,011 meters TVD. Corrected porosity from the NPHI logs were difficult to analyze since the potassium within the Gamma Ray log deflects in the same way shale would. Therefore, the corrections applied to the NPHI log have been modified to omit any 'shale presence' corrections, which results in an increase in uncertainty in Φ_{cn} (see Chapter 2.5). It appears that with increasing potassium content, the porosity also increases (Figure 3.17). The point at which the potassium log value is greatest (at 9856 feet TVD) is also the point at which corrected porosity is at one of its highest points at the Potsdam (15%). The same maximum porosity of the Potsdam is calculated for the Avoca 4 well, and is also the highest porosity value found in the Beekmantown Group for this well. For both wells, shale corrections had been omitted to properly calculate porosity of the feldspathic sands.

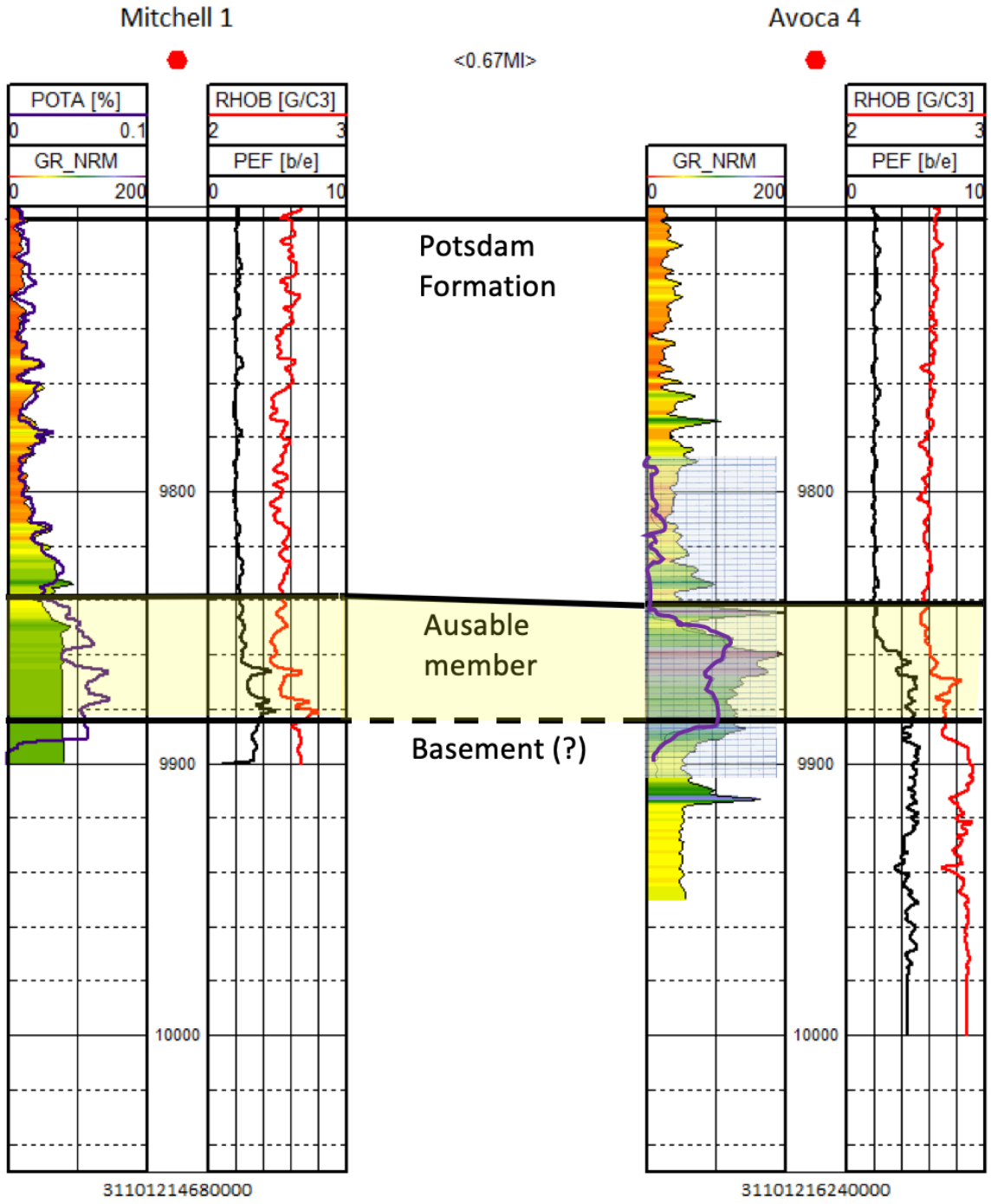

Figure 3.16: Logs of the Mitchell 1 (M1) and Avoca 4 wells in Steuben County, central NY. Avoca 4 is 0.67 miles west of M1. The basement is estimated to be at horizons where the PEF and RHOB logs begin to sharply increase, and its uncertain top is depicted in a dashed line. For Mitchell 1, the potassium spectral log of the GR log (POTA), in purple, is overlaid on the GR log. For Avoca 4, the Spectral GR log is drawn using its raster image, and is also depicted in a bold purple line. It appears that the Ausable arkosic sandstone member of the Potsdam 40 feet in thickness for both wells, and is highlighted in yellow.

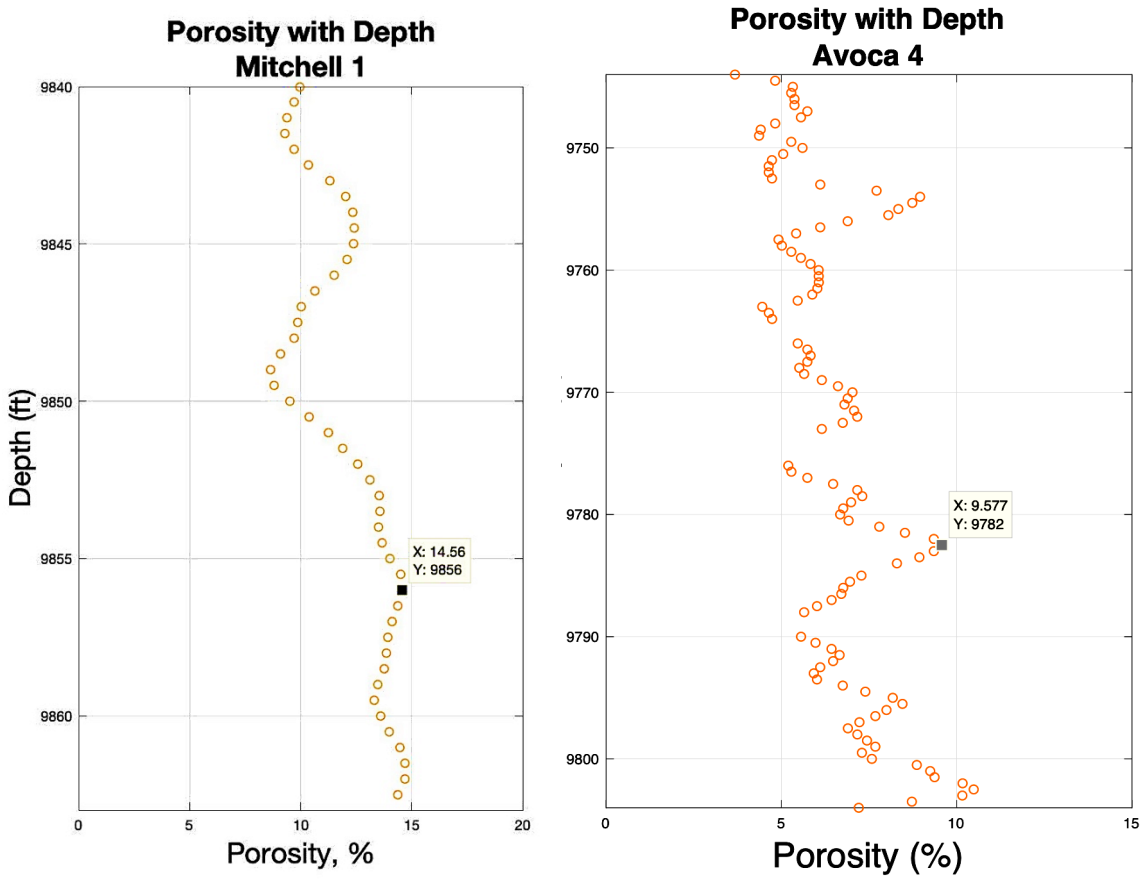

Figure 3.17: Left: NPHI log porosity of the Potsdam sandstone Ausable member to the top of the basement, from 9,840 to 9,863 feet (~3,000 – 3,006 meters) at the Mitchell 1 (M1) well in Steuben County, central NY. NPHI porosity corrected for gas, but not shale. The point at 9,856 feet is highlighted here to link with the point at which the potassium content is highest, according to the Spectral GR log. Right: Porosity of the Potsdam sandstone Ausable member, from 9,744 -9,804 feet (~2,970 – 2,988 meters) at the Avoca 4 well in Steuben County, central NY. NPHI porosity corrected for gas, but not shale .The point at 9,782 feet (~2,982 meters) is highlighted here to link with the point at which the potassium content is highest, according to the Spectral GR log.

Reports of cuttings of the Mitchell 3 (M3) well are available and indicate the presence of 'wash' (here interpreted as part of the Ausable member) as well as anhydrite at the bottom of the Potsdam.

Based on porosity observations and cuttings reports, the depth spanned by the Ausable member at M3 is interpreted to be 30 feet (9 meters) thick, from ~9,770 – 9,815 feet (~2,980 - 2,990 meters) TVD (Figure 3.18). The maximum porosity at this zone is around 24%. This is the only well that contains a zone of relatively high (> 20%) porosity that may be related to the presence of the Ausable. It is also the only well that exhibits this zone of very low density of about 2.2 – 2.5 g/cm^3.

There are many possible reasons for the M3 anomaly. The first is that the strata in M3 may be less compacted than those at the other wells. The second is that its location at a paleogeographic low may have allowed for primary or diagenetic sedimentary rock properties to differ at this particular location in a manner that is favorable for porosity. Alternatively, the data itself is unique in its high porosity (for the Galway, corrected porosity is up to 50%), which may indicate that the data may have errors, or higher uncertainty associated with it. Finally, the presence of faults that are located only at M3 may also be the cause for this increased porosity.

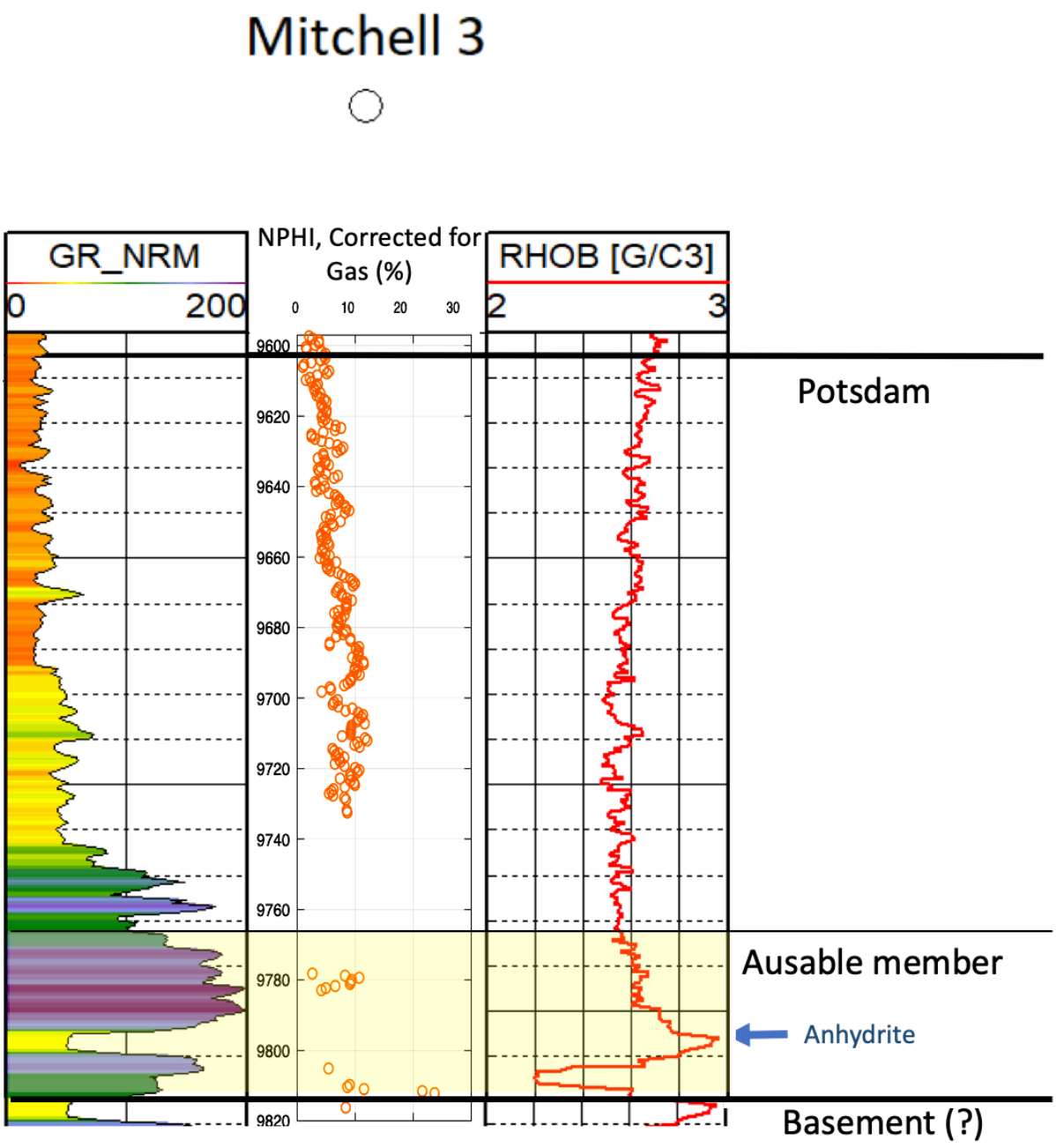

Figure 3.18: Well logs of the Mitchell 3 (M3) well in Steuben County, central NY from the Potsdam to the basement. The interval interpreted to be the Ausable member is highlighted in yellow, and is only 10 feet thick. Depths here are in TVD. The Ausable member here is interpreted to be at ~9,770 to 9,815 feet, or ~ 2,980 – 2,990 meters TVD. In the NPHI log, sandstone is displayed in orange. Cutting reports indicate the presence of anhydrite, which is dense and labeled with a blue arrow. Relatively high porosity of 3-24% exists at the Ausable.

In outcrop, the Ausable member has a discontinuous lateral and isopach distribution and its presence is tied to the presence of faults Figure (3.19) (Lowe et al., 2017). It was reported that the Ausable is typically present and thickest within grabens, and thin toward hanging walls. This may be the case with the Ausable at M3 and F6, which are deeper than the Ausable at the Avoca 4, Mitchell 1 and Hubbard No. 1 wells.

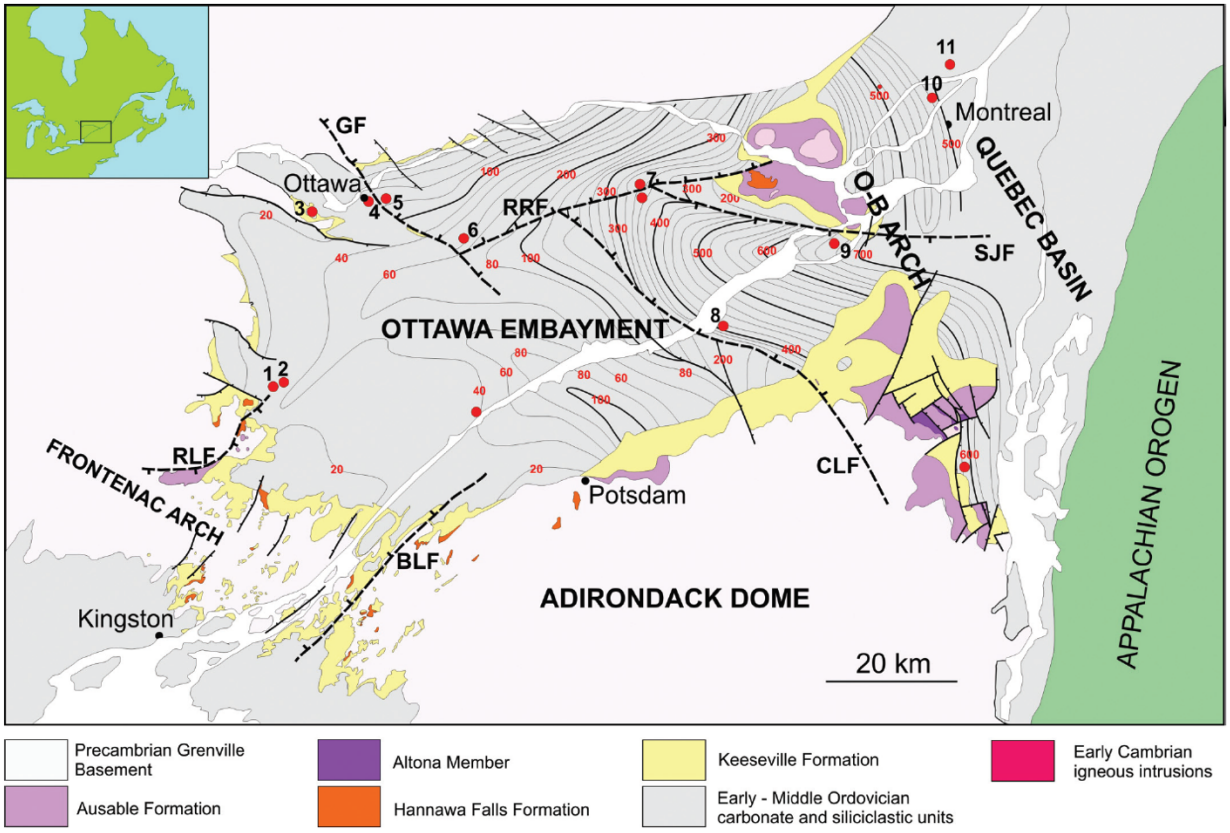

Figure 3.19: Geologic and isopach map of the Potsdam in the Ottawa Embayment and Quebec Basin. The Ausable member is in purple, and bounded by faults (from Lowe et al., 2017).

3.10 Synthesis of Overall Regional Analysis of Porosity and Permeability

Reported studies of porosity from cores, plugs and thin sections have been compared to NPHI porosity logs that have been corrected for presence of gas and shale across central and western New York. Boxplots of all wells analyzed for true NPHI porosity, corrected for the presence of gas and shale, have been generated to analyze porosity trends by formation (Figure 3.20). The average Φ_{cn} of 5 - 12% is similar across the Beekmantown Group formations. The Little Falls and Galway Formations have the greatest amount of outliers and the highest maximum porosity of about 40% and 55%, respectively. Porosity does not appear to change regionally (for example, the porosity of the Galway formation in central NY is similar to its porosity at western NY), but sandy beds appear to predominantly have higher porosity than others.

Studies conducted by Kolkas (1998), Lugert et al. (2006), and Smith et al. (2005; 2010), were conducted regionally to assess the reservoir quality of the Beekmantown Group. All studies conclude that the Potsdam Formation is likely to be the best reservoir. This study partially agrees with the conclusions of previous assessments: although the Potsdam Formation has a reportedly high permeability of almost one darcy, the report is singular in its findings and the source of the data is difficult to trace (Guo et al., 1996). It is ambiguous which section of the Potsdam Formation is attributed to this reportedly high permeability, and no other nearby wells have any reports of this high permeability. While the Potsdam Formation is still considered to have a high potential as a reservoir at the Ausable member, this study will also err on the cautious side and recommend the Galway as another potential formation with higher porosity and permeability, especially at the informal Rose Run sand member.

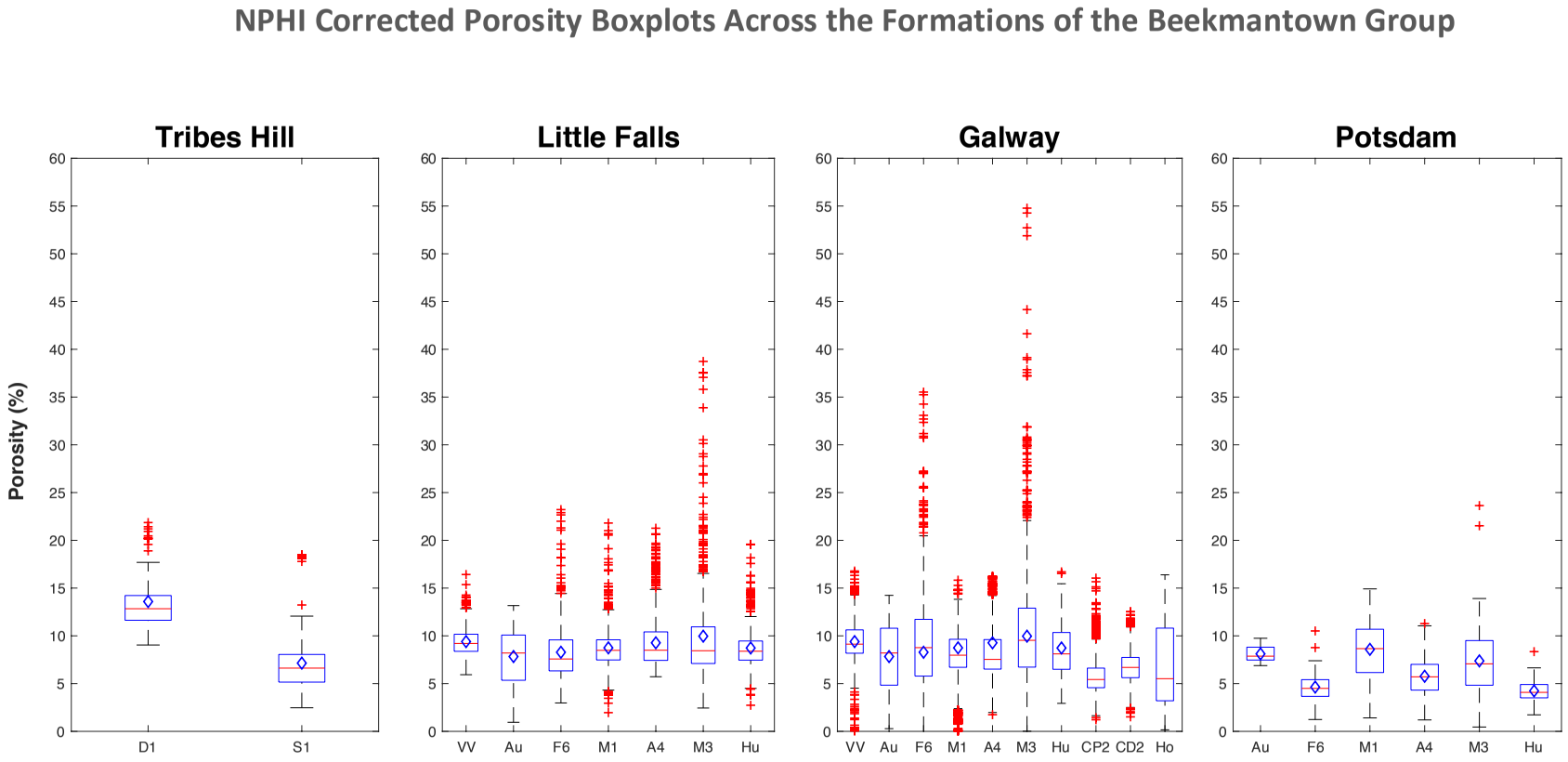

Figure 3.20: Box and whiskers plots of formations of the Beekmantown Groups and their corrected porosities. Well names, on the x-axis, are abbreviated. A full list of wells used and their corrected porosities can be found in Appendix D. Porosity means are represented by red horizontal lines, medians are represented by blue diamonds, and outliers are represented by red plus symbols. Whiskers at the bottom of the box represent the smallest non-outlier, and at the top represent the largest non-outlier. The box consists of data from the first quartile (bottom of box) to the third quartile (top of box).

3.11 Interpolation of Subsurface Stratigraphic Tops at Cornell University

Along with cuttings analyses, the Petra software was used to pick formation tops from logs of wells at western and central NY (see Appendices A and C). Cornell's location and elevation were used to estimate the depths and thicknesses of the sub-Knox formations in the subsurface beneath Cornell University. Cornell University is investigating the viability of all subsurface strata found at depths with suitable temperature gradients at 2.3 km or below. Based on interpolations from other nearby wells on a N-S cross-section, the shallowest formation expected to be encountered at that depth is the Black River Group (Figure 3.21). The contact of Trenton and Black River Groups is expected to be at 2.28 +/- 0.2 km TVD. The top of the Beekmantown Group at Cornell, the Tribes Hill Formation, is expected to be encountered at 2.36 km +/- 0.2 km. The top of the Little Falls Formation is expected to be at 2.38 km +/- 0.2 km TVD. The top of the Little Falls Formation is expected to be at 7,955 ft or 2.425 km TVD. At 2.56 km +/- 0.2 km, the top of the Rose Run Member of the Galway Formation is interpolated at Cornell's location. The Yellowjacket member of the Galway is estimated to be at about 2.60 +/- 0.2 km TVD. The top of the Vespa member of the Galway is estimated to be at 2.70 +/- 0.3 km TVD. Finally, the top of the Potsdam is expected to be found at 2.76 +/- 0.2 km TVD and have a thickness of about 0.4 km. Thus, the depth to basement is expected to be 2.80 km +/- 0.2 km.

The top of the Ausable member of the Potsdam Formation appears to be variably present. It is possible that the presence of the Ausable is more likely to be found at paleovalleys, and that factors such as the presence of fault may present some relatively favorable reservoir quality at the Potsdam. The Ausable Member is present at the Shepard 1 well just 6 miles away from Cornell. Therefore, there is a chance that it is also present at the location Cornell chooses as its drill site.

North South

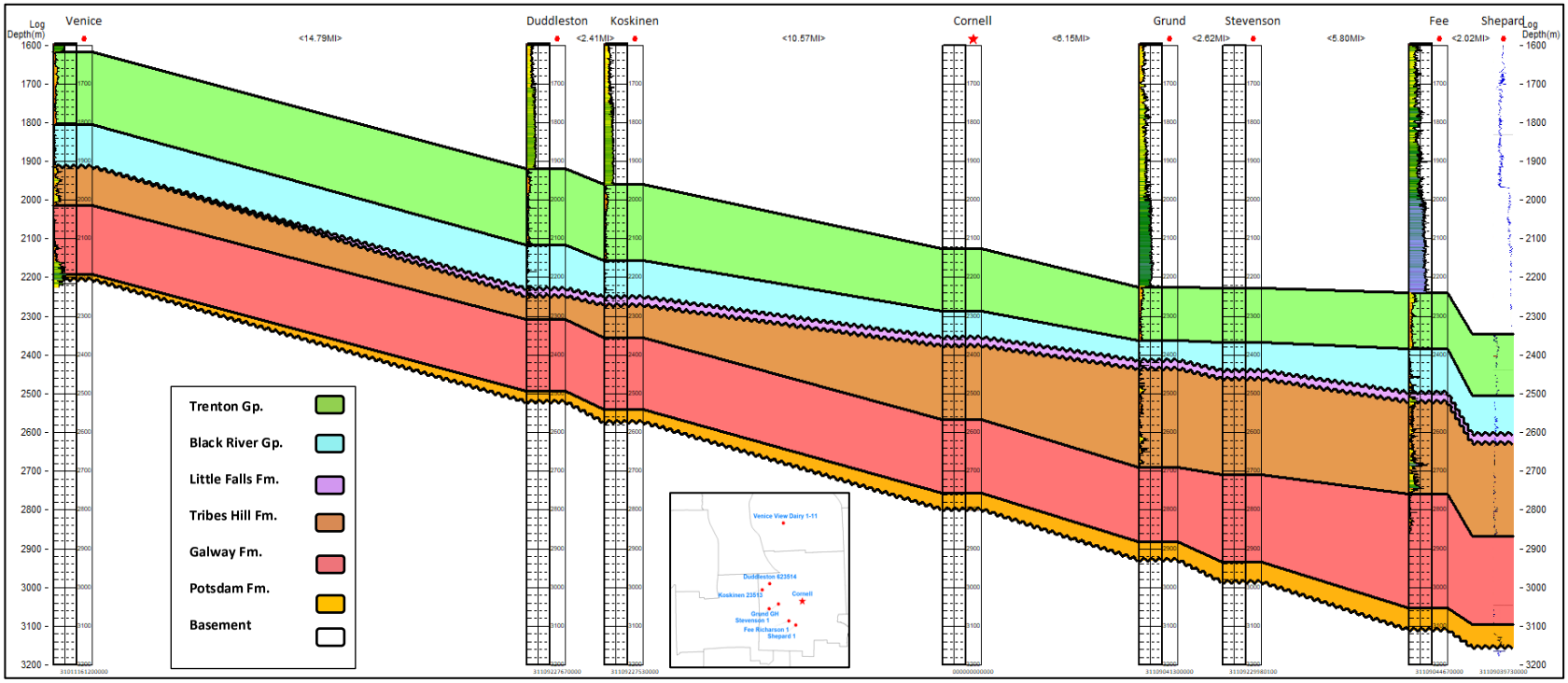

Figure 3.21: North-South cross-section of wells used for the interpolation of Cambro-Ordovician strata at Cornell's subsurface. To the sides are depths, in meters TVD. Wavy lines denote tops directly below an unconformity. An inset map is included with the geographic locations of wells used for the cross-section. In brackets are distances between wells. The raster image of the Shepard 1 GR log, digitized by Teresa E. Jordan, is included in the analysis.

REFERENCES

American Petroleum Institute, 1998, Recommended practices for core analysis: Recommended Practice, v. 40, 236 pp.

Bastedo, J.C. and Van Tyne, A.M., 1990. Geology and Oil and Gas Exploration in Western New York. Fieldtrip Guidebook Western New York and Ontario, NYSGA 62nd Annual Meeting.

Braun, M. and Friedman, G.M., 1969, Carbonate lithofacies and environments of the Tribes Hill Formation (Lower Ordovician) of the Mohawk Valley, New York: Journal of Sedimentary Petrology, v. 39, p. 113-135.

Curl, M.W., Zagorski, T.W., and Friedman, G.M., 1984, Depositional environments and diagenesis of subsurface Tribes Hill Formation (Lower Ordovician), Mohawk Valley, New York: The Compass of Sigma Gamma Epsilon, v. 61, no. 4, p. 216-243.

Empire State Organized Geologic Information System (ESOGIS), New York State Museum, www.esogis.nysm.nysed.com (April 2019)

Fisher, D.W., 1954, Lower Ordovician (Canadian) stratigraphy of Mohawk Valley, New York: Geological Society of America Bulletin, v. 65, p. 71- 96.

Fisher, D.W., 1977, Correlation of the Hadrynian, Cambrian and Ordovician rocks in New York State: New York State Museum Map and Chart Series No. 25, 75 p.

Guo, B., Friedman, G.M., Bass, J.P., and Sarwar, G., 1996, Underground gas storage in the Cambro-Ordovician succession of southeastern New York: A preliminary study: Northeastern Geology and Environmental Sciences, v. 18, nos. 1/2, p. 49-58

Harris, R.L. and Friedman, G.M., 1982, Depositional environments of the subsurface Ogdensburg Formation (Lower Ordovician) in northern New York State: Northeastern Geology, v. 4, p. 151-166.

Husinec, A., and Donaldson, J.A., 2014, Lower Paleozoic Sedimentary Succession of the St. Lawrence River Valley, New York and Ontario: Field Trip A-1, *in* Chiarenzelli, J., and Valentino, D., eds., Geology of the Northwestern Adirondacks and St. Lawrence River Valley, p. A1 – A28

Landing, E., 2012, The great American carbonate bank in eastern Laurentia: Its births, deaths, and linkage to paleoceanic oxygenation (Early Cambrian – Late Ordovician), *in* J.R. Derby, R.D. Fritz, S.A. Longacre, W.A. Morgan, and C.A. Sternbah, eds., The great American carbonate bank: The geology and economic resources of the Cambrian—Ordovician Sauk megasequene of Laurentia: AAPG Memoir 98, p. 451-492.

Lowe, D.G., Arnott, R.W.C., Nowlan, G.S., and McCracken, A.D., 2017, Lithostratigraphic and allostratigraphic framework of the Cambrian-Ordovician Potsdam Group and correlations across Early Paleozoic southern Laurentia: Canadian Journal of Earth Sciences, v. 54, p. 550-585.

Lugert, C., Smith, L., and Nyahay, R., 2006, Systematic technical innovations initiative: Brine disposal in the Northeast. Final Report. Albany, NY, New York State Energy Research and Development Authority, 269 pp.

Martin, J., 2010, New York geothermal overview. Powerpoint presentation.

McCann T. P., Privrasky, N. C., Stead, F. L., and Wilson J. E, 1968, Possibilities for disposal of industrial wastes in subsurface rocks on north flank of Appalachian Basin in New York: *in* Subsurface disposal in Geologic Basins: AAPG Memoir 10, 10 pp.

New York State Energy Research and Development Authority, 2011, Carbon sequestration feasibility study in the Chautauqua County, New York Area: Final Report.

Rickard, L. V., 1973, Stratigraphy and structure of the subsurface Cambrian and Ordovician carbonates of New York : New York State Museum and Science Service, Map and Chart Series 18, 50 pp.

Smith, L., Nyahay, R., and Slater, B., 2010: Integrated reservoir characterization of the subsurface Cambrian and lower Ordovician Potsdam, Galway and Theresa Formations in New York: Albany, NY, New York State Energy Research and Development Authority, 69 pp.

Smith, L., Lugert, C., Bauer, S., Ehgartner, B., and Nyahey, R., 2005, Systematic technical innovations initiative: Brine disposal in the Northeast: Albany, NY, New York State Energy

Zenger, D. H., 1981. Stratigraphy and Petrology of the Little Falls Dolostone (Upper Cambrian), East-Central New York: New York State Museum Map and Chart Series No. 34.

CHAPTER 4:

THE EFFECT OF THE KNOX UNCONFORMITY ON THE POROSITY OF UNDERLYING STRATA:

A COMPARISON OF WESTERN AND CENTRAL NEW YORK

4.1 Abstract

The erosional effects of an unconformity may increase the porosity of the strata directly beneath it. In western New York, the increased porosity caused by contact with the Knox Unconformity has made the Galway Formation a prolific gas reservoir. By contrast, the Galway Formation in central New York is not commonly a producing reservoir. To characterize the possible effects of the Knox Unconformity on reservoir quality, this study compares the porosity of the Galway in two places: Wyoming County, western New York, where the formation directly underlies the unconformity, and Steuben County, central New York, where it is separated from the Knox Unconformity by the Little Falls Formation. Gamma ray, neutron porosity, density, and photoelectric factor well logs of the Galway formation in 3 wells in Wyoming County, western New York and 5 wells in Steuben County, central New York are used to calculate effective porosity and examine the possible effects of the contact of the Knox Unconformity to the porosity of these strata. Results indicate that the section of the Galway that produces gas in western New York is actually the interbedded sands and dolomites below the Rose Run member of the Galway. Porosity values of this interval in central New York appear to be similar to porosity of the same interval in western New York. This suggests that the Knox Unconformity may not have a great effect on the porosity of underlying strata.

4.2 Introduction

Studies on hydrocarbon accumulation in the Cambro-Ordovician Beekmantown Group dolomites of Ohio, known there as the Beekmantown Dolomite, have concluded that production was confined to about 150 feet below the Knox Unconformity (Figure 4.1). A study by Smosna et al in 2005 was conducted on the karst-hydrogeologic system that formed within the Beekmantown Dolomite. Lateral and vertical distribution of porosity within the Beekmantown Dolomite was determined to be controlled by proximity to the Knox Unconformity, and possibly facilitated by fractures and hydrothermal fluids in areas of structural flexing. Higher porosity was also observed on paleohighs on which the unconformity occurred, and lower porosity was observed in paleovalleys. It was concluded that three factors have possibly contributed to the high porosity and permeability of the reservoirs: prolonged subaerial erosion from the Knox Unconformity, locations at structural highs, and the paleotopography of the Precambrian when sediments were deposited where paleohighs increased porosity and permeability (Dolly, 1969).

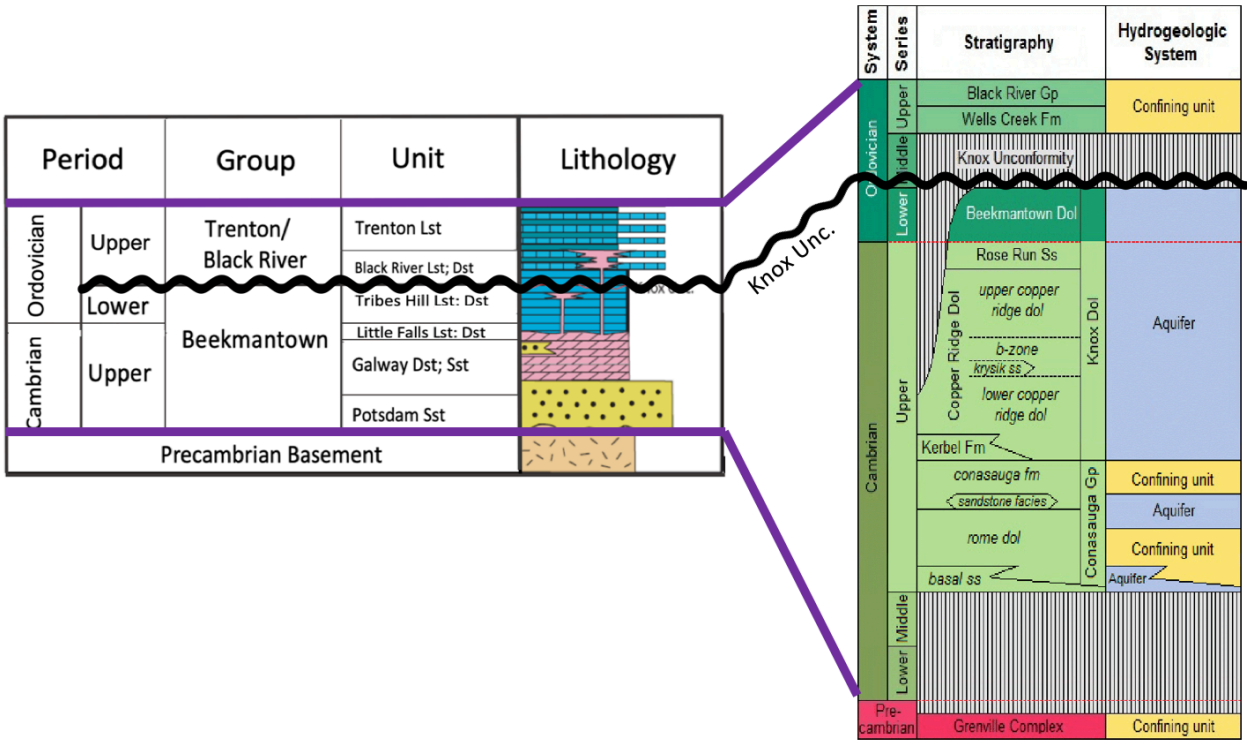

Figure 4.1: Comparison of stratigraphy of the Sauk megasequance at central NY (left) with the stratigraphy of the Sauk megasequence in Ohio (right). Images from Smith, 2006, and Gupta et al., 2017. The Beekmantown Dolomite directly subcrops the Knox Unconformity, and overlies the Rose Run sandstone. Both of these are established gas reservoirs due to their proximity to the Knox unconformity. Bold purple lines connect the stratigraphy based on age. The wavy red line symbolizes an unconformity.

Surveys found that the Galway Formation in western New York, which also subcrops the Knox Unconformity (yellow and orange zones, Figure 4.2), is likewise a viable play (Fagan and Copley, 1998). The findings of the report indicate that, similar to Ohio, increased reservoir quality of the Galway in western NY may be due paleogeographic, structural, and/or erosional factors. Of the three factors, this study will focus on the erosional effects of the Knox Unconformity on underlying strata. The Galway is not known to be a producing reservoir east of western NY, and the effect of the unconformity on reservoir quality is unknown in central New York. Given that the purpose of producing hot water for geothermal energy transfer is different than the purpose of most reservoir analyses of the Galway equivalent reservoir in Ohio, which is to find natural gas or oil, I examine the Galway play concept in a somewhat different manner.

The Knox Unconformity cuts deeper into the strata to the north and west so that it overlies the Galway Formation in western NY (Figure 4.2). This pattern makes it possible to observe the effect of the Knox Unconformity on the porosity of underlying strata by comparing the porosity of the Galway when it is in direct contact with the unconformity within western NY to the porosity where the Galway is in contact with the Little Falls Formation rather than with the unconformity, in central New York. At Steuben County, central NY, the Galway is conformably overlain by the Little Falls Formation.

The portion of the Galway in western NY is analogous to the Yellowjacket member of the Galway in central NY due to the thickness of the interbedded interval of the Galway in western NY, which is hundreds of feet or tens of meters. The thickness rules out the possibility of this interbedded interval being the basal Little Falls, which is much thinner.

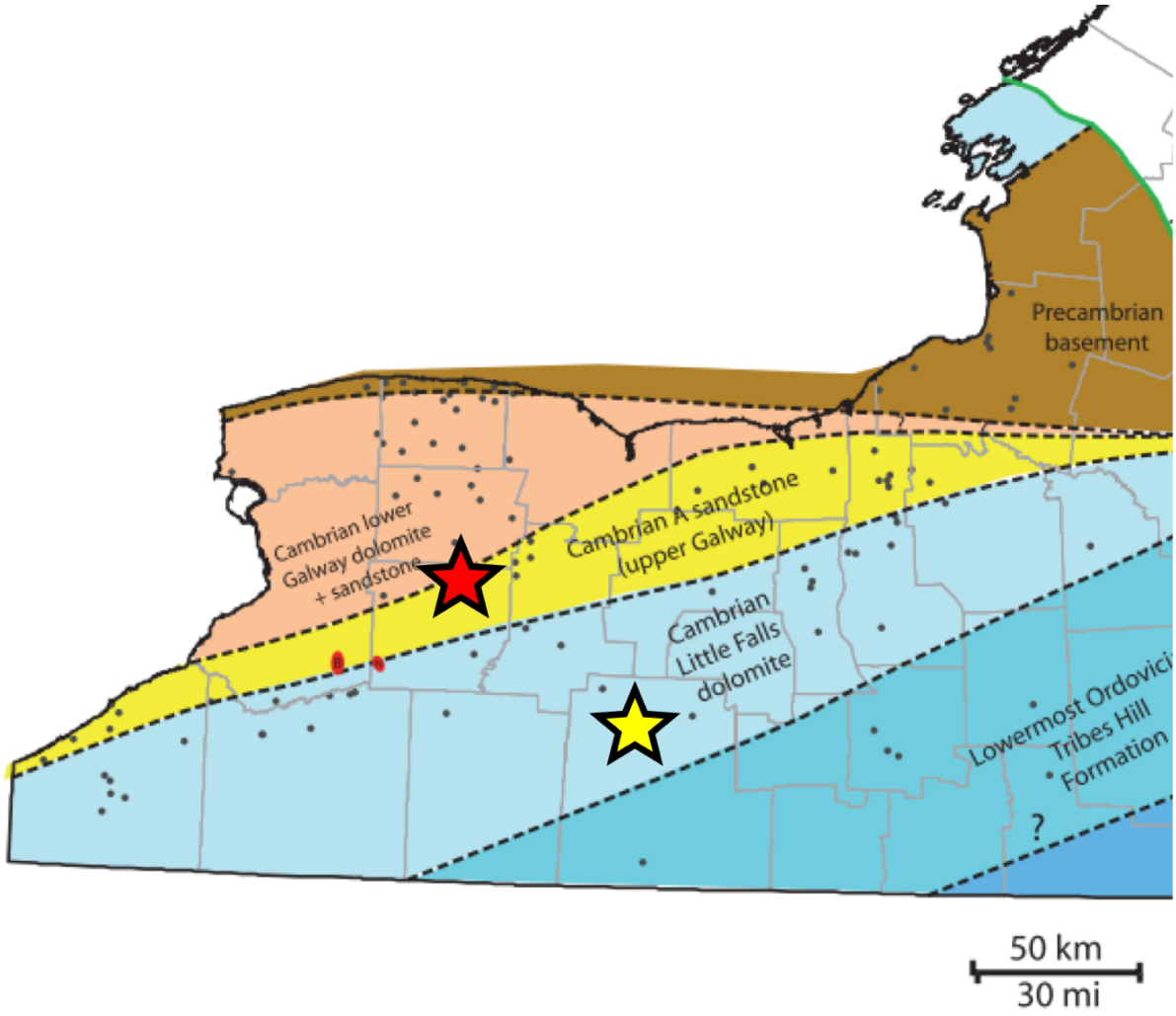

Figure 4.2: Map of formations that directly subcrop the Knox Unconformity in western and central New York. The location of a cluster of three wells used to conduct porosity analysis of the Rose Run member of the Galway Formation in western New York, where it is in direct contact with the Knox Unconformity, is denoted by the red star. Location of a cluster of five wells in Central New York, where the Rose Run is separated from the unconformity by the Little Falls Formation, is marked by the yellow star (modified from Smith et al, 2010).

4.3 Well Selection

The wells in Wyoming County and Steuben County were selected based on their proximity to one another (wells are < 2 miles or < 3 kilometers apart for each cluster of wells), drilled to depths of at least 100 feet below the Galway Formation, and the availability of GR, NPHI and RHO logs for each well (Figure 4.3.) The methods used to calculate Φ_n (raw NPHI porosity) and Φ_{cn} (corrected NPHI porosity, for both gas and shale presence) on the NPHI log are discussed in Section 2.4.

In Wyoming County, western New York, three wells fit the criteria: Howes A 2 (API: 31-121-21909-0000), Chamberlain D 2 (API: 31-121-21907-0000) and Chamberlain P 2 (API: 31-121-22053-0000). In Steuben County, central New York, five wells fit the criteria: the Hubbard No.1 (API: 31-101-21496-0000), Mitchell 1 (API: 31-101-21468-0000), Avoca 4 (API: 31-101-21624-0000), Mitchell 3 (API: 31-101-21633-0000), and Fee 6 (API: 31-101-21636-0000) wells.

The wells in western NY were not the ones where the Galway was the most productive because those wells did not have the required well logs for the NPHI log correction. However, one of the wells, the Howes A 2 well, was a well in which the Galway was a gas producer.

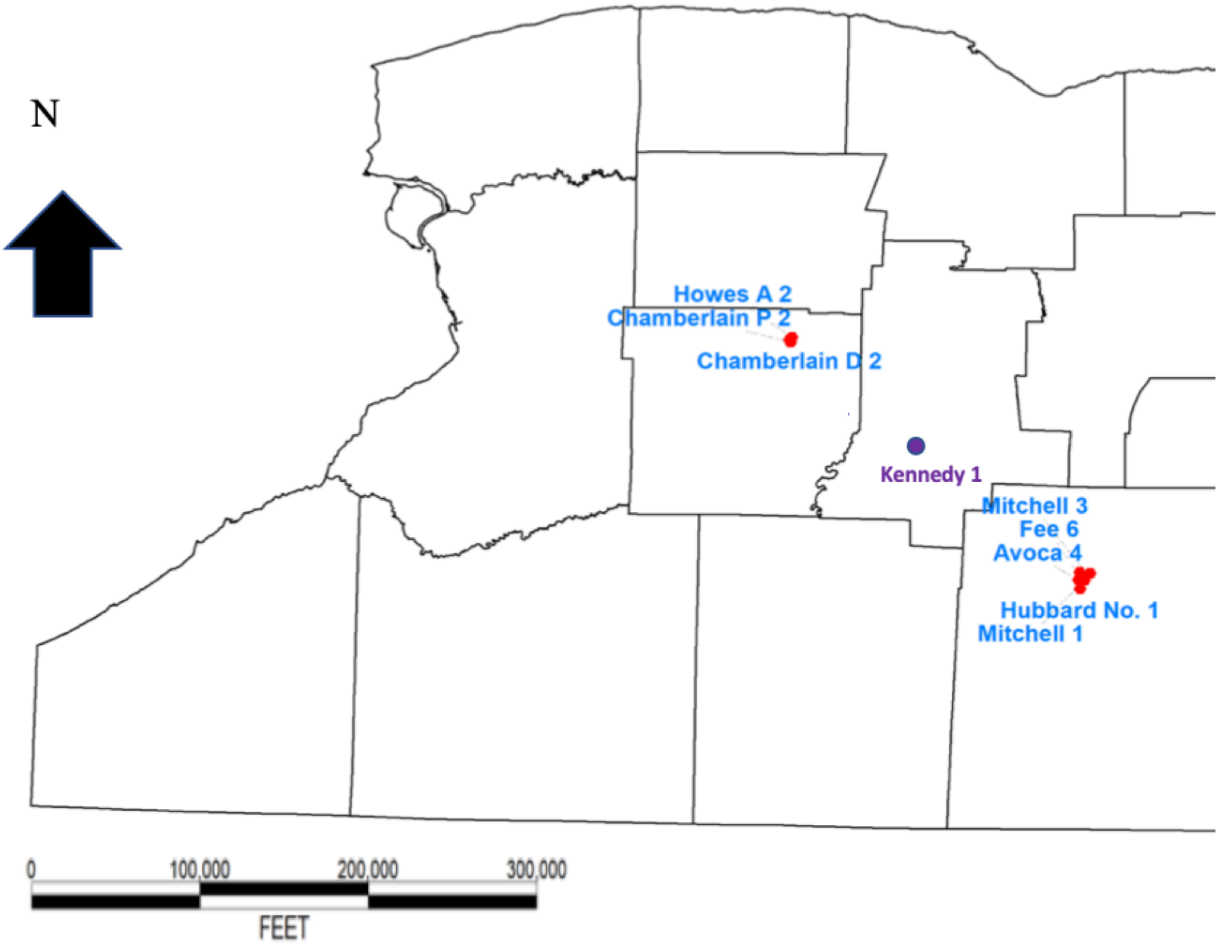

Figure 4.3: Map of approximate locations of the three wells located in Wyoming County, western New York, and 5 wells used in Steuben County, central New York, for the analyses conducted in this chapter. Included in purple are locations of wells with cores, plugs, or thin section reports that have been incorporated in this chapter.

4.4 Results and Discussion

Histograms of Φ_{cn} and their frequencies are compared for the Galway Formation in wells in central NY with the wells in western NY. For the five wells at central NY, the range of Φ_{cn} is 0 - 31 % (Figure 4.4 and 4.5A). The histograms for central NY are unimodal, with an average of 7% across all wells examined. The distribution of Φ_{cn} in western NY is bimodal (Figure 4.5), with a range of 0 -16% and lower average of 6%.

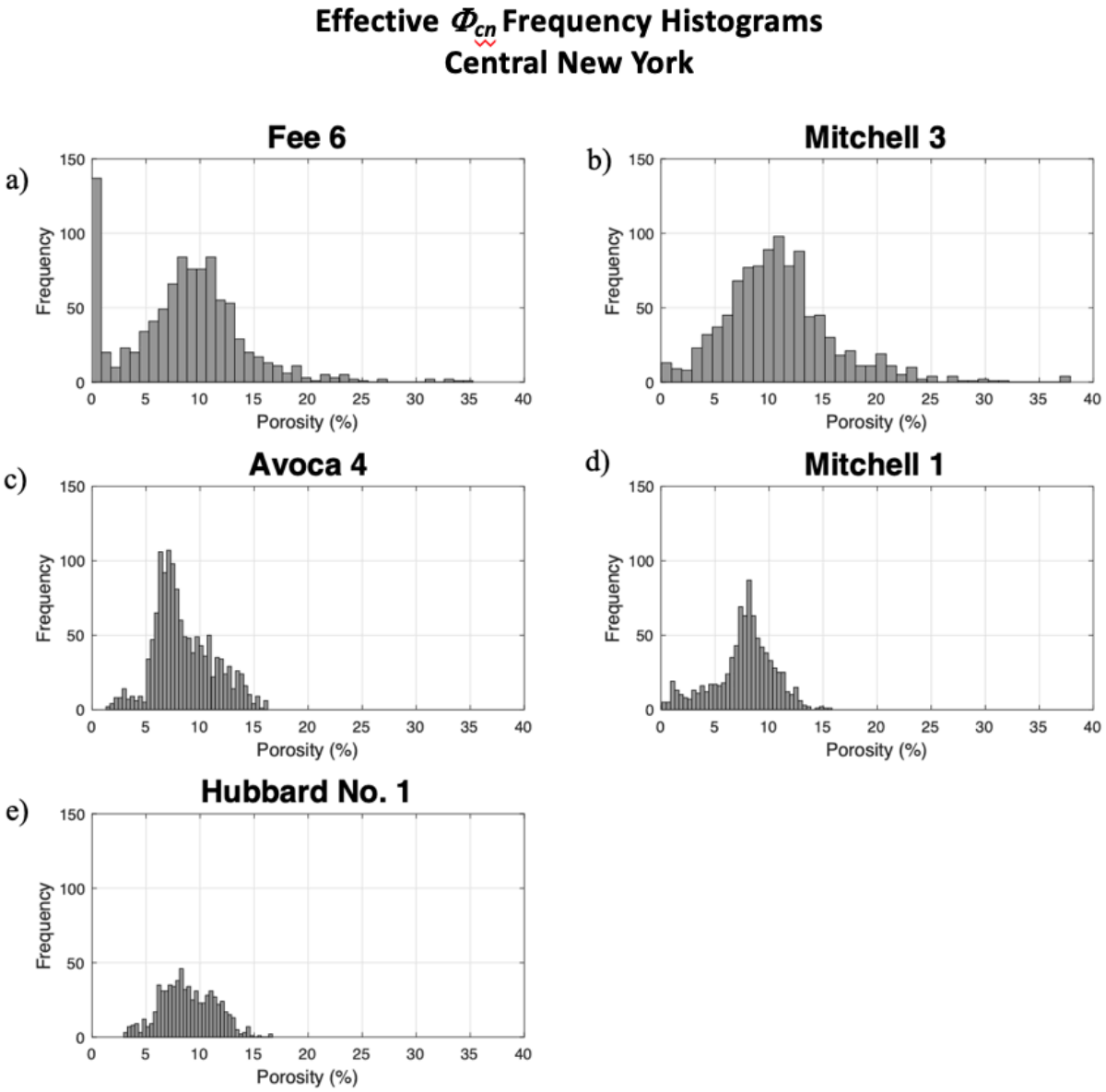

Figure 4.4: Histograms of porosity (%) and their frequencies for the Galway Formation in the five wells in central NY. The wells, from a) to e), are arranged from northernmost to southernmost locations. The porosity distribution is unimodal, with an average of ~7% porosity.

A.

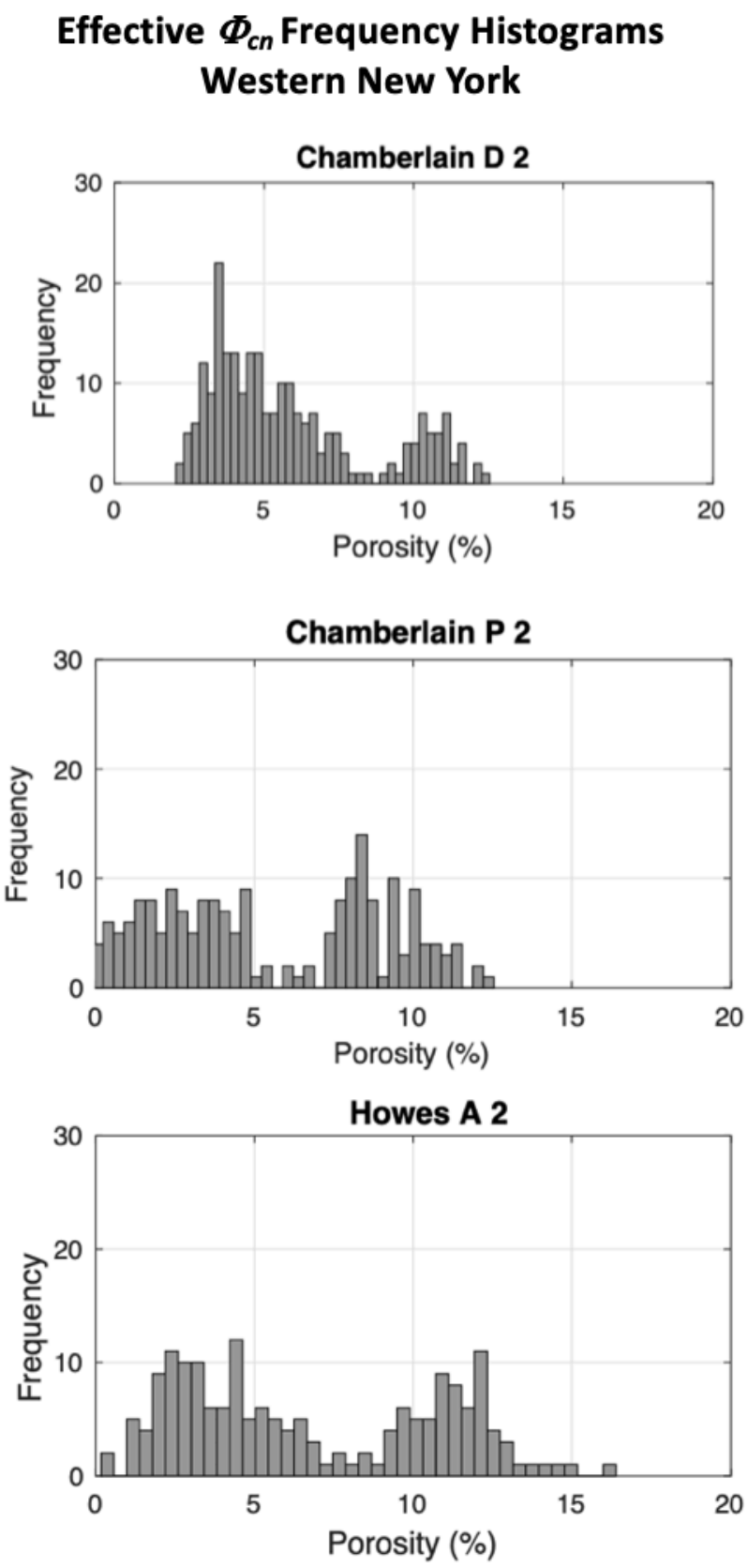
Effective Φ_{cn} Frequency Histograms
Western New York
Chamberlain D 2
Frequency
Porosity (%)
Chamberlain P 2
Frequency
Porosity (%)
Howes A 2
Frequency
Porosity (%)

B.

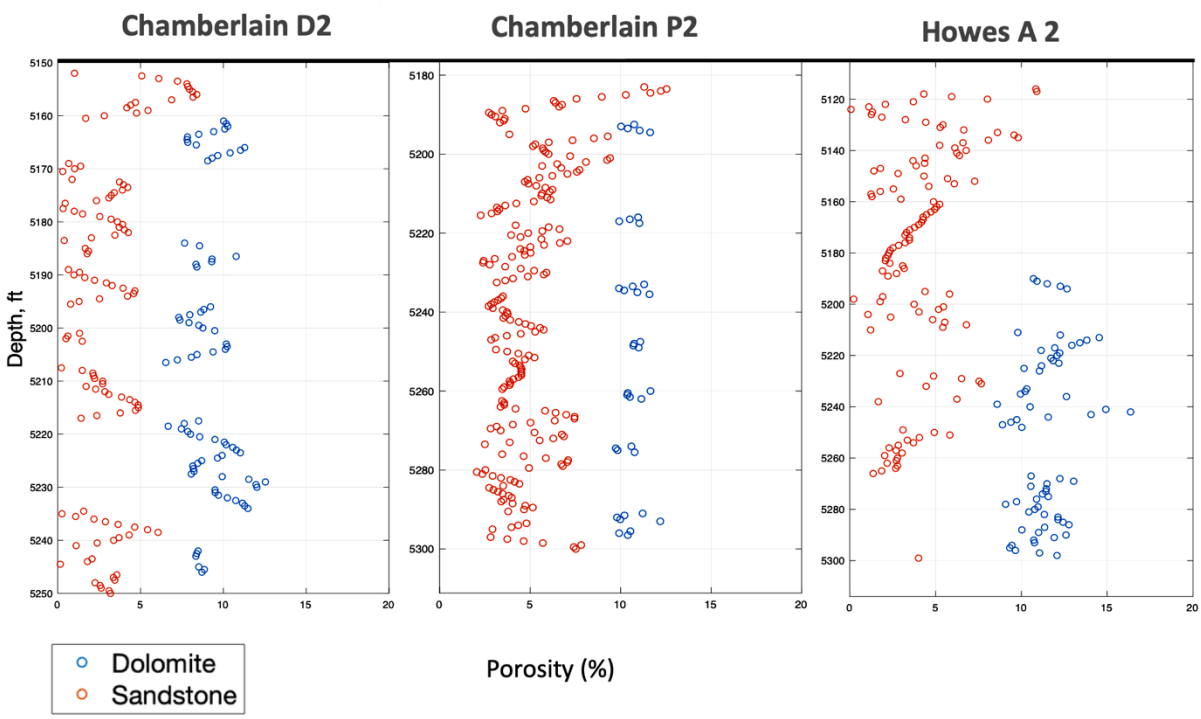

Figure 4.5: A: Bimodal histograms of porosity (%) and their frequencies for the three wells in western NY. B: NPHI porosity values corrected for shale and gas across the same wells, flattened to the top of the portion of the Galway Formation that directly underlies the Knox Unconformity. Here, several intervals of increased porosity are present, especially where dolomite is present. Intervals of higher porosity are 5-20 feet or 1-6 meters thick.

Although paleotopography may have some influence in central NY, in terms of higher porosity at paleovalleys, the geographical location (location-to-location trend) of the wells in central NY preclude any observable trend in maximum Φ_{cn}. However, the average Φ_{cn} appears to generally increase from the northernmost well (Figure 4.4a) to the southernmost well (Figure 4.4e): the average Φ_{cn} of the Fee 6 well, which is the farthest north, is only 6%. The M3 well, which is 1.69 miles south of Fee 6 on a north-south cross-section, has an average Φ_{cn} of 8%. The Avoca 4 well is 1.75 miles south of M3 on the cross-section, and has an average Φ_{cn} of 7%. The distance between the Avoca 4 well and the neighboring Mitchell 1 (M1) well in the cross-section is only 0.67 miles. This may explain why the M1 well has a similar mean Φ_{cn} of 7%. Finally, the southernmost well, Hubbard No. 1, is set apart from the M1 well by 1.11 miles and has a similar Φ_n as the other wells: 8 %.

The M3 well has an anomalously high maximum Φ_{cn} of 31% compared to the 12-19% maximum Φ_{cn} of the other wells. As was reasoned (Section 3.8) for the underlying Potsdam sandstone, this may be influenced by several possible reasons discussed in Chapter 3.9.

The maximum porosity found in western NY is almost half of that found in central NY: ~16% compared to central NY's ~31% (Figure 4.4 and 4.5A). Nevertheless, the average porosity in the western NY set of wells is comparable, ~6% average effective Φ_{cn} as compared to central New York's ~7% average porosity.

An investigation of the density and PEF logs associated with the Galway Φ_{cn} assessed in this study reveals that the bimodal nature is due to lithological differences: in western NY, the Galway comprises both sandstones and dolomite (Figure 4.5). Across the three wells, the sandstones are associated with the lower porosities, 0-8%, while the dolomites are associated with high porosities, ~6-13%.

The reservoir quality of the Yellowjacket member of the Galway in western NY may be controlled by the presence of dolomites and the possible presence of features formed by secondary porosity, like fractures and vugs, that may have increased permeability.

Given the correlation proposed in this thesis that the Galway of western NY is the same as the upper part of the Yellowjacket member, then the porosity data of the same stratigraphic interval in the two areas should be compared. An analysis of porosity for Yellowjacket yields results in central NY similar to the Galway in western New York, in that the dolomites are associated with the higher porosities and the trend is much less unimodal (Figure 4.6). For example, the Avoca well of central NY has similar porosity trends to those of western NY at the Yellowjacket member: the maximum porosity of the Avoca 4 well is ~14 %, which is similar to the maximum porosity of the three wells in western NY.

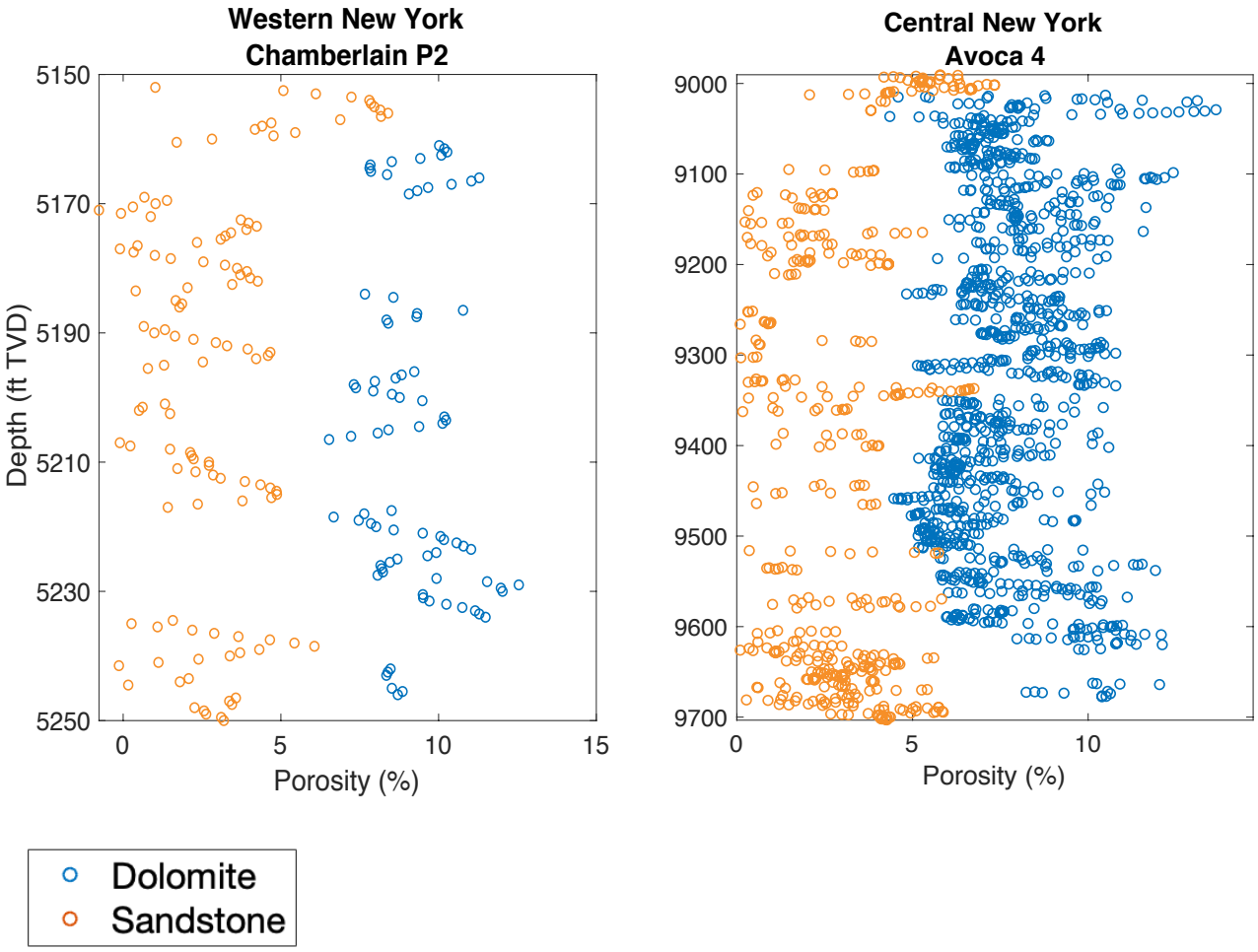

Figure 4.6: Effective porosity, in percent, versus depth, in feet, of the Yellowjacket member of the Galway for one well in western New York (left) versus one well in central New York (right). The dolomites found at both locations are associated with consistently higher porosity than the sandstone. Average and maximum effective porosities appear to be similar at both locations.

It is likely that the source of the high reservoir quality is the dolomites of interbedded sandstones and dolomites that constitute the Yellowjacket member. Corrected effective porosity of wells penetrating the Yellowjacket interval in central NY are comparable in porosity to those in Western NY, with the exception of wells that appear to drill through strata deposited on paleovalleys, such as Fee 6 and Mitchell 3. This may suggest that the Knox Unconformity does not have much of an effect on the porosity of the underlying formations, but that strata deposited on paleovalleys may increase porosity, which is opposite to the findings in Ohio (Smith et al., 2010). However, confirmation of this is not possible since no current permeability data exists for the Yellowjacket member of the Galway for wells in central NY, and more studies will need to be conducted on the permeability of the Yellowjacket member of the Galway.

4.5 Conclusion

The results of this study suggest that the high porosity of Yellowjacket is controlled by dolomite, and that, because average Φ_n does not differ much in western and central NY, the proximity of this stratigraphic interval to the Knox Unconformity has little to no effect on porosity. The other two factors attributed to the high reservoir quality in western NY were the locations at structural highs, and the effect of the paleotopography of the Precambrian on the deposition and porosity of the Rose Run.

REFERENCES

Dolly, E.D., 1969, Stratigraphic, structural and geomorphological factors controlling oil accumulation in Upper Cambrian strata of central Ohio. PhD dissertation. University of Oklahoma, Norman, OK.

Fagan, J. Jr., Copley, D.L., 1998, Aeromag interpretation technology helps chase Cambrian in New York. The Oil and Gas Journal, p.63

Gupta, N., Haagsma, A., Howat, E., Kelley, M., Hawkins, J., Fukai, I., Conner, A., Babrinde, O., Larsen, G., Main, J., McNeil, C., and Sullivan, C., 2016, Integrated sub -basin scale exploration for carbon storage targets: advanced characterization of geologic reservoirs and caprocks in the Upper Ohio River Valley. International Conference on Greenhouse Gas Technologies, Lausanne, Switzerland, GHGT-13; 14-18 N

Jacobi, R.D., Fountain, J.C., 2002. The character and reactivation history of the southern extension of the seismically active Clarendon –Linden Fault System, western New York State. Tectonophysics, 353, p. 215 – 262

Lowe, D.G., Arnott, R.W.C., Nowlan, G.S., and McCracken, A.D., 2017, Lithostratigraphic and allostratigraphic framework of the Cambrian-Ordovician Potsdam Group and correlations across Early Paleozoic southern Laurentia: Canadian Journal of Earth Sciences, v. 54, p. 550-585

New York State Energy Research and Development Authority, 2011, Carbon sequestration feasibility study in the Chautauqua County, New York Area: Final Report.

Riley, R.A., 1995, Ohio Rose Run, Beekmantown exploration heats Appalachians, Oil & Gas Journal, v. 93., p. 61-64.

Smith, L., Nyahay, R., and Slater, B., 2010, Integrated Reservoir Characterization of the subsurface Cambrian and Lower Ordovician Potsdam, Galway and Theresa Formations in New York: Albany, NY, New York State Energy Research and Development Authority, 69 p.

CHAPTER 5:

CONCLUSIONS AND RECOMMENDATIONS

Three zones have been identified as potential reservoirs at depths suitable for geothermal energy extraction from the subsurface at Cornell University, Ithaca, central New York (NY), ≥ 2.3 km depth below the surface. The zone with the highest reservoir potential is the Potsdam Formation, which overlies the unconformity above the crystalline basement. Allaz et al. (2013) have shown that diagenesis in the Potsdam Formation at multiple times in the Paleozoic was facilitated by circulation of relatively hot (~200°C) fluids within the Potsdam at locations spanning from as close as Steuben County to the east flank of the Adirondack Mountains. Whether a similar capacity for fluid flow persists today has been the focus of several lines of analysis presented in this thesis.

The top of the Potsdam Formation is predicted to be at about 2.76 km depth at Cornell's location, and to be about 200 meters thick. Reported permeability on the Mitchell 1 (M1) well at Steuben County, central NY indicate permeability at this zone is orders of magnitude higher than any other zone (up to ~960 md) (Guo et al., 1996). However, it is unclear whether the permeability results refer uniquely to the Potsdam, or to the Potsdam, Galway and Little Falls., and it is important to note this anomalously high permeability is singular in its report, and the source of the data is unknown. Regardless, the presence of the Ausable arkosic sand member of the Potsdam is a possible factor in increased porosity and permeability at the Potsdam. It is also likely that the Ausable has better reservoir quality when it is preserved or deposited in pockets of low basement paleotopography (possibly paleovalleys) at the the Mitchell 3 (M3) well at Steuben County, central New York, and in outcrop in paleo-structural lows at the Adirondack mountains. Evidence of the presence of the Ausable member, its reservoir quality and its

preservation is inconclusive, however, and will require further study. The permeability of the Potsdam is also variable, as some tests of wells in western NY are much lower (~0.01 md).

As reviewed in this work, multiple data sources have been unable to reproduce the Guo et al. report of high permeability in the Mitchell 1 well. Therefore, despite the report on the Mitchell 1 well having an exceptional permeability of ~1 darcy at the Potsdam, further tests on the permeability of the Potsdam are recommended. Regardless, the Potsdam's contact with the basement and the presence of the Ausable member make it a zone of interest for exploration of its potential as a reservoir in Cornell's location.

The second zone of interest is the Rose Run member of the Galway and the basal Little Falls, in which the dolomites of the Little Falls Formation grade to the sandstones of the Rose Run member of the Galway Formation. Reported laboratory measurements on the permeability of this zone indicate that this interval is highest in permeability below the Knox Unconformity at the Miller 2 well (New York State Energy Research and Development Authority, 2011). This interval is suspected to have relatively good reservoir quality, and is expected to be about 60 meters in thickness with the top of the reservoir at approximately 2.55 kilometers in depth at Cornell's location. This is predicted based on a N-S cross-section generated from wells nearby Cornell.

The third zone of interest is the Yellowjacket member of the Galway Formation. The proximity of the Yellowjacket member of the Galway Formation to the Knox Unconformity within western NY, combined with structural closures and locations at paleo-highs, have been assumed by Dolly (1969) to be the reason why this zone has been a prolific gas reservoir at western NY. To apply similar reasoning to the Tribes Hill below Cornell, which subcrops the Knox Unconformity, we need to test the validity of the postulated role of the unconformity. The

test is provided by comparison of the porosity of the informal Yellowjacket member of the Galway, where it subcrops the unconformity at western NY, with its porosity at central NY, where the Yellowjacket member is separated from the unconformity by the Rose Run member of the Galway, and the Little Falls and Tribes Hill Formation. This study has found no correlation of proximity to the unconformity with increased porosity, and I interpret that the Tribes Hill Formation will not be very porous. This interpretation also assumes low permeability due to the common presence of shale beds within the Tribes Hill. Although the unconformity may not increase porosity of underlying strata, the porosity of Yellowjacket remains similar at western and central NY. This suggests that the interval may be a potential reservoir for geothermal production at Cornell's subsurface, as well.

The Vespa member of the Galway emerged as a possible zone of interest due to a suite of data from logs at the Auburn Geothermal well in Cayuga County, central NY, which indicate a possible permeable zone. Permeability tests on this section at the Olin well indicate that this zone has little potential as a reservoir (Kolkas, 1998).This lithologic zone is predicted to be encountered at roughly 2.6 km depth at Cornell's location and to span roughly 160 meters in thickness, based on the cross-section. Permeability tests on this portion of the Galway are negligible, however, and inconclusive (Smith et al., 2010). It does appear that there are specific intervals of spiked porosity associated with some dolomite beds, which may be interpreted as a result of the presence of vugs or fractures. Many of the intervals found in well logs that present this pattern of spiked porosity are interpreted here as zones where vugs or possibly fractures are present.

The Potsdam Formation and its lower Ausable member, the basal Little Falls Formation and Rose Run member of the Galway, and Yellowjacket member of the Galway offer the best

potential to be reservoirs for geothermal production from natural porosity at Cornell University's location in Ithaca, NY (Figure 5.1). However, there is no guarantee that the properties examined in this study that have contributed to the reservoir quality of these zones will be found, since no well has been drilled into Cornell's deep subsurface before. The quality of these reservoirs is highly variable from location to location, and is dependent on several factors that may or may not be present in Cornell's subsurface, such as locations of structural highs or the presence of fractures or vugs. Also, as documented by Camp and Jordan (2017), although at a slightly shallower depth with lower temperatures, the uppermost Black River Group has high potential as a thin reservoir interval. It is highly recommended that a test well be drilled to corroborate the theories posited in this thesis.

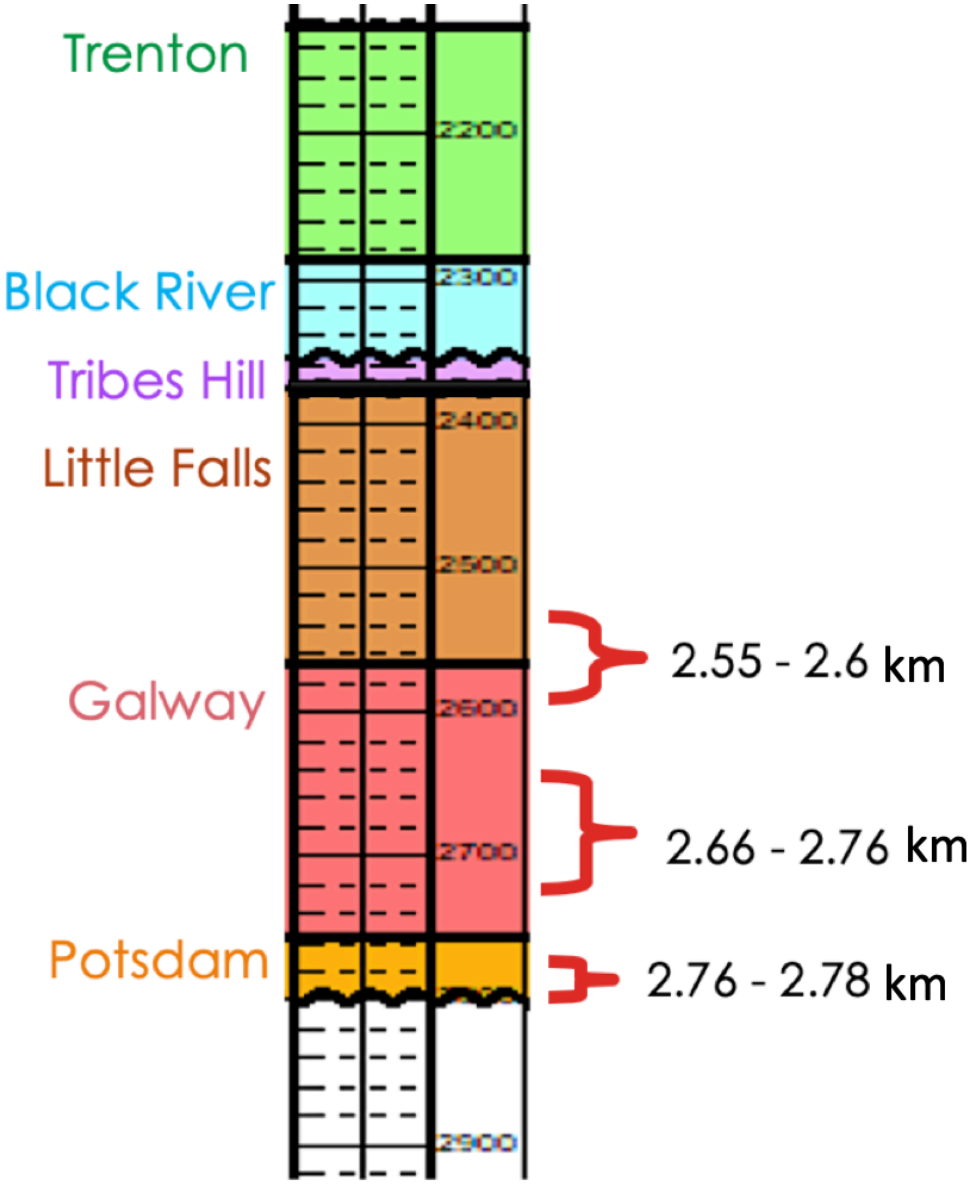

Figure 5.1: Stratigraphic column of expected depths (in meters) to the Trenton-Black River and Beekmantown Groups in central New York, at Cornell's location. Stratigraphic names are to the left, tops are in bolded black, and unconformities are in wavy black lines. Reservoir candidates and their expected depths (in kilometers) are to the right.

REFERENCES

Allaz, J., Selleck, B., Williams, M., and Jercinovic, M. , 2013, Microprobe analysis and dating of monazite from the Potsdam Formation, New York: A progressive record of chemical reaction and fluid interaction. American Mineralogist. 98. 1106-1119. 10.

Dolly, E.D., 1969, Stratigraphic, structural and geomorphological factors controlling oil accumulation in Upper Cambrian strata of central Ohio. PhD dissertation. University of Oklahoma, Norman, OK.

Guo, B., Friedman, G.M., Bass, J.P., and Sarwar, G., 1996, Underground gas storage in the Cambro-Ordovician succession of Southeastern New York: A preliminary study. Northeastern Geology and Environmental Sciences, v. 18, pp. 49-58.

Kolkas, M. M., 1998, Subsurface brine disposal in the Sauk Sequence of central and western New York: Implications for new salt cavern gas-storage reservoirs. PhD dissertation. The City University of New York, New York City, New York.

Lugert, C., Smith, L., and Nyahay, R., 2006, Systematic technical innovations initiative: Brine disposal in the Northeast. Final Report. Albany, NY, New York State Energy Research and Development Authority

New York State Energy Research and Development Authority, 2011, Carbon sequestration feasibility study in the Chautauqua County, New York Area: Final Report.

Smith, L., Nyahay, R., and Slater, B., 2010, Integrated Reservoir Characterization of the subsurface Cambrian and Lower Ordovician Potsdam, Galway and Theresa Formations in New York: Albany, NY, New York State Energy Research and Development Authority, 69 p.

APPENDIX A:

TOP PICKS OF WELLS AT CENTRAL AND WESTERN NEW YORK

This Appendix provides a list of all tops picked for every well used in this thesis to generate structural and stratigraphic maps. Tops for Tribes Hill and Little Falls are difficult to find for some wells, so a '?' symbol represents a top that is too uncertain to confidently pic. Blank spaces or spaces wit 'N/A' indicate that there is no log data available to pick the top. Surface latitude, longitude and elevations are included for each well.

UWI/API		31011900010000	31101216240000	31097214950000
WELLNAME		Auburn Geothermal	Avoca 4	Bale 1
SURFLAT		42.94479	42.42005	42.27001
SURFLON		-76.54432	-77.46718	-76.71356
ELEVATION		70	984	1785
MARCELLUS	(MD)	12		
MARCELLUS	(TVD)	12		
ONONDAGA	(MD)	46		
ONONDAGA	(TVD)	46		
HELDERBERG	(MD)	141		
HELDERBERG	(TVD)	141		
BERTIE	(MD)	190		
BERTIE	(TVD)	190		
CAMILLUS	(MD)	223		
CAMILLUS	(TVD)	223		
SYRACUSE	(MD)	238		
SYRACUSE	(TVD)	238		
VERNON	(MD)	638		
VERNON	(TVD)	638		
LOCKPORT	(MD)	1231		
LOCKPORT	(TVD)	1231		
CLINTON	(MD)	1420		
CLINTON	(TVD)	1420		
MEDINA	(MD)	1711		
MEDINA	(TVD)	1711		
QUEENSTON	(MD)	1789		
QUEENSTON	(TVD)	1789		
OSWEGO	(MD)	2308		
OSWEGO	(TVD)	2308		
LORRAINE/UTICA	(MD)	2861	6541	8140
LORRAINE/UTICA	(TVD)	2861	6535.9	8140
TRENTON	(MD)	3460	7177	8847
TRENTON	(TVD)	3460	7171	8847
BLACK_RIVER	(MD)	4164	7815	9319
BLACK_RIVER	(TVD)	4164	7808	9319
LITTLE_FALLS	(MD)	3393	8320	
LITTLE_FALLS	(TVD)	3393	8313	
GALWAY	(MD)	4659	8775	
GALWAY	(TVD)	4659	8765.65	
POTSDAM	(MD)	5002	9700	
POTSDAM	(TVD)	5002	9667.67	
PRECAMBRIAN	(MD)	5049	9890	
PRECAMBRIAN	(TVD)	5049	9853.14	

UWI/API		31109260390000	31069048710000	31025044550000
WELLNAME		Barron 1	Bowerman Ralph 1	C E Leslie Caroline
SURFLAT		42.586091	43.02164	42.39048
SURFLON		-76.575199	-77.33506	-75.04415
ELEVATION		984	556	497
TULLY	(MD)	513		
TULLY	(TVD)	513		
MARCELLUS	(MD)	1513		
MARCELLUS	(TVD)	1512.99		
CHERRY VALLEY	(MD)	1556		
CHERRY VALLEY	(TVD)	1555.99		
ONONDAGA	(MD)	1587		
ONONDAGA	(TVD)	1586.99		
HELDERBERG	(MD)	1661		
HELDERBERG	(TVD)	1660.99		
BERTIE	(MD)	1831		
BERTIE	(TVD)	1830.98		
CAMILLUS	(MD)	1943		
CAMILLUS	(TVD)	1942.98		
SYRACUSE	(MD)	2030		
SYRACUSE	(TVD)	2029.98		
VERNON	(MD)	2650		
VERNON	(TVD)	2649.98		
LOCKPORT	(MD)	3264		
LOCKPORT	(TVD)	3263.97		
CLINTON	(MD)	3427		
CLINTON	(TVD)	3426.42		
MEDINA	(MD)	3806		
MEDINA	(TVD)	3805.32		
QUEENSTON	(MD)	3950		
QUEENSTON	(TVD)	3949.3		
OSWEGO	(MD)	4461		
OSWEGO	(TVD)	4460.24		
LORRAINE/UTICA	(MD)	5133	2200	
LORRAINE/UTICA	(TVD)	5132.16	2200	
TRENTON	(MD)	5836	2813	5919
TRENTON	(TVD)	5834.91	2813	5919
BLACK RIVER	(MD)	6759	3486	6170
BLACK RIVER	(TVD)	6535.57	3486	6170
LITTLE FALLS	(MD)	N/A	N/A	6710
LITTLE FALLS	(TVD)	N/A	N/A	6710
GALWAY	(MD)	N/A	3911	7068
GALWAY	(TVD)	N/A	3911	7068
POTSDAM	(MD)	N/A	4165	7828
POTSDAM	(TVD)	N/A	4165	7828
PRECAMBRIAN	(MD)	N/A	4204	7878
PRECAMBRIAN	(TVD)	N/A	4204	7878

UWI/API		31025042140000	31121219070000	31121220530000
WELLNAME		Campbell H A and M W	Chamberlain D 2	Chamberlain P 2
SURFLAT		42.18284	42.81819	42.81387
SURFLON		-74.92141	-78.11616	-78.11311
ELEVATION		10992	1420	1380
TRENTON	(MD)	8237	4200	4162
TRENTON	(TVD)	8237	4200	4162
BLACK_RIVER	(MD)	?	4746	4736
BLACK_RIVER	(TVD)	?	4746	4736
GALWAY	(MD)	9790	5173	5152
GALWAY	(TVD)	9790	5173	5152
POTSDAM	(MD)	10850	N/A	N/A
POTSDAM	(TVD)	10850	N/A	N/A
PRECAMBRIAN	(MD)	10965	N/A	N/A
PRECAMBRIAN	(TVD)	10965	N/A	N/A

UWI/API		**31099204460000**	**31029129100000**	**31109227670000**
WELLNAME		**Compton 1 (4177)**	**Darling 1**	**Duddleston 62351**
SURFLAT		**42.70864**	**42.46651**	**42.51203**
SURFLON		**-76.80819**	**-78.8033**	**-76.63581**
ELEVATION		**761**	**1145**	**1030**
LORRAINE/UTICA	(MD)	3982	4015	5605
LORRAINE/UTICA	(TVD)	3982	4015	5605
TRENTON	(MD)	4534	4855	6296
TRENTON	(TVD)	4534	4855	6296
BLACK RIVER	(MD)	5367	?	6941
BLACK RIVER	(TVD)	5367	?	6941
LITTLE FALLS	(MD)	5762	N/A	7319
LITTLE FALLS	(TVD)	5762	N/A	7319
GALWAY	(MD)	6028	5692	N/A
GALWAY	(TVD)	6028	5692	N/A

UWI/API		31009038680000	31009092350000	31029066680000
WELLNAME		Ellis I-1710	Enterprise Transit	Fee 1
SURFLAT		42.45515	42.00872	42.80331
SURFLON		-79.03965	-78.56849	-78.84418
ELEVATION		1328	2294	6.8
TRENTON	(MD)	4820	8433	2987
TRENTON	(TVD)	4820	8433	2987
BLACK RIVER	(MD)	5270	8925	3480
BLACK RIVER	(TVD)	5270	8925	3480
LITTLE FALLS	(MD)	?	9331	N/A
LITTLE FALLS	(TVD)	?	9331	N/A
GALWAY	(MD)	5620	9720	3820
GALWAY	(TVD)	5620	9720	3820
POTSDAM	(MD)	6303	10610	4130
POTSDAM	(TVD)	6303	10610	4130
PRECAMBRIAN	(MD)	6450	10989	4210
PRECAMBRIAN	(TVD)	6450	10989	4210

UWI/API		31101216360000	31063066690000	31109044670000
WELLNAME		Fee 6	Fee Hooker Chemical	Fee Richarson 1
SURFLAT		42.42904	43.07998	42.38444
SURFLON		-77.46566	-79.00651	-76.54041
ELEVATION		1721	582	1041
TULLY	(MD)			980
TULLY	(TVD)			980
MARCELLUS	(MD)			2160.5
MARCELLUS	(TVD)			2160.5
ONONDAGA	(MD)			2263.5
ONONDAGA	(TVD)			2263.5
HELDERBERG	(MD)			2375
HELDERBERG	(TVD)			2375
BERTIE	(MD)			2564
BERTIE	(TVD)			2564
CAMILLUS	(MD)			2730
CAMILLUS	(TVD)			2730
SYRACUSE	(MD)			2850
SYRACUSE	(TVD)			2850
VERNON	(MD)			3662
VERNON	(TVD)			3662
LOCKPORT	(MD)			4425
LOCKPORT	(TVD)			4425
CLINTON	(MD)			4604
CLINTON	(TVD)			4604
MEDINA	(MD)			5040
MEDINA	(TVD)			5040
QUEENSTON	(MD)			5185
QUEENSTON	(TVD)			5185
OSWEGO	(MD)			5741
OSWEGO	(TVD)			5741
LORRAINE/UTICA	(MD)	6582		6560
LORRAINE/UTICA	(TVD)	6527.66		6560
TRENTON	(MD)	7294	2114	7346
TRENTON	(TVD)	7154.81	2114	7346
BLACK_RIVER	(MD)	8119	2568	7820
BLACK_RIVER	(TVD)	7787.83	2568	7820
TRIBES_HILL	(MD)	N/A	N/A	8191
TRIBES_HILL	(TVD)	N/A	N/A	8191
LITTLE_FALLS	(MD)	8757	N/A	8275
LITTLE_FALLS	(TVD)	8297.43	N/A	8275
GALWAY	(MD)	9312	2837	9048
GALWAY	(TVD)	8711.01	2837	9048
POTSDAM	(MD)	10506	2995	
POTSDAM	(TVD)	9589.34	2995	
PRECAMBRIAN		10783	3028	
PRECAMBRIAN		9777.27	3028	

UWI/API		31109041300000	31067213350000	31117051160000
WELLNAME		Grund GH	Halloran 1	Hammond F W 1
SURFLAT		42.44218	43.06607	43.15204
SURFLON		-76.59246	-76.35257	-77.0695
ELEVATION		1454	529	8
TULLY	(MD)	1255		
TULLY	(TVD)	1255		
MARCELLUS	(MD)	2405		
MARCELLUS	(TVD)	2405		
ONONDAGA	(MD)	2500		
ONONDAGA	(TVD)	2500		
HELDERBERG	(MD)	2618		
HELDERBERG	(TVD)	2618		
BERTIE	(MD)	2851		
BERTIE	(TVD)	2851		
CAMILLUS	(MD)	2958		
CAMILLUS	(TVD)	2958		
SYRACUSE	(MD)	3046		
SYRACUSE	(TVD)	3046		
VERNON	(MD)	3765		
VERNON	(TVD)	3765		
LOCKPORT	(MD)	4419		
LOCKPORT	(TVD)	4419		
CLINTON	(MD)	4588		
CLINTON	(TVD)	4588		
MEDINA	(MD)	5025		
MEDINA	(TVD)	5025		
QUEENSTON	(MD)	5152		
QUEENSTON	(TVD)	5152		
OSWEGO	(MD)	5729		
OSWEGO	(TVD)	5729		
LORRAINE/UTI	(MD)	6572		
LORRAINE/UTI	(TVD)	6572		
TRENTON	(MD)	7299	2748	2442
TRENTON	(TVD)	7299	2744.22	2442
BLACK RIVER	(MD)	7750	3416	3187
BLACK RIVER	(TVD)	7750	3359.59	3187
TRIBES HILL	(MD)	8120	N/A	N/A
TRIBES HILL	(TVD)	8120	N/A	N/A
LITTLE FALLS	(MD)	?	3794	N/A
LITTLE FALLS	(TVD)	?	3709.67	N/A
GALWAY	(MD)	8824	3805	3476
GALWAY	(TVD)	8824	3719.83	3476
POTSDAM	(MD)	N/A	N/A	3662
POTSDAM	(TVD)	N/A	N/A	3662
PRECAMBRIAN	(MD)	N/A	N/A	3690
PRECAMBRIAN	(TVD)	N/A	N/A	3690

UWI/API		31013044370000	31051137000000	31065039280000
WELLNAME		Harrington 1	Hilts 20617-T	Homer A Keith 1
SURFLAT		42.18364	42.69726	42.86804
SURFLON		-79.33754	-77.89168	-75.42618
ELEVATION		1773	890	1319
TRENTON	(MD)	5968	4430	3190
TRENTON	(TVD)	5968	4430	3190
BLACK RIVER	(MD)	6375	5020	3545
BLACK RIVER	(TVD)	6375	5020	3545
LITTLE FALLS	(MD)	6770	5430	3635
LITTLE FALLS	(TVD)	6770	5430	3635
GALWAY	(MD)	6852	5482	3895
GALWAY	(TVD)	6852	5482	3895
POTSDAM	(MD)	7548	6187	4297
POTSDAM	(TVD)	7548	6187	4297
PRECAMBRIAN	(MD)	N/A	6321	4316
PRECAMBRIAN	(TVD)	N/A	6321	4316

UWI/API		**31121219090000**	**31101214960000**	**31011175080000**
WELLNAME		**Howes A 2**	**Hubbard No. 1**	**Hunter A & B 1**
SURFLAT		**42.82218**	**42.40532**	**43.12905**
SURFLON		**-78.11061**	**-77.4632**	**-76.5614**
ELEVATION			**1775**	**449**
LORRAINE/UTICA	(MD)			1814
LORRAINE/UTICA	(TVD)			1814
TRENTON	(MD)	4125	7315	2436
TRENTON	(TVD)	4125	7315	2436
BLACK_RIVER	(MD)	4682	7985	3125
BLACK_RIVER	(TVD)	4682	7985	3125
LITTLE_FALLS	(MD)	N/A	8450	N/A
LITTLE_FALLS	(TVD)	N/A	8450	N/A
GALWAY	(MD)	5109	8950	3473
GALWAY	(TVD)	5109	8950	3473
POTSDAM	(MD)	N/A	9859	N/A
POTSDAM	(TVD)	N/A	9859	N/A
PRECAMBRIAN	(MD)	N/A	10025	N/A
PRECAMBRIAN	(TVD)	N/A	10025	N/A

UWI/API		31015229240000	31051046300000	31015004430000
WELLNAME		Johnson 1	Kennedy 1	Kesselring 1
SURFLAT		42.26898	42.6503	42.19869
SURFLON		-76.75087	-77.75568	-76.53735
ELEVATION		1509	599	1081
TULLY	(MD)			1622.5
TULLY	(TVD)			1622.5
MARCELLUS	(MD)			2865
MARCELLUS	(TVD)			2865
ONONDAGA	(MD)			2971
ONONDAGA	(TVD)			2971
HELDERBERG	(MD)			3234
HELDERBERG	(TVD)			3234
BERTIE	(MD)			3420
BERTIE	(TVD)			3420
CAMILLUS	(MD)			3610
CAMILLUS	(TVD)			3610
SYRACUSE	(MD)			3826
SYRACUSE	(TVD)			3826
VERNON	(MD)			4866
VERNON	(TVD)			4866
LOCKPORT	(MD)			5640
LOCKPORT	(TVD)			5640
CLINTON	(MD)			5830
CLINTON	(TVD)			5830
MEDINA	(MD)			6373
MEDINA	(TVD)			6373
QUEENSTON	(MD)			6535
QUEENSTON	(TVD)			6535
OSWEGO	(MD)			7237
OSWEGO	(TVD)			7237
LORRAINE/UTICA	(MD)	7800		8123
LORRAINE/UTICA	(TVD)	7800		8123
TRENTON	(MD)	8603	4491	8900
TRENTON	(TVD)	8603	4491	8900
BLACK_RIVER	(MD)	9403	5083	9340
BLACK_RIVER	(TVD)	9403	5083	9340
TRIBES_HILL	(MD)	9860	N/A	9700
TRIBES_HILL	(TVD)	9860	N/A	9700
LITTLE_FALLS	(MD)	N/A	5541	N/A
LITTLE_FALLS	(TVD)	N/A	5541	N/A
GALWAY	(MD)	N/A	5620	10402
GALWAY	(TVD)	N/A	5620	10402
POTSDAM	(MD)	N/A	6295	
POTSDAM	(TVD)	N/A	6295	
PRECAMBRIAN	(MD)	N/A	6324	
PRECAMBRIAN	(TVD)		6324	

UWI/API		**31011175100000**	**31099108930000**	**31037051170000**
WELLNAME		**Keysor H 1**	**Kinney 1**	**Klotzbach 1**
SURFLAT		**43.13841**	**42.94135**	**43.040518**
SURFLON		**-76.55184**	**-76.87629**	**-78.38964**
ELEVATION		**420**	**500**	**870**
TRENTON	(MD)	2402	3184	2728
TRENTON	(TVD)	2402	3184	2728
BLACK_RIVER	(MD)	3070	3975	3182
BLACK_RIVER	(TVD)	3070	3975	3182
GALWAY	(MD)	3450	4402	3584
GALWAY	(TVD)	3450	4402	3584
POTSDAM	(MD)	?	N/A	3677
POTSDAM	(TVD)	?	N/A	3677
PRECAMBRIAN	(MD)	3900	N/A	3870
PRECAMBRIAN	(TVD)	3900	N/A	3870

UWI/API		**31109227530000**	**31013076490000**	**31109260560000**
WELLNAME		**Koskinen 23513**	**Langworthy 1**	**Lansing T-1**
SURFLAT		**42.49038**	**42.40715**	**42.622127**
SURFLON		**-76.67302**	**-79.1663**	**-76.533969**
ELEVATION		**1100**	**1615**	**1100**
TULLY	(MD)	762		200
TULLY	(TVD)	762		200
MARCELLUS	(MD)	1800		1207
MARCELLUS	(TVD)	1800		1207
ONONDAGA	(MD)	1882		1290
ONONDAGA	(TVD)	1882		1290
HELDERBERG	(MD)	1980		1355
HELDERBERG	(TVD)	1980		1355
BERTIE	(MD)	2146		1507
BERTIE	(TVD)	2146		1507
CAMILLUS	(MD)	2257		1607
CAMILLUS	(TVD)	2257		1607
SYRACUSE	(MD)	2345		1689
SYRACUSE	(TVD)	2345		1689
VERNON	(MD)	3041		2272
VERNON	(TVD)	3041		2272
LOCKPORT	(MD)	3690		2886
LOCKPORT	(TVD)	3690		2886
CLINTON	(MD)	3852		3062
CLINTON	(TVD)	3852		3062
MEDINA	(MD)	4265		3425
MEDINA	(TVD)	4265		3425
QUEENSTON	(MD)	4376		3531
QUEENSTON	(TVD)	4376		3531
OSWEGO	(MD)	4919		4053
OSWEGO	(TVD)	4919		4053
LORRAINE/UTI	(MD)	5757		4800
LORRAINE/UTI	(TVD)	5757		4800
TRENTON	(MD)	6430	5133	5473
TRENTON	(TVD)	6430	5133	5473
BLACK_RIVER	(MD)	7075		6270
BLACK_RIVER	(TVD)	7075		6200.39
PRECAMBRIAN	(MD)		5922	
PRECAMBRIAN	(TVD)		5922	

UWI/API		**31015228620000**	**31025043790000**	**31053011730000**
WELLNAME		**Lant 1**	**Lanzilotta 1**	**Letts 1**
SURFLAT		**42.26828**	**42.27354**	**42.86118**
SURFLON		**-76.81321**	**-74.62734**	**-75.40207**
ELEVATION		**1134**	**1847**	**1255**
LORRAINE/UTICA	(MD)	7500		
LORRAINE/UTICA	(TVD)	7500		
TRENTON	(MD)	8237	6765	3078
TRENTON	(TVD)	8237	6765	3078
BLACK_RIVER	(MD)	8753	6908	3415
BLACK_RIVER	(TVD)	8753	6908	3415
TRIBES_HILL	(MD)	9165	7265	3488
TRIBES_HILL	(TVD)	9165	7265	3488
LITTLE_FALLS	(MD)	N/A	?	?
LITTLE_FALLS	(TVD)	N/A	?	?
GALWAY	(MD)	N/A	7505	3765
GALWAY	(TVD)	N/A	7505	3765
POTSDAM	(MD)	N/A	8790	4155
POTSDAM	(TVD)	N/A	8790	4155
PRECAMBRIAN	(MD)	N/A	8920	4162
PRECAMBRIAN	(TVD)	N/A	8920	4162

UWI/API		**31077040550000**	**31107229340000**	**31117067190000**
WELLNAME		**Lum B Paul et al 1**	**Manwaring 62447**	**Martin 1**
SURFLAT		**42.63099**	**42.05783**	**43.02908**
SURFLON		**-74.70775**	**-76.40979**	**-76.94349**
ELEVATION		**1979**	**1341**	**392**
TRENTON	(MD)	4264	10510	2791
TRENTON	(TVD)	4264	10510	2791
BLACK_RIVER	(MD)	4280	11091	3530
BLACK_RIVER	(TVD)	4280	11091	3530
TRIBES_HILL	(MD)	4305	11434	N/A
TRIBES_HILL	(TVD)	4305	11434	N/A
LITTLE_FALLS	(MD)	?		N/A
LITTLE_FALLS	(TVD)	?		N/A
GALWAY	(MD)	4925		3963
GALWAY	(TVD)	4925		3963
POTSDAM	(MD)	5250		
POTSDAM	(TVD)	5250		
PRECAMBRIAN	(MD)	5362		
PRECAMBRIAN	(TVD)	5362		

UWI/API		**31015103350000**	**31121225200000**	**31051045520000**
WELLNAME		**Matejka 1**	**Matusik, J 1**	**McClurg 1**
SURFLAT		**42.16908**	**42.55355**	**42.83535**
SURFLON		**-76.65865**	**-78.43856**	**-77.93674**
ELEVATION		**1435**	**1633**	**1002**
LORRAINE/UTICA	(MD)	8581		
LORRAINE/UTICA	(TVD)	8581		
TRENTON	(MD)	9329	5279	3861
TRENTON	(TVD)	9329	5279	3861
BLACK_RIVER	(MD)	9829	5750	4478
BLACK_RIVER	(TVD)	9829	5750	4478
TRIBES_HILL	(MD)	10233	N/A	N/A
TRIBES_HILL	(TVD)	10233	N/A	N/A
LITTLE_FALLS	(MD)	N/A	6104	N/A
LITTLE_FALLS	(TVD)	N/A	6104	N/A
GALWAY	(MD)	N/A	6158	4883
GALWAY	(TVD)	N/A	6158	4883
POTSDAM	(MD)	N/A	N/A	5443
POTSDAM	(TVD)	N/A	N/A	5443
PRECAMBRIAN	(MD)	N/A	N/A	5560
PRECAMBRIAN	(TVD)	N/A	N/A	5560

UWI/API		31015231860100	31101214680000	31101216330000
WELLNAME		**Messing 1-A**	**Mitchell 1**	**Mitchell 3**
SURFLAT		**42.05234**	**42.41965**	**42.42791**
SURFLON		**-76.90128**	**-77.45324**	**-77.44556**
ELEVATION		**1434**	**1680**	**1680**
LORRAINE/UTICA	(MD)	9600		6564
LORRAINE/UTICA	(TVD)	9600		6522.79
TRENTON	(MD)	10313	7166	7280
TRENTON	(TVD)	10313	7166	7148.92
BLACK_RIVER	(MD)	10873	7817	8169
BLACK_RIVER	(TVD)	10873	7817	7794.64
TRIBES_HILL	(MD)	11307	8303	N/A
TRIBES_HILL	(TVD)	11307	8303	N/A
LITTLE_FALLS	(MD)	N/A	8780	8895
LITTLE_FALLS	(TVD)	N/A	8780	8297.77
GALWAY	(MD)	N/A	9700	9543
GALWAY	(TVD)	N/A	9700	8746.22
POTSDAM	(MD)	N/A	9890	10910
POTSDAM	(TVD)	N/A	9890	9596.74
PRECAMBRIAN	(MD)	N/A	N/A	11210
PRECAMBRIAN	(TVD)	N/A	N/A	9778.19

UWI/API		**31099227630000**	**31101136990000**	**31101039240000**
WELLNAME		**Murray 2587-01**	**NYS Reforestation 6**	**Olin [N-650-S]**
SURFLAT		**42.82845**	**42.46624**	**42.063401**
SURFLON		**-76.83749**	**-77.2651**	**-77.429976**
ELEVATION		**644**	**4027**	**1658**
LORRAINE/UTICA	(MD)	3170		8913
LORRAINE/UTICA	(TVD)	3170		8254.82
TRENTON	(MD)	3736	7093	9672
TRENTON	(TVD)	3736	7093	9013.74
BLACK_RIVER	(MD)	4587	7869	10230
BLACK_RIVER	(TVD)	4587	7869	9551.97
TRIBES_HILL	(MD)	N/A	N/A	10728
TRIBES_HILL	(TVD)	N/A	N/A	10049.96
LITTLE_FALLS	(MD)	5037	8314	?
LITTLE_FALLS	(TVD)	5037	8314	?
GALWAY	(MD)	5137	8812	11788
GALWAY	(TVD)	5137	8812	11009.47
POTSDAM	(MD)			12610
POTSDAM	(TVD)			11827.25
PRECAMBRIAN	(MD)			13300
PRECAMBRIAN	(TVD)			11916.78

UWI/API		**31117051140000**	**31011050110000**	**31121045360000**
WELLNAME		**Olson H v 1**	**O'Neill 1**	**Page Henry 1**
SURFLAT		**43.11158**	**43.146152**	**42.82678**
SURFLON		**-77.02032**	**-76.553139**	**-78.13817**
ELEVATION		**8**	**404**	**1501**
LORRAINE/UTICA	(MD)		1700	
LORRAINE/UTICA	(TVD)		1700	
TRENTON	(MD)	2488	2327	
TRENTON	(TVD)	2488	2327	
BLACK_RIVER	(MD)	2847	3003	
BLACK_RIVER	(TVD)	2847	3003	
TRIBES_HILL	(MD)	N/A	N/A	
TRIBES_HILL	(TVD)	N/A	N/A	
LITTLE_FALLS	(MD)	N/A	N/A	
LITTLE_FALLS	(TVD)	N/A	N/A	
GALWAY	(MD)	3213	3376	5200
GALWAY	(TVD)	3213	3376	5200
POTSDAM	(MD)	3660	?	5600
POTSDAM	(TVD)	3660	?	5600
PRECAMBRIAN	(MD)	3710	3570	5790
PRECAMBRIAN	(TVD)	3710	3570	5790

UWI/API		**31011049990000**	**31099258610000**	**31029250050000**
WELLNAME		**Parker Robert A 1**	**Poorman 2586-01**	**Porter 1**
SURFLAT		**43.02606**	**42.83934**	**42.54597**
SURFLON		**-76.5285**	**-76.83667**	**-78.61204**
ELEVATION		**589**	**600**	**1725**
LORRAINE/UTICA	(MD)	2511	3100	
LORRAINE/UTICA	(TVD)	2511	3100	
TRENTON	(MD)	3116	3681	5211
TRENTON	(TVD)	3116	3681	5211
BLACK_RIVER	(MD)	3789	4520	5644
BLACK_RIVER	(TVD)	3789	4520	5644
LITTLE_FALLS	(MD)	4160	4968	
LITTLE_FALLS	(TVD)	4160	4968	
GALWAY	(MD)	4190	5080	6045
GALWAY	(TVD)	4190	5080	6045

UWI/API		**31011175580000**	**31011175590000**	**31109227890000**
WELLNAME		**Provo 7271**	**Quill 725-1**	**Rehebein/Call 1 A**
SURFLAT		**43.01115**	**42.924114**	**42.54291**
SURFLON		**-76.52119**	**-76.69931**	**-76.27994**
ELEVATION		**600**	**510**	**1150**
TULLY	(MD)			602
TULLY	(TVD)			601.81
MARCELLUS	(MD)			1810
MARCELLUS	(TVD)			1809.43
ONONDAGA	(MD)			1920
ONONDAGA	(TVD)			1919.4
HELDERBERG	(MD)			2017
HELDERBERG	(TVD)			2016.37
BERTIE	(MD)			2241
BERTIE	(TVD)			2240.3
CAMILLUS	(MD)			2365
CAMILLUS	(TVD)			2364.26
SYRACUSE	(MD)			2470
SYRACUSE	(TVD)			2469.22
VERNON	(MD)			3098
VERNON	(TVD)			3097.03
LOCKPORT	(MD)			3805
LOCKPORT	(TVD)			3803.87
CLINTON	(MD)			3961
CLINTON	(TVD)			3959.82
MEDINA	(MD)			4391
MEDINA	(TVD)			4387.16
QUEENSTON	(MD)			4500
QUEENSTON	(TVD)			4489.7
OSWEGO	(MD)			5052
OSWEGO	(TVD)			4972.62
LORRAINE/UTI	(MD)	2511	2652	5805
LORRAINE/UTI	(TVD)	2511	2652	5605.98
TRENTON	(MD)	3140	3260	6692
TRENTON	(TVD)	3140	3260	6415.75
BLACK_RIVER	(MD)	3823	4067	7120
BLACK_RIVER	(TVD)	3823	4067	6808.91
TRIBES_HILL	(MD)			7400
TRIBES_HILL	(TVD)			7064.3
LITTLE_FALLS	(MD)	4139	4498	
LITTLE_FALLS	(TVD)	4139	4498	
GALWAY	(MD)	4275	4481	
GALWAY	(TVD)	4275	4481	
POTSDAM	(MD)		4816	
POTSDAM	(TVD)		4816	
PRECAMBRIAN	(MD)		4900	
PRECAMBRIAN	(TVD)		4900	

UWI/API		31007050870000	31099042030000	31109039730000
WELLNAME		Richards 1	Schaffer 2	Shepard 1
SURFLAT		42.32353	42.87627	42.37027
SURFLON		-75.94751	-76.85822	-76.50596
ELEVATION		1008.7	543.1	1295
TULLY	(MD)			1050
TULLY	(TVD)			1050
MARCELLUS	(MD)			2244
MARCELLUS	(TVD)			2244
ONONDAGA	(MD)			2343
ONONDAGA	(TVD)			2343
HELDERBERG	(MD)			2440
HELDERBERG	(TVD)			2440
BERTIE	(MD)			2632
BERTIE	(TVD)			2632
CAMILLUS	(MD)			2801
CAMILLUS	(TVD)			2801
SYRACUSE	(MD)			2954
SYRACUSE	(TVD)			2954
VERNON	(MD)			4105
VERNON	(TVD)			4105
LOCKPORT	(MD)			4980
LOCKPORT	(TVD)			4980
CLINTON	(MD)			5108
CLINTON	(TVD)			5108
MEDINA	(MD)			5430
MEDINA	(TVD)			5430
QUEENSTON	(MD)			5584
QUEENSTON	(TVD)			5584
OSWEGO	(MD)			5960
OSWEGO	(TVD)			5960
LORRAINE/UTICA	(MD)		2995	6436
LORRAINE/UTICA	(TVD)		2995	6436
TRENTON	(MD)	7547	3553	7693
TRENTON	(TVD)	7547	3553	7693
BLACK_RIVER	(MD)	7907	4380	8217
BLACK_RIVER	(TVD)	7907	4380	8217
TRIBES_HILL	(MD)	8175	N/A	8595
TRIBES_HILL	(TVD)	8175	N/A	8595
LITTLE_FALLS	(MD)	?	4827	?
LITTLE_FALLS	(TVD)	?	4827	?
GALWAY	(MD)	9090	4907	9407
GALWAY	(TVD)	9090	4907	9407
POTSDAM	(MD)		5259	10154
POTSDAM	(TVD)		5259	10154
PRECAMBRIAN	(MD)		5375	10352
PRECAMBRIAN	(TVD)		5375	10352

UWI/API		**31053095780000**	**31067213360000**	**31109229980000**
WELLNAME		**Shepard Helen 1**	**Stell 1**	**Stevenson 1**
SURFLAT		**42.95119**	**43.12284**	**42.42457**
SURFLON		**-75.80746**	**-76.40045**	**-76.63839**
ELEVATION		**1358**	**660**	**1255**
TULLY	(MD)			1160
TULLY	(TVD)			1159.93
MARCELLUS	(MD)			2222
MARCELLUS	(TVD)			2221.87
ONONDAGA	(MD)			2302
ONONDAGA	(TVD)			2301.87
HELDERBERG	(MD)			2386
HELDERBERG	(TVD)			2385.86
BERTIE	(MD)			2560
BERTIE	(TVD)			2559.85
CAMILLUS	(MD)			2776
CAMILLUS	(TVD)			2775.84
SYRACUSE	(MD)			2874
SYRACUSE	(TVD)			2873.84
VERNON	(MD)			3653
VERNON	(TVD)			3652.79
LOCKPORT	(MD)			4314
LOCKPORT	(TVD)			4313.75
CLINTON	(MD)			4491
CLINTON	(TVD)			4490.74
MEDINA	(MD)			4914
MEDINA	(TVD)			4913.72
QUEENSTON	(MD)			5074
QUEENSTON	(TVD)			5073.71
OSWEGO	(MD)			5660
OSWEGO	(TVD)			5659.7
LORRAINE/UTICA	(MD)			6453
LORRAINE/UTICA	(TVD)			6452.67
TRENTON	(MD)	3782	2684	7217
TRENTON	(TVD)	3782	2684	7216.17
BLACK_RIVER	(MD)	4080	3403	7662
BLACK_RIVER	(TVD)	4080	3403	7660.94
TRIBES_HILL	(MD)	N/A	N/A	8000
TRIBES_HILL	(TVD)	N/A	N/A	7998.76
LITTLE_FALLS	(MD)	4256	N/A	N/A
LITTLE_FALLS	(TVD)	4256	N/A	N/A
GALWAY	(MD)	4460	3802	N/A
GALWAY	(TVD)	4460	3802	N/A
POTSDAM	(MD)	4809	N/A	N/A
POTSDAM	(TVD)	4809	N/A	N/A
PRECAMBRIAN	(MD)	4866	N/A	N/A
PRECAMBRIAN	(TVD)	4866	N/A	

UWI/API		**31015231140000**	**31037045930000**	**31023195400000**
WELLNAME		**Strouse 1**	**Tyler 1**	**Vander Ploeg 1**
SURFLAT		**42.05261**	**43.04293**	**42.55436**
SURFLON		**-76.96368**	**-78.07707**	**-76.02057**
ELEVATION		**1746**	**716**	**1573**
TRENTON	(MD)	10717	2454	6641
TRENTON	(TVD)	10716.05	2454	6641
BLACK_RIVER	(MD)	11351	3056	7008
BLACK_RIVER	(TVD)	11349.98	3056	7008
TRIBES_HILL	(MD)	11650	N/A	7290
TRIBES_HILL	(TVD)	11648.91	N/A	7290
LITTLE_FALLS	(MD)		N/A	7500
LITTLE_FALLS	(TVD)		N/A	7500
GALWAY	(MD)		3520	N/A
GALWAY	(TVD)		3520	N/A
POTSDAM	(MD)		3850	N/A
POTSDAM	(TVD)		3850	N/A
PRECAMBRIAN	(MD)		4000	N/A
PRECAMBRIAN	(TVD)		4000	N/A

UWI/API		**31121044360000**	**31055047240000**	**31121040920000**	
WELLNAME		**Wellman L 1**	**Yantz 1**	**Veith D 1**	
SURFLAT		**42.81827**	**43.15095**	**42.61736**	
SURFLON		**-78.13836**	**-77.97494**	**-78.07991**	
ELEVATION		**1576**	**651**	**1575**	
TRENTON	(MD)	4336	2120	5310	
TRENTON	(TVD)	4336	2120	5310	
BLACK_RIVER	(MD)	4892	2797	5850	
BLACK_RIVER	(TVD)	4892	2797	5850	
LITTLE_FALLS	(MD)	N/A	N/A	6240	
LITTLE_FALLS	(TVD)	N/A	N/A	6240	
GALWAY	(MD)	5321	3137	6366	
GALWAY	(TVD)	5321	3137	6366	
POTSDAM	(MD)			7020	
POTSDAM	(TVD)			7020	
PRECAMBRIAN	(MD)		3274		
PRECAMBRIAN	(TVD)		3274		

APPENDIX B:

MATLAB CODE FOR NPHI POROSITY CORRECTIONS

```
%Corrections for Shale and Gas Effects in Neutron Logs

%Coded by Jood Ahmad A. Al Aswad      jaa378@cornell.edu

%Calculations from Bassiouni, 1994

%Modified from Erin Camp's 'Correcting Neutron Logs'   erc85@cornell.edu

%% Expected Output
%Data is loaded in with the first 6 columns. The rest are
%calculated here.

   % Column 1 = TVD; be sure to remove all basement data from this input
   % Column 2 = GR ; normalized high-low from 0-200 API
   % Column 3 = neutron porosity in decimal.
   % Column 4 = bulk density
   % Column 5 = photoelectric factor
   % Column 6 = lithology partition (1 = dolomite, 2 = limestone, 3 = sandstone)

   % Column 7 = volume of shale
   % Column 8 = density porosity
   % Column 9 = true porosity, corrected for shale


%% Assumptions
nsh = .045; % average nphi of nearby shale unit Utica Fm.
rhof= 1.19; % assuming mud with some brine
rhomad = 3; %based on densities of lithologies identified using PEF logs
rhomal = 2.82;
rhomas = 2.73;

%% Preparing Data
well = load('logs_WellName.txt');
col = zeros(length(well),1);
new_well = [well col];

for a = 1:length(new_well)

%calculation for shale index
gr=  new_well(:,2);
maxgr= max(gr);
mingr= min(gr);
```

```
new_well(a,7)=((new_well(a,2)-mingr)/(maxgr-mingr));

%Shale index to be corrected to get shale volume. Since this data is based
%on Cambro-Ordovician layers, Larionov Equation for older rocks is used.

new_well(a,7)= (0.33*(2^(2*new_well(a,7))-1));

%Correction for shale presence
 if new_well(a,7) > 0.2
   new_well(a,3) = NaN;
 end

 %% Calculate dphi, column 8
 if new_well(a,6) == 1 %dolomite
    new_well(a,8) =  (rhomad- new_well(a,4))/(rhomad-rhof);
 elseif new_well(a,6) == 2  %limestone
    new_well(a,8) = (rhomal - new_well(a,4))/(rhomal -rhof);
 elseif new_well(a,6) == 3 %sandstone
    new_well(a,8) = (rhomas - new_well(a,4))/(rhomas-rhof);
 end

 %% Corrections for "Gas" Presence
if abs(new_well(a,8)) > abs(new_well(a,3))
   new_well(a,9) =  100* ( sqrt(((new_well(a,8)^2) + (new_well(a,3)^2))/2));
else
   new_well(a,9) =  100* ((new_well(a,8)) + (new_well(a,3))/2);
end

%% Find effective porosity
S = (new_well(a,7) * 0.06);
new_well(a,9) = (new_well(a,9) -S);

end

%% Figures
  dol_nphi =  new_well(find(new_well(:,6) == 1),9);
  dline = new_well(find(new_well(:,6) == 1),1);
  dol_rho = new_well(find(new_well(:,6) == 1),4);
  lim_nphi = new_well(find(new_well(:,6) == 2),9);
  lline = new_well(find(new_well(:,6) == 2),1);
  lim_rho = new_well(find(new_well(:,6) == 2),4);
  san_nphi = new_well(find(new_well(:,6) == 3),9);
  sline = new_well(find(new_well(:,6) == 3),1);
  san_rho = new_well(find(new_well(:,6) == 3),4);
```

```
  x = linspace(0,40);

%% Figure of Porosity with Depth
  figure
  plot(dol_nphi,dline,'o','Color', [50/255,205/255, 50/255])
  hold on
  plot(lim_nphi,lline,'ro', 'Color', [30/255,144/255, 255/255])
  hold on
  plot(san_nphi,sline,'o', 'Color', [255/255,20/255, 147/255])
  hold on
  set(gca,'YDir','reverse')
  hold on
  title({'Porosity with Depth at WellName,'Trenton - Precambrian'},'FontSize',20)
  xlabel('Porosity, %', 'FontSize',20)
  ylabel('Depth, ft', 'FontSize', 20)
  legend({'Dolomite','Limestone','Sandstone'},'FontSize',16,'Location','southeast');

%% Histogram of true porosity values
binsporo = linspace(-2,2,50);
binsExpporo = 10.^binsporo;
figure
hist( new_well(:,9),40)
grid on
% set(gca,'XScal','log')
set(get(gca,'child'),'FaceColor',[0.6 0.6 0.6],'EdgeColor','k');
axis([0 40 0 1000])
xlabel('Porosity, %','FontSize',18)
ylabel('Frequency','FontSize',18)
title({'Well Log Derived Porosity in WellNAME','Trenton - Precambrian'},'FontSize',20)

%% CSV output file
output = new_well;
headers = {'TVD', 'GR','NPHI', 'RHO', 'PEF', 'LITH', 'VSHALE', 'DPHI', 'TRUE POROSITY'};
csvwrite_with_headers('WellName_porosity_calc.csv',output, headers);
```

APPENDIX C

WELL CUTTINGS ANALYSIS

	Shepard (API: 31-053-09578-0000)	
Depth	**Description**	**Formation**
5460 - 65	SHALE, medium to dark grey, silty,small amounts of PYRITE (10-15%)	ONEIDA
5480-85	SILTSTONE (80%), medium brownish red, sub-rounded, with some SHALE (20%), med-dark grey	MEDINA
5535 - 40	SHALE (60%), medim to dark grey, sub-angular, with some interbedded SILTSTONE (40%), dark brownish red, sub-rounded	
5570 -75	SILTSTONE (60%), lightish orange-brown or pinkish red, rounded, with SHALE (40%), medium-light grey	
5595-5600	SILTSTONE (75%), light pinkish-red, rounded, with SHALE (25%) medium-light grey	
5640-45	SANDSTONE (85%), clear/white/light-pink, rounded, with SHALE (10%), medium grey, subangular, and PYRITE (5%)	QUEENSTON
5705-10	SANDSTONE (95%), clear/white/light-pink, rounded, with SHALE (4%), light grey, subangular, and PYRITE (1%)	
5780- 85	SANDSTONE (93%), dark red, sub-rounded, with SHALE (7%), medium grey, sub-angular	
5860-70	SANDSTONE (93%), clear/white/light-pink, silty, sub-rounded, with SHALE (7%), light-grey	

5970-80	SANDSTONE (90%), clear/white/light-pink, silty, sub-rounded, with SHALE (10%), sub-rounded, medium-light grey	
6050-55	SANDSTONE (50%), clear/pink, sub-rounded, with SHALE (50%), sub-angular, medium-grey	
6140-50	SANDSTONE (100%) white/pale-yellow, silty,	
6250-60	SANDSTONE (100%) white/white-grey, very silty	
6380-90	SANDSTONE (100%) mostly grey/some white/clear (foggy),	OSWEGO
6490 - 6500	SANDSTONE (100%) mostly white, foggy, silty	
6600-10	SANDSTONE (100%) light grey, foggy, silty	
6720-30		
6860-70		
6980-90	SILTSTONE (100%) light grey, very fine, some pyrite	
7090-7100	SILTSTONE (100%) light grey, very fine	LORRAINE
7210-20		
7320-30	SHALE (100%) medium to dark grey, sub-angular	UTICA
7430-40		
7550-60		
7670-80	SHALE (100%) dark grey, silty, sub angular	
7780-90	LIMESTONE (100%) medium-dark grey, argillicious	TRENTON
7890-7900	SHALE (100%) dark grey,sub angular	
8000-10	LIMESTONE (100%) medium-dark grey, argillicious	
8120-30		
8258-66	DOLOMITE (100%), dark-medium grey, argilicious	BLACK RIVER
8364-74		
8476-86	DOLOMITE (100%) light grey/white, some frosted quartz grains	
8595-8600	DOLOMITE (>95%), medium-light grey, some PYRITE (<5%)	TRIBES HILL
8625-30	SILTSTONE (100%) light-grey, very fine, silty	
8655-60		
8685-90		
8740-45	DOLOMITE (100%) light grey/white, some frosted quartz grains	
8770-8775		

8800-05		
8830-35		
8905-8910		TRIBES HILL
8915-20		
8980-85		
9010-15		
9040-45	CHERT? (100%) light grey, does not react to HCl even when powdered	
9075-80		
9130-35	DOLOMITE, light grey/white, some frosted quartz grains with CHERT	LITTLE FALLS
9160-65		
9190-95		
9220-25	DOLOMITE, dark grey, very fine, silty/sandy with CHERT	
9245-50		
9265-70		
9290-95		
9345-50		
9370-75		
9385-90		
9415-20	DOLOMITE (100%) yellow-green, very fine	GALWAY
9425-30		
9445-50		
9470-75	SILTSTONE (100%) all quartz, pale yellow, fine, rounded, some small amounts of shale	
9500-05	SILTSTONE, pale yellow, fine, with DOLOMITE traces	
9516-20	DOLOMITE, light, medium dark grey/white, very fine interbedded with SANDSTONE, light grey/white/ very fine (50/50)	
9524-30		
9550-56		
9570-78		
9602-08		
9672-78		
9702-12		
9732-38		
9752-58		
9778-82		
9804-08		
9818-22		

9838-44		
9858-62		
9872-78		
9896-9902		
9912-18		
9932-38		
9952-58		
9964-68		
9984-88		
10004-08		
10022-28		
10042-48		
10058-68		
10084-88		
10104-10		
10128-34		
10152-58		
10172-78		
10192-98		
10212-18		
10234-38		
10244-48		
10248-54	SANDSTONE, white/light-grey/clear, sub-angular, fine, some DOLOMITE, light/medium/dark grey (20%)	
10258-60		
10260-68		
9415-20	DOLOMITE (100%) yellow-green, very fine	GALWAY
9425-30		
9445-50		
9470-75	SILTSTONE (100%) all quartz, pale yellow, fine, rounded, some small amounts of shale	
9500-05	SILTSTONE, pale yellow, fine, with DOLOMITE traces	
9516-20	DOLOMITE, light, medium dark grey/white, very fine interbedded with SANDSTONE, light grey/white/ very fine (50/50)	
9524-30	SANDSTONE, white/light-grey/clear, sub-angular, fine, some DOLOMITE, light/medium/dark grey (20%)	
9550-56	SANDSTONE, and DOLOSTONE (30-50%)	
9570-78		

9602-08		
9672-78		
9702-12		
9732-38		
9752-58		
9778-82		
9804-08		
9818-22		
9838-44		
9858-62		
9872-78		
9896-9902		
9912-18		
9932-38		
9952-58		
9964-68		
9984-88		
10004-08		
10022-28		
10042-48		
10058-68		
10084-88		
10104-10		
10128-34		
10152-58		
10172-78		
10192-98		
10212-18		
10234-38		
10244-48		
10248-54		
10258-60	SANDSTONE, white/light-grey/clear, sub-angular, fine, some DOLOMITE, light/medium/dark grey (20%)	POTSDAM
10260-68		
10274-78	SANDSTONE, grey, sub-angular, with some pyrite, with FELDSPAR (50%?)	

10288-94	K-SPAR (50%), sub-angular (do not appear to have been rounded) , pink, 40% AMPHIBOLE, 10% ROCK FRAGMENTS (granitic, black, with quartz imbedded)	BASEMENT ?
10294-10298		
10298-10304		
10314- 1-318		
10330-10336		
10342-10346		
10346 - 10352		
10352-10358		

	Mitchell 1 (API: 31-101-21468-0000)	
Depth	**Description**	**Formation**
9770 - 9800	DOLOMITE (70%), SHALE (30%) with some PYRITE	POTSDAM
9810 - 9820	SANDSTONE/QUARTZ (80%), DOLOMITE (20%) with some PYRITE (?)	
9820 - 9830		
9830 - 9840		
9850 - 9860		
9860 - 9870		
9870 - 9880		
9875		
9884	SANDSTONE/QUARTZ (80%), DOLOMITE (20%) with some PYRITE	
9885		

	Olin (API: 31-101-03924-0000)	
11785 - 90	SANDSTONE/QUARTZ (65%), clear/orange, sub-rounded, DOLOMITE (35%)	GALWAY
11800 - 05		
11845 - 50	SANDSTONE/QUARTZ (50%), DOLOMITE (50%)	
11895 - 11900		
11945 - 50		
11965 - 70		
11970 -75	SANDSTONE/QUARTZ (70%), DOLOMITE (30%)	
11985 - 90		
11990 -13318 NO SAMPLES		
13318 - 13322	QUARTZ (100%), white, light - dark-grey, sub-angular	POTSDAM
13322 - 13326	QUARTZ SS FRAGMENTS (50%), light-dark grey, PINKISH	
13326 -30		
13330 - 36		

APPENDIX D

POROSITY LOGS CORRECTED FOR PRESENCE OF GAS AND SHALE

POROSITY WITH DEPTH (TVD), IN WHICH POROSITY VALUES INCREASE TO THE RIGHT

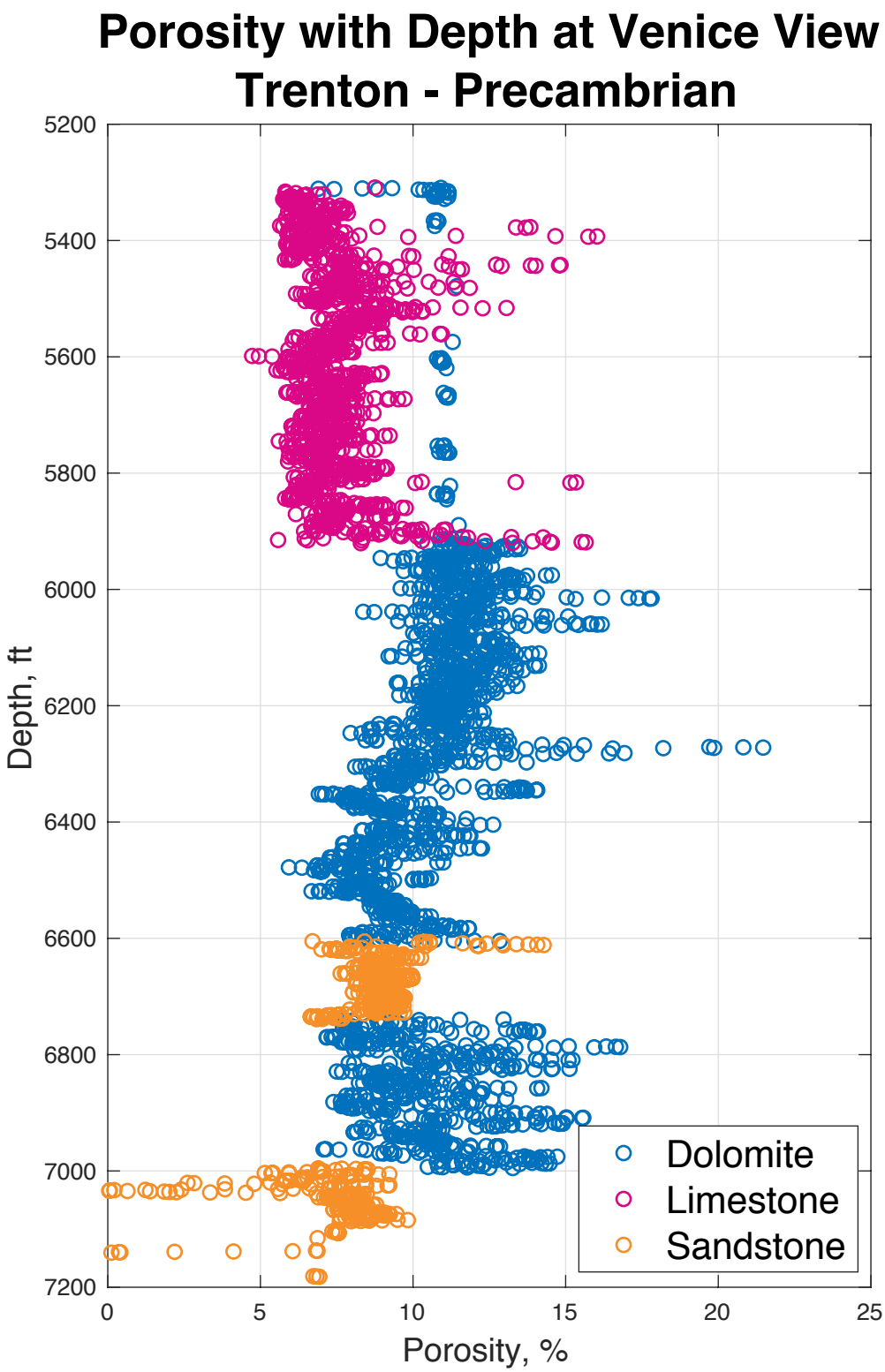
Porosity with Depth at Venice View
Trenton - Precambrian
Depth, ft
Porosity, %
5200
5400
5600
5800
6000
6200
6400
6600
6800
7000
7200
0
5
10
15
20
25
Dolomite
Limestone
Sandstone

Porosity with Depth at Stevenson Well
Trenton - Little Falls

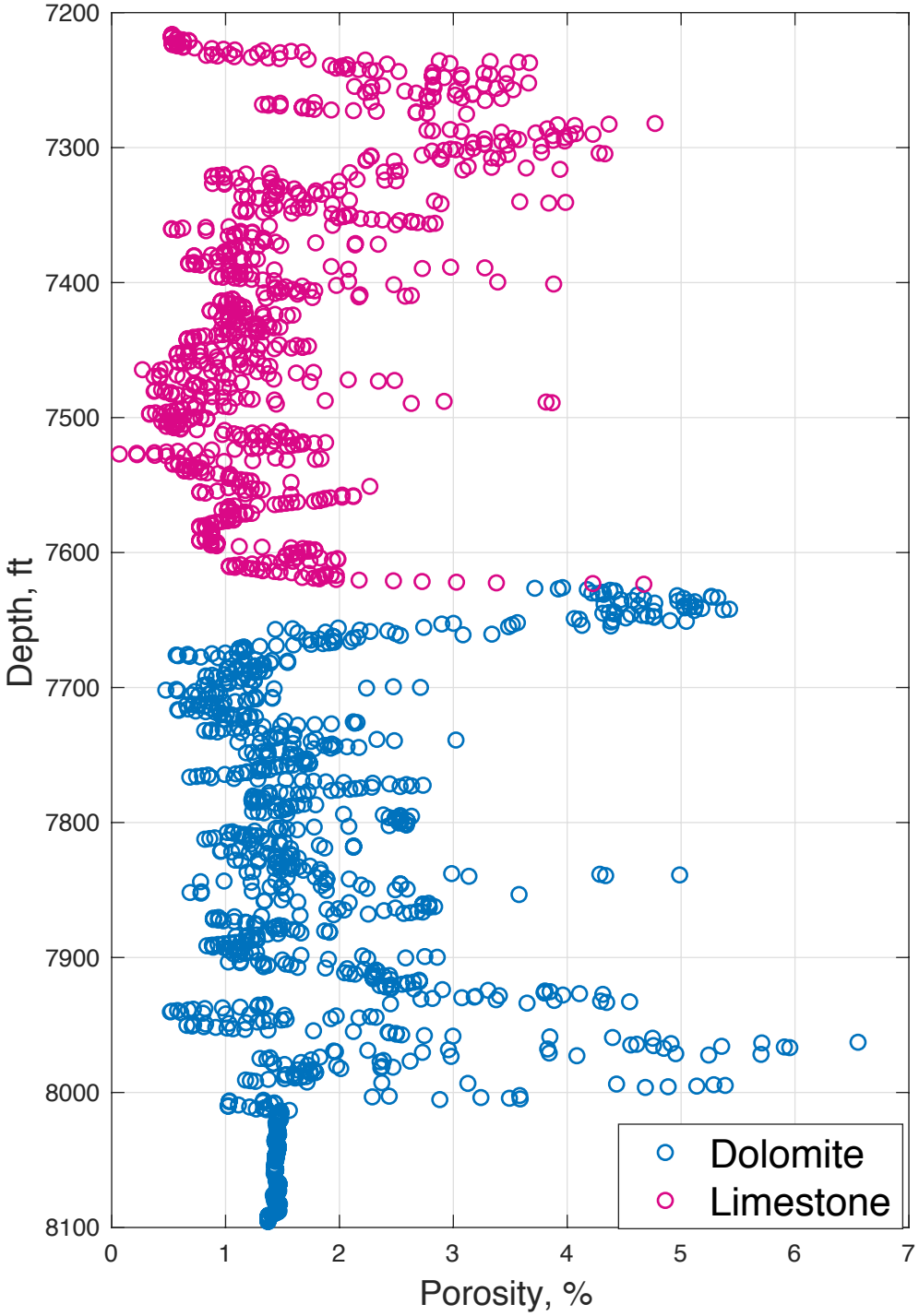

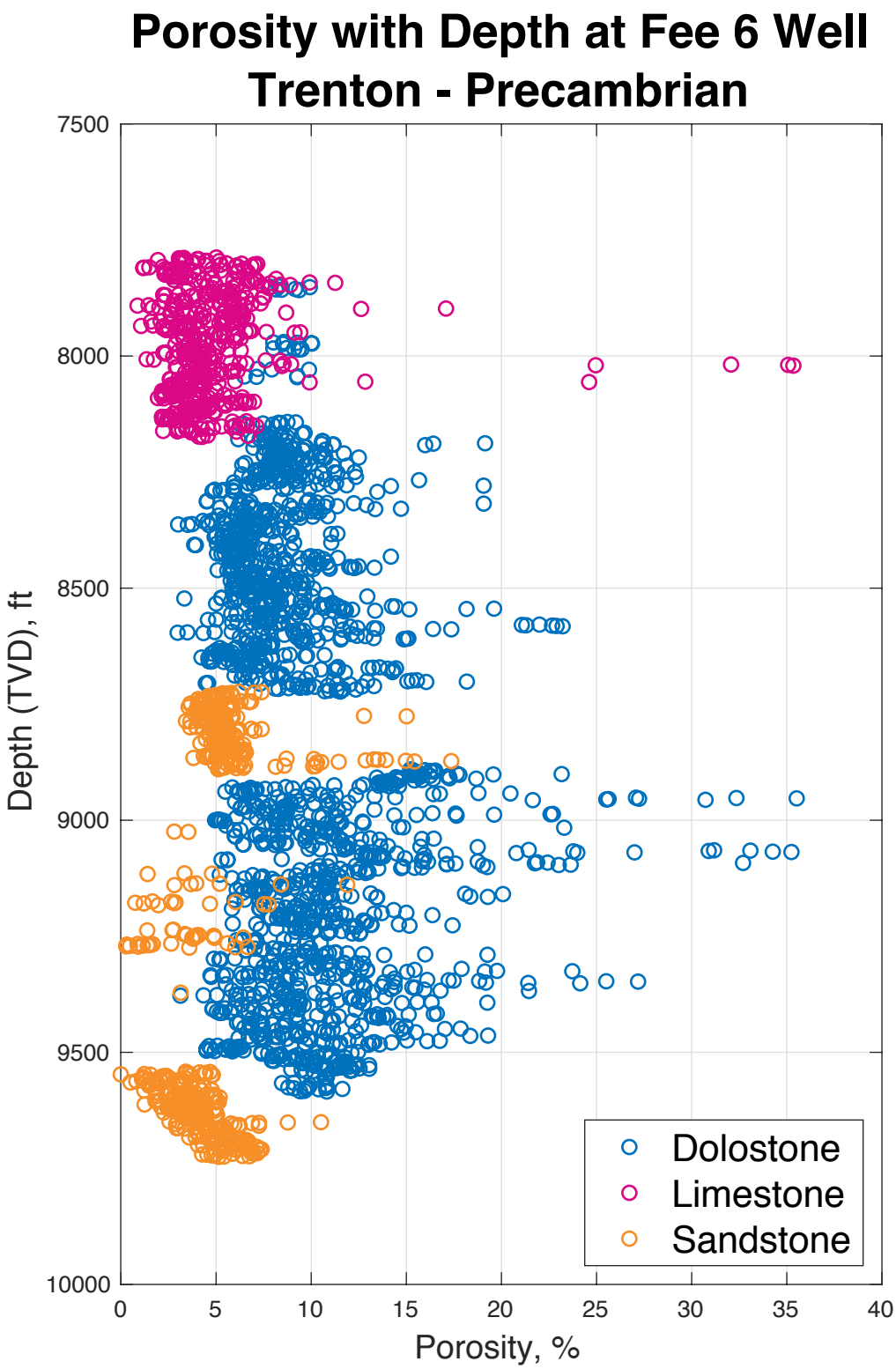
Porosity with Depth at Fee 6 Well
Trenton - Precambrian
Depth (TVD), ft
7500
8000
8500
9000
9500
10000
0
5
10
15
20
25
30
35
40
Porosity, %
Dolostone
Limestone
Sandstone

Porosity with Depth at Mitchell 1 Well
Tompkins Group - Precambrian

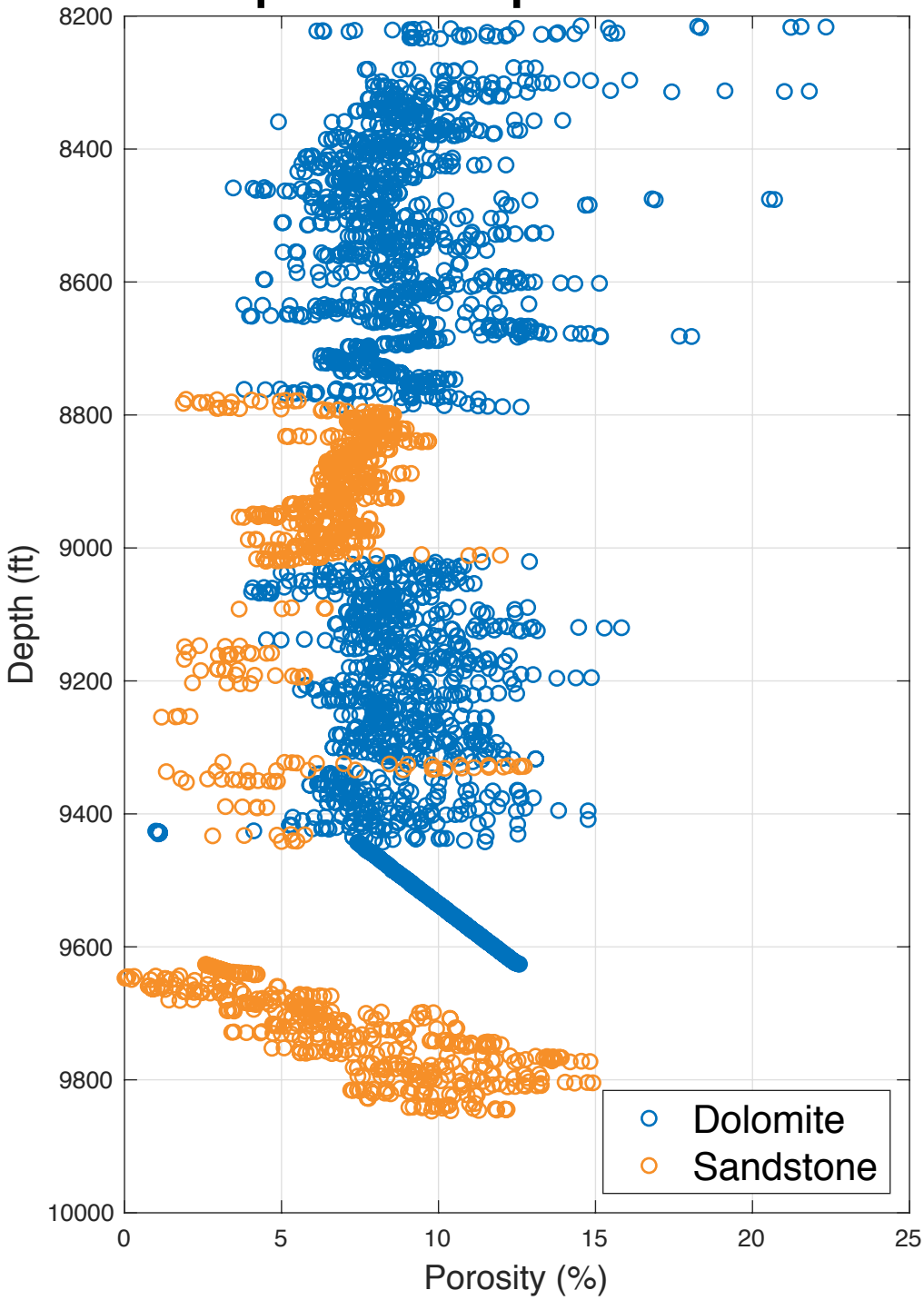

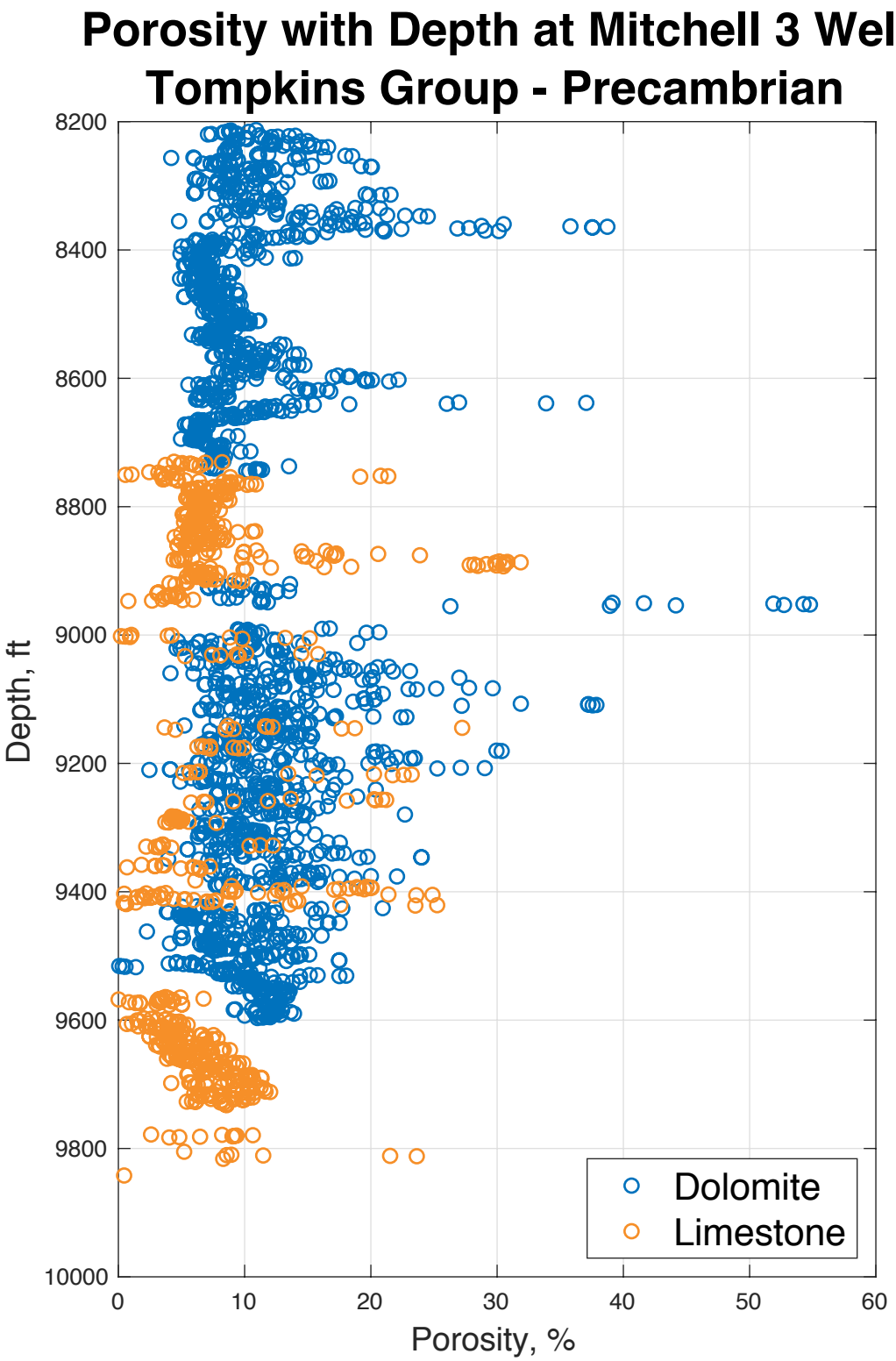
Porosity with Depth at Mitchell 3 Well
Tompkins Group - Precambrian
Depth, ft
8200
8400
8600
8800
9000
9200
9400
9600
9800
10000
0
10
20
30
40
50
60
Porosity, %
Dolomite
Limestone

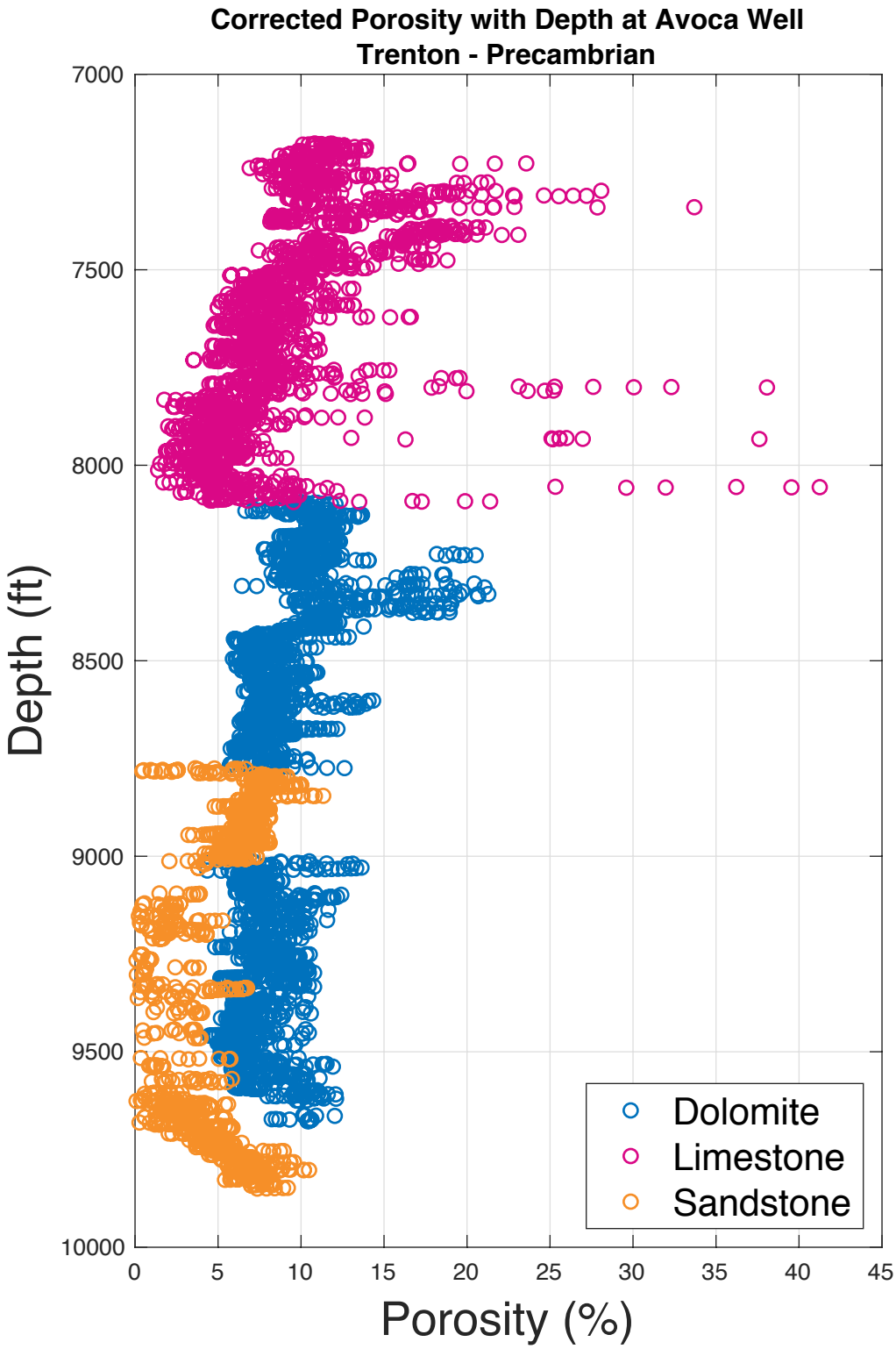
Corrected Porosity with Depth at Avoca Well
Trenton - Precambrian
Depth (ft)
7000
7500
8000
8500
9000
9500
10000
0
5
10
15
20
25
30
35
40
45
Porosity (%)
Dolomite
Limestone
Sandstone

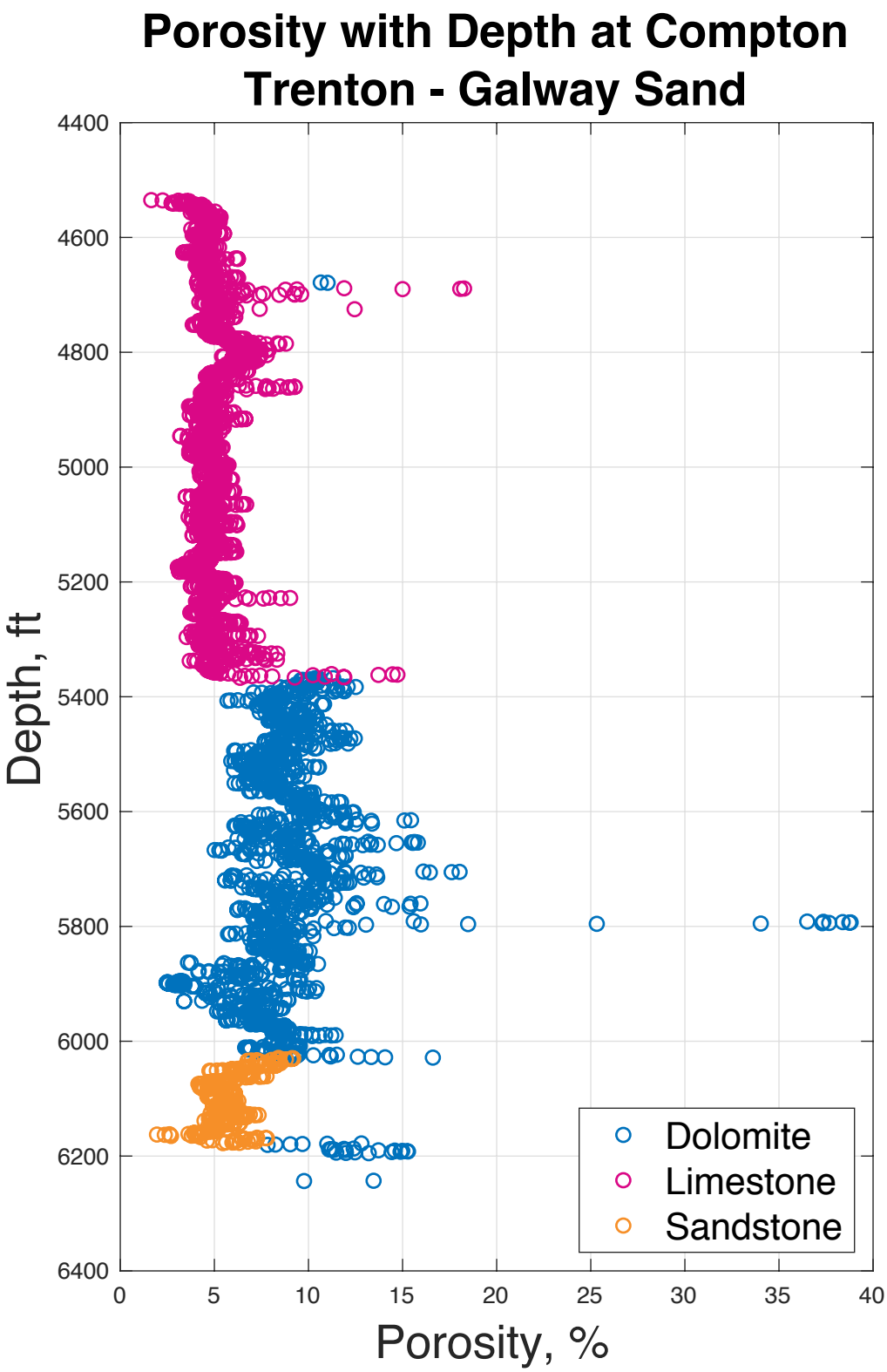
Porosity with Depth at Compton
Trenton - Galway Sand
Depth, ft
Porosity, %
4400
4600
4800
5000
5200
5400
5600
5800
6000
6200
6400
0
5
10
15
20
25
30
35
40
Dolomite
Limestone
Sandstone

Porosity with Depth at Hubbard Well
Tompkins - Potsdam

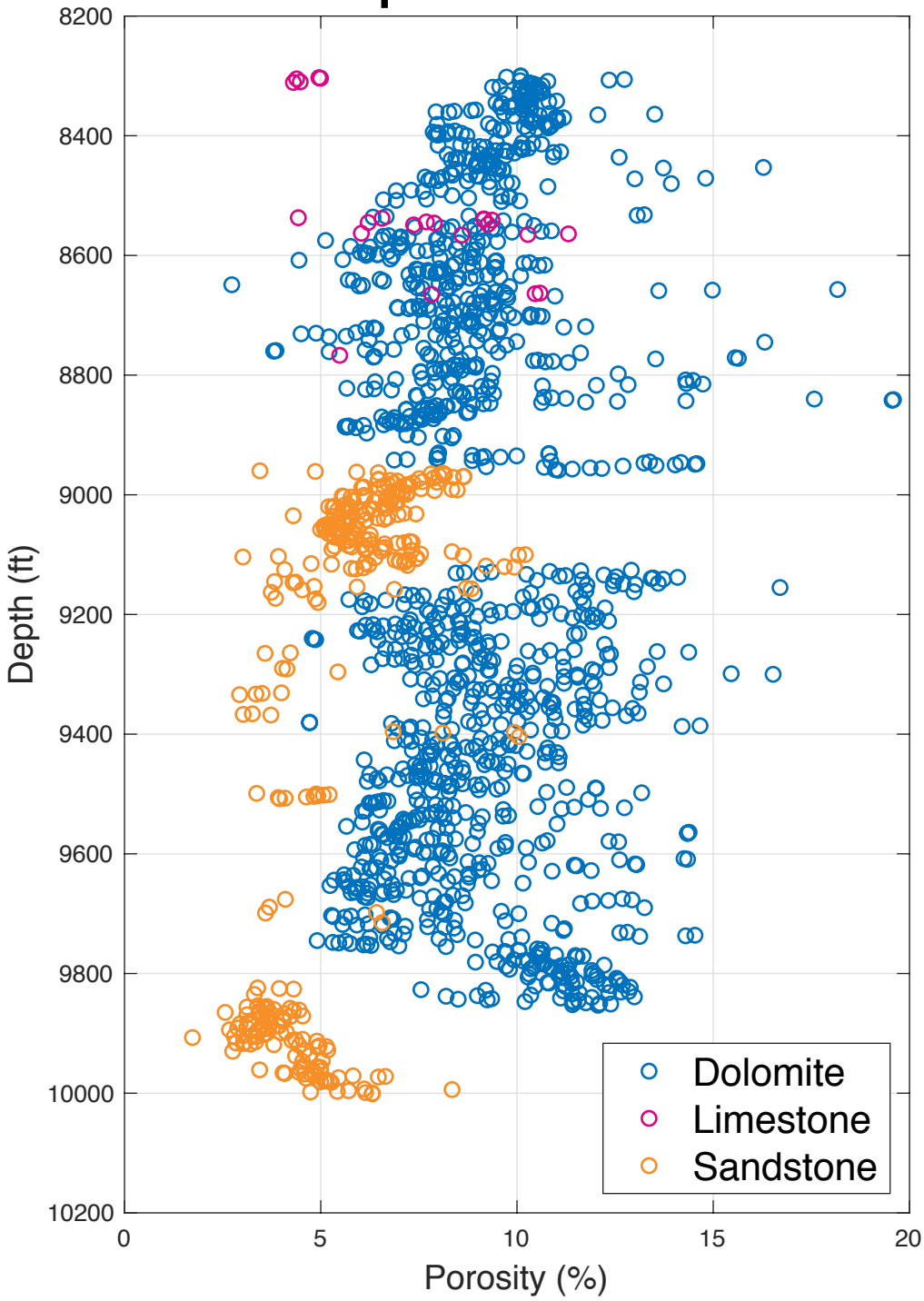

Porosity with Depth at Chamberlain P2
Trenton - Galway Sand

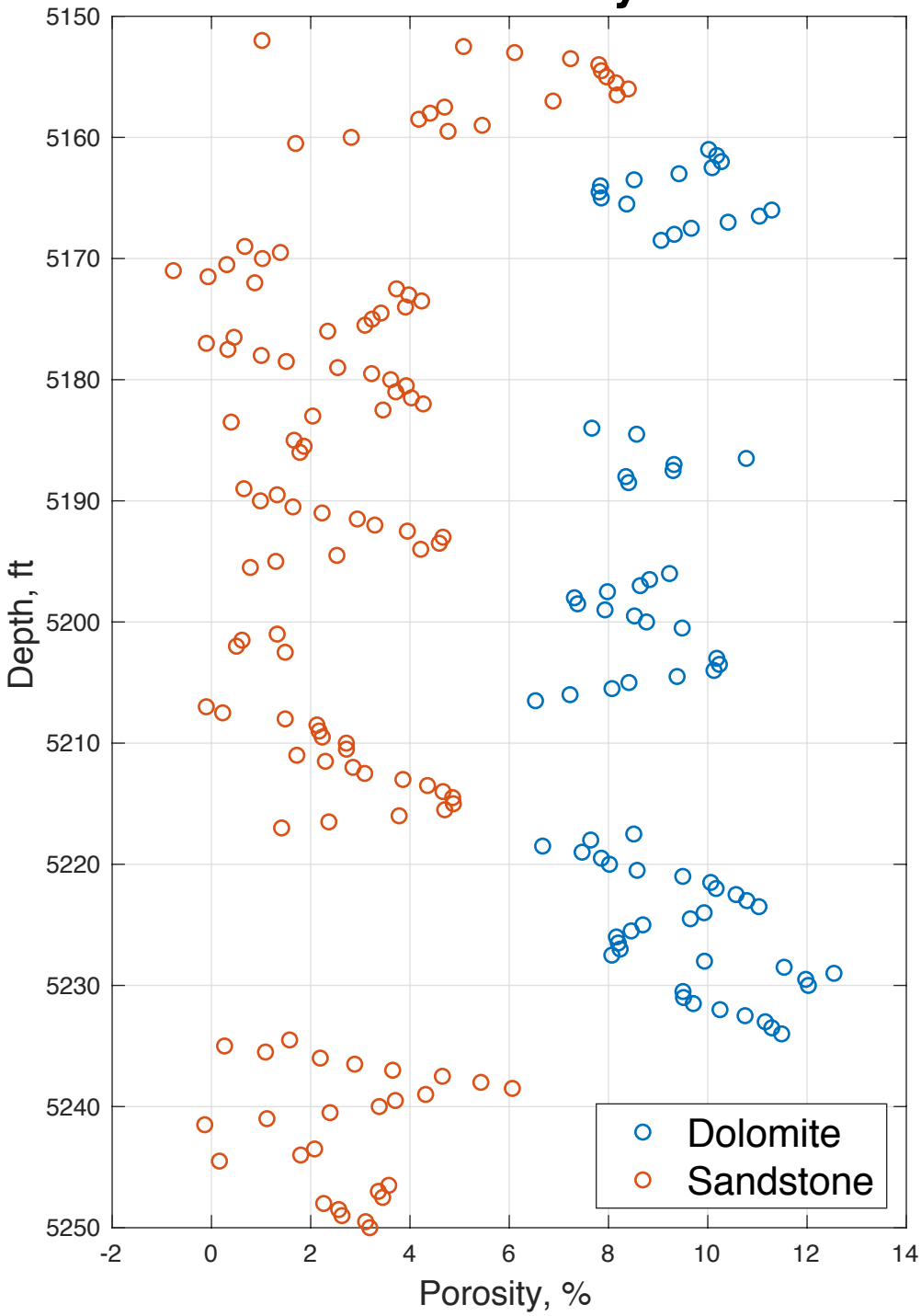

Porosity with Depth at Chamberlain D2
Trenton - Galway Sand

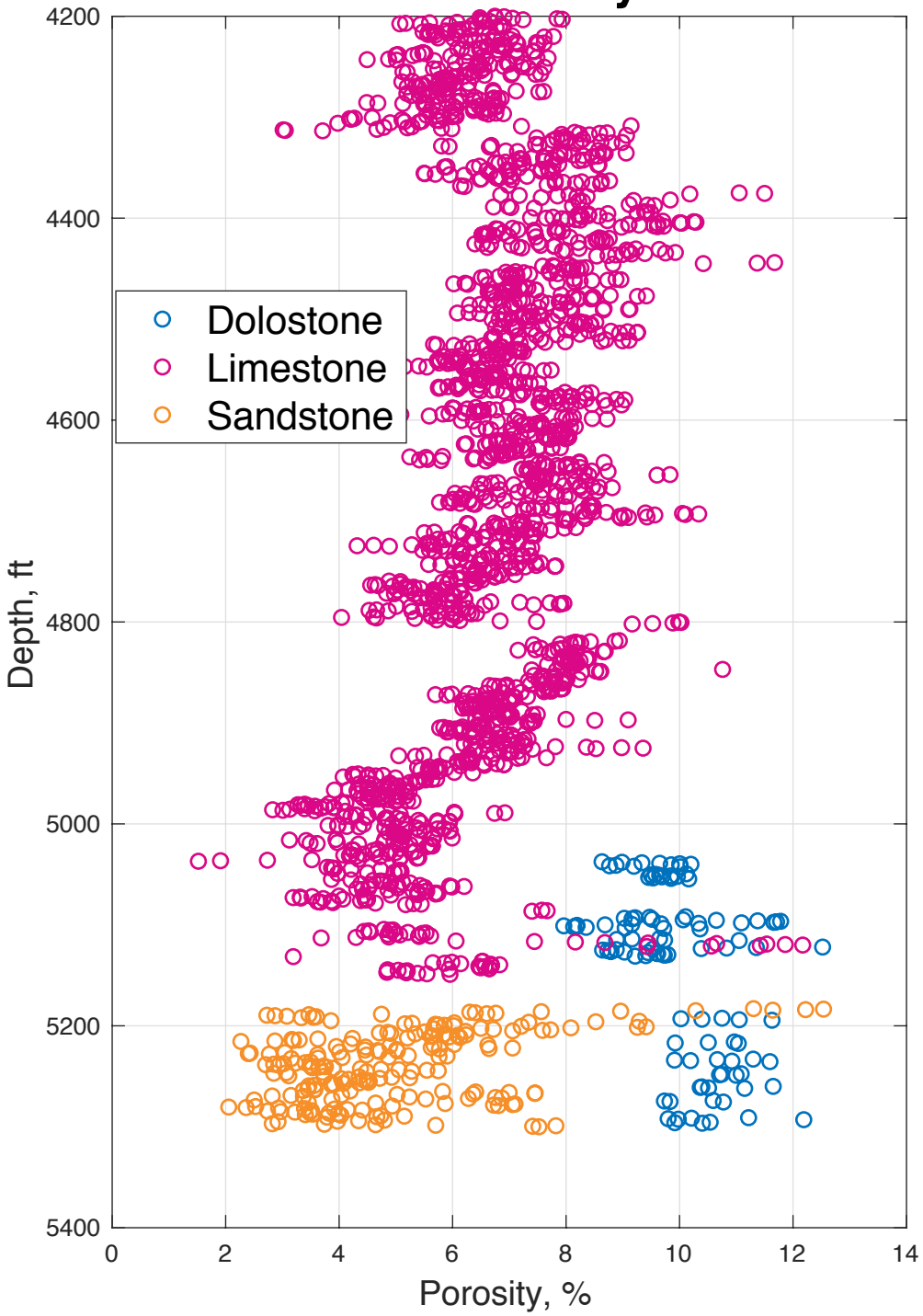

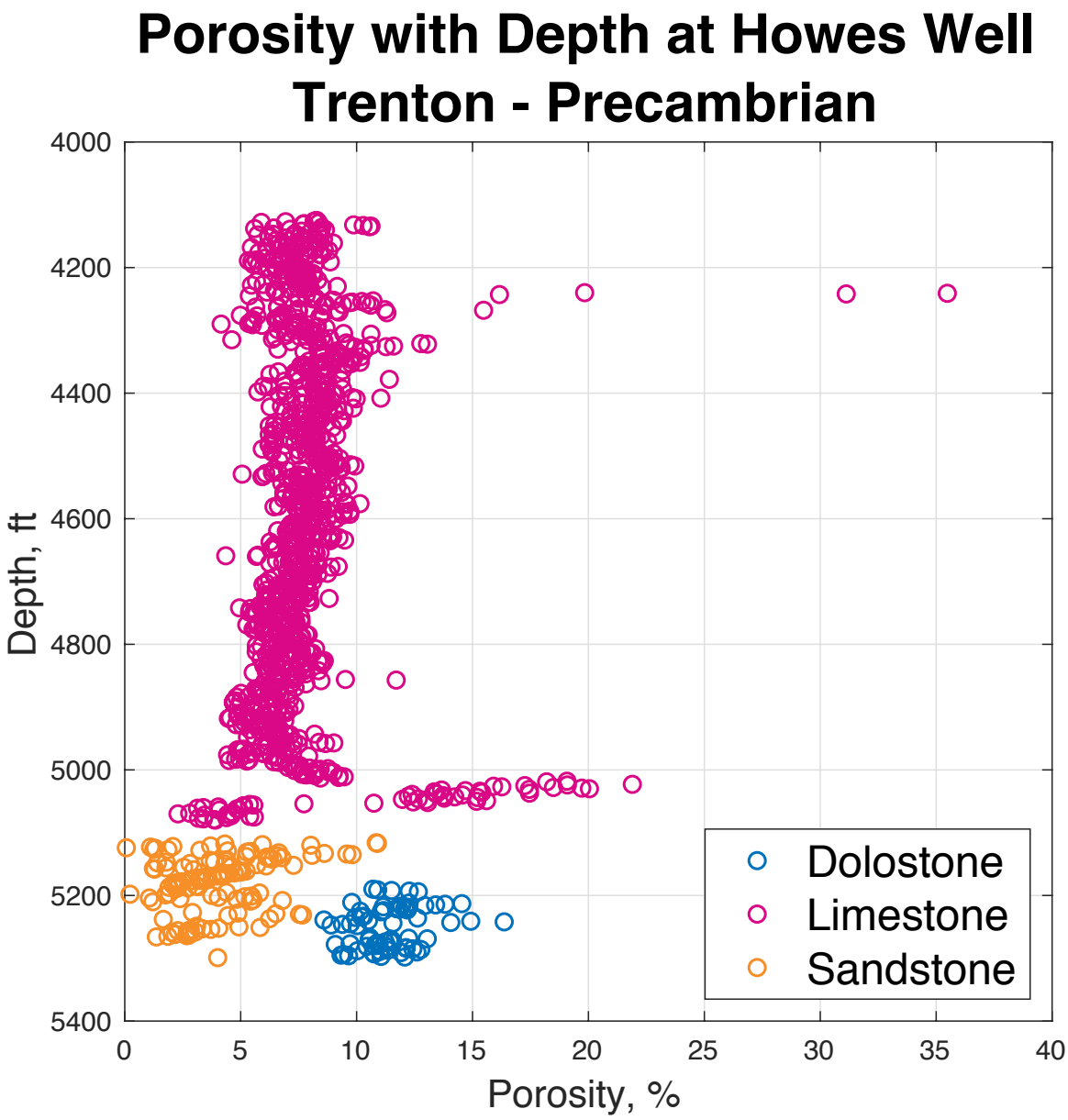
Porosity with Depth at Howes Well
Trenton - Precambrian
Depth, ft
Porosity, %
4000
4200
4400
4600
4800
5000
5200
5400
0
5
10
15
20
25
30
35
40
Dolostone
Limestone
Sandstone